

**Flanders**  
State of  
the Art

13\_131\_11  
FHR reports

## Integraal Plan Boven-Zeeschelde

Deelrapport 11  
Effect of B-alternatives on Sand Transport

DEPARTMENT  
MOBILITY &  
PUBLIC  
WORKS

[www.flandershydraulicsresearch.be](http://www.flandershydraulicsresearch.be)

# Integraal Plan Boven-Zeeschelde

## Sub report 11 – Effect of B-alternatives on Sand Transport

Smolders, S.; Plancke, Y.; Vanlede, J.; Mostaert, F.

### Legal notice

Flanders Hydraulics Research is of the opinion that the information and positions in this report are substantiated by the available data and knowledge at the time of writing.  
 The positions taken in this report are those of Flanders Hydraulics Research and do not reflect necessarily the opinion of the Government of Flanders or any of its institutions.  
 Flanders Hydraulics Research nor any person or company acting on behalf of Flanders Hydraulics Research is responsible for any loss or damage arising from the use of the information in this report.

### Copyright and citation

© The Government of Flanders, Department of Mobility and Public Works, Flanders Hydraulics Research 2019  
 D/2019/3241/218

This publication should be cited as follows:

**Smolders, S.; Plancke, Y.; Vanlede, J.; Mostaert, F.** (2019). Integraal Plan Boven-Zeeschelde: Sub report 11 – Effect of B-alternatives on Sand Transport. Version 3.0. FHR Reports, 13\_131\_11. Flanders Hydraulics Research: Antwerp.

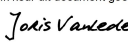
Reproduction of and reference to this publication is authorised provided the source is acknowledged correctly.

### Document identification

Customer:	Flanders Hydraulics Research	Ref.:	WL2019R13_131_11
Keywords (3-5):	Scaldis Sand transport, scenario analysis		
Text (p.):	45	Appendices (p.):	13
Confidentiality:	<input checked="" type="checkbox"/> No	<input checked="" type="checkbox"/> Available online	

Author(s)	Smolders, S.
-----------	--------------

### Control

	Name	Signature
Reviser 1:	Plancke, Y.	Getekend door: Yves Plancke (Signature) Getekend op: 2020-01-29 09:01:54 +01:00 Reden: Ik keur dit document goed 
Project leader:	Joris Vanlede	Getekend door: Joris Vanlede (Signature) Getekend op: 2020-01-22 11:03:11 +01:00 Reden: Ik keur dit document goed 

### Approval

Head of Division:	Mostaert, F.	Getekend door: Frank Mostaert (Signature) Getekend op: 2020-01-21 15:29:07 +01:00 Reden: Ik keur dit document goed 
-------------------	--------------	--



# Samenvatting

Een zandtransportmodel werd eerder reeds binnen het project Integraal Plan Boven-Zeeschelde gemaakt. Dit model werd “Scaldis Zand” genoemd. Het werd gevalideerd aan de hand van 13-uursmetingen langsheen de Zeeschelde. Dit model is bedoeld om zandtransport te simuleren en dus geen morfologie. Aangezien er over het ganse modeldomein ongelimiteerd zand aanwezig is, berekent dit model eerder de zandtransport*capaciteit* dan het ogenblikkelijke zandtransport. Er wordt een uniforme korrelgrootte van 150 µm gebruikt, samen met de transportformule volgens Engelund en Hansen.

In dit rapport wordt dit model gebruikt om enkele scenario's met B-alternatieven te berekenen. Onder scenario's worden twee verschillende randvoorwaarden bedoeld die het effect van klimaatverandering trachten na te bootsen. Het gaat hier over een hoog (AplusCH) en een laag (AminCL) klimaatscenario. Onder B-alternatieven worden enkele bathymetrische aanpassingen aan de planvorm van het estuarium in de Boven-Zeeschelde bedoeld en dit in het jaar 2050. Het gaat over drie alternatieven onder de naam VaG, Chafing en VaH. Deze alternatieven en de klimaatrandvoorwaarden worden in het rapport uitgebreid beschreven.

In eerste instantie beschrijft dit rapport de effecten van de autonome ontwikkeling van het estuarium op het zandtransport in de Boven-Zeeschelde. Deze autonome ontwikkeling houdt alle ontwikkelingen van de bodem en planvorm in tussen de situatie 2013 en 2050. De randvoorwaarden blijven deze van 2013. Voor effecten wordt er gekeken naar verschillen in netto zandtransport over verschillende dwarssecties langsheen heel het estuarium. Verder wordt met behulp van al deze dwarssecties een massabalans opgemaakt voor zand voor het gebied tussen de dwarssecties.

In een tweede stap worden voor de situatie in 2050 de twee voornoemde klimaatrandvoorwaarden doorgerekend. Hiermee worden effecten van stijgende zeespiegel en veranderende getijslag op de zandtransportcapaciteit in 2050 in kaart gebracht.

Vervolgens worden de drie alternatieven doorgerekend met het meest ingrijpende klimaatscenario, AplusCH. De resultaten worden vergeleken met de resultaten van de 2050 situatie met dezelfde AplusCH randvoorwaarden. Op deze manier worden enkel de effecten van het aanpassen van de bodem en planvorm van de Boven-Zeeschelde onder het zwaarste klimaatscenario uitgelicht. Voor het VaG alternatief wordt ook de vergelijking met de referentie gemaakt voor het AminCL klimaatscenario.

Algemeen kan gesteld worden dat het effect van de klimaatscenario's, en dan vooral AplusCH, op de zandtransportcapaciteit veel groter is dan de veranderingen in de bodem en planvorm binnen de alternatieven. De effecten van de alternatieven Chafing en VaH zijn in grootteorde gelijk aan de effecten van de autonome ontwikkeling. Het effect van het VaG alternatief is groter dan alle andere.

## Abstract

A sand transport model for the Scheldt estuary was made in the framework of the integrated plan Upper Sea Scheldt. This model is called “Scaldis Sand” and was able to reproduce sand transport rates measured along the Sea Scheldt and was as such validated. In this report this model is used to simulate some of the B-alternatives.

The B-alternatives are three bathymetrical variations on the Scheldt estuary plan form in 2050 to allow larger vessels of class Va to reach Ghent via the Sea Scheldt. These alternatives are called VaG, Chafing and VaH and are described in detail in this report. Alongside the bathymetrical changes the boundary conditions were changed to include climate change. In this report only two types are taken into account: a climate high (AplusCH) and a climate low (AminCL).

First the effect of the autonomous development of the estuary, i.e. the bathymetrical changes between 2013 and 2050, on sand transport is discussed. Sand transport rates are given for different transects along the estuary. The transport direction is explained by the asymmetry between ebb and flood in the cross sectionally averaged flow velocity to the power five. The net sand transport rate over the transects is used to determine a mass balance for the areas in between transects.

Secondly the 2050 reference is compared with the two climate scenarios 2050 AplusCH and 2050 AminCL. Sand transport rates and mass balances are compared.

Next the 2050 AplusCH will act as a reference for the alternatives simulated with the same climate boundary conditions. The sand transport rates and mass balances of 2050 AplusCH, Chafing AplusCH, VaG AplusCH and VaH AplusCH are compared. For the VaG alternative the AminCL scenario was also compared with the reference.

The climate boundary conditions had a larger effect on the sand transport rates and the mass balances than the changes in bathymetry in the B-alternatives. Comparing only the alternatives, the effect of Chafing and VaH was in the same order of magnitude as the effect of the autonomous development. VaG had a much larger effect.

# Contents

Samenvatting.....	III
Abstract .....	IV
Contents .....	V
List of tables.....	VII
List of figures .....	VIII
1 Introduction.....	1
1.1 project Integrated Plan Upper Sea Scheldt .....	1
1.2 Evaluation framework .....	2
2 Units and reference plane .....	4
3 Summary of Scaldis sand transport model.....	5
3.1 Scaldis HD 2013 .....	5
3.2 Sand transport model in SISYPHE.....	6
3.2.1 model parameters .....	6
3.2.2 Boundary conditions.....	7
3.2.3 Initial conditions .....	7
3.2.4 Bottom friction coefficient .....	7
3.2.5 Bottom update in hydrodynamic model switched off .....	8
4 Alternatives and Scenarios .....	9
4.1 Alternatives.....	9
4.1.1 Bathymetry Updates from Scaldis 2013 to Scaldis 2050 .....	9
4.1.2 The B alternatives: Chafing.....	13
4.1.3 The B alternatives: VaG .....	14
4.1.4 The B alternatives: VaH .....	15
4.2 Scenarios.....	16
4.2.1 Normal and events discharge scenarios.....	16
4.2.2 Tidal range scenarios .....	16
4.2.3 Sea level rise scenarios .....	16
4.3 Simulation period .....	17
4.4 Overview of Model Runs .....	18
5 Methodology of scenario analysis.....	19
5.1 Calculating sand transport.....	19
5.2 Tidal asymmetry effects on sand transport.....	24

5.3	Erosion and sedimentation patterns .....	24
6	Scenario Results.....	25
6.1	Scaldis 2013 REF QN A0CN .....	25
6.2	Scaldis 2050 REF QN: A0CN, AplusCH and AminCL.....	29
6.3	VaG alternative.....	32
6.3.1	AplusCH scenario .....	32
6.3.2	AminCL scenario .....	35
6.4	VaH alternative .....	37
6.5	Chafing alternative .....	39
6.6	Synthesis of alternatives with AplusCH boundary condition .....	41
7	Conclusions.....	44
7.1	Autonomous development from 2013 to 2050.....	44
7.2	Climate scenarios in 2050: AplusCH and AminCL .....	44
7.3	Alternatives: Chafing, VaG and VaH .....	44
8	References .....	45
	Appendix A: Mass balance for USS for different scenarios .....	A1
	Appendix B: Net sand transport figures for scenarios .....	A7

## List of tables

Table 1 – The Evaluation parameters in the framework of the “Sediment and morphology” theme.....	3
Table 2 – Tidal range scenarios .....	16
Table 3 – List of the simulation periods .....	17
Table 4 – List of the different scenarios/alternatives runs.....	18
Table 5 – Cumulative potential sand transport per polygon extrapolated from a spring/neap tidal cycle to one year [x 10 <sup>3</sup> tons/year].....	A6

## List of figures

Figure 1 – Changes in bathymetry going from 2013 to 2050.....	10
Figure 2 – Biggest changes in bathymetry in the sustainable bathymetry (circled in red) for the Upper Sea Scheldt compared to the 2013 situation.....	11
Figure 3 – Future bathymetry of the tidal tributary Durme.....	11
Figure 4 – Future development of the Heusden are with a new sluice.....	12
Figure 5 – Difference in bathymetry (Chafing – Reference 2050) part 1 of 2.....	13
Figure 6 – Difference in bathymetry (Chafing – Reference 2050) part 2 of 2.....	13
Figure 7 – Difference in bathymetry (VaG – Reference 2050).....	14
Figure 8 – Difference in bathymetry (VaH – Reference 2050).....	15
Figure 9 – Map of the Scheldt estuary with main tributaries and most important locations.....	20
Figure 10 – boxes of the ecosystem model used in the calculation of the sand transport (Western Scheldt).....	20
Figure 11 – boxes of the ecosystem model used in the calculation of the sand transport (Lower Sea Scheldt).....	21
Figure 12 – boxes of the ecosystem model used in the calculation of the sand transport (Upper Sea Scheldt Part 1).....	21
Figure 13 – boxes of the ecosystem model used in the calculation of the sand transport (Upper Sea Scheldt Part 2).....	22
Figure 14 – Difference in transects (transect 48) between the 2050 REF and VaG alternative for location around km 130-131 (Uitbergen).....	22
Figure 15 – Difference in transects (transect 62) between the 2050 REF and VaG alternative for location around km 152 (Bergenmeersen).....	23
Figure 16 – Difference in transects (transect 48) between the 2050 REF and Chafing alternative for location around km 130-131 (Uitbergen).....	23
Figure 17 – Net sand transport over different cross sections along the Scheldt estuary calculated and plotted for a neap and spring tide and a full spring/neap tidal cycle. Scenario 2013 QN REF AOCN.....	25
Figure 18 – Net sand transport over different cross sections of the Upper Sea Scheldt calculated and plotted for a neap and spring tide and a full spring/neap tidal cycle. Scenario 2013 QN REF AOCN.....	26
Figure 19 – Asymmetry between flood and ebb over time integrated cross sectional averaged flow velocity to the power five for scenario 2013 QN REF AOCN.....	27
Figure 20 – Asymmetry between flood and ebb over time integrated cross sectional averaged flow velocity to the power five for scenario 2013 QN REF AOCN focused on the Upper Sea Scheldt.....	27
Figure 21 – Mass balance of potential sand transport over spring/neap tidal cycle for polygons along the Upper Sea Scheldt. Scenario QN 2013 REF AOCN.....	28
Figure 22 – Schematic view of the two step path from Scaldis model 2013 to Scaldis model 2050.....	29

Figure 23 – Bar graph of net potential sand transport over different transects along the Upper Sea Scheldt calculated over a full spring/neap tidal cycle for scenarios 2013 REF QN A0CN, 2050 REF QN A0CN, 2050 REF QN AplusCH and 2050 REF QN AminCL. .... 30

Figure 24 – Asymmetry between flood and ebb over time integrated cross sectional averaged flow velocity to the power five for scenario 2013 QN REF A0CN, 2050 QN REF A0CN, 2050 REF QN AplusCH and 2050 REF QN AminCL..... 30

Figure 25 – Asymmetry between flood and ebb over time integrated cross sectional averaged flow velocity to the power five for scenario 2013 QN REF A0CN, 2050 QN REF A0CN, 2050 REF QN AplusCH and 2050 REF QN AminCL. Focus on the Upper Sea Scheldt. .... 31

Figure 26 – Potential sedimentation erosion rates extrapolated from a spring/neap tidal cycle to one year for different polygons along the Upper Sea Scheldt for scenarios 2013 REF QN A0CN, 2050 REF QN A0CN, 2050 REF QN AplusCH and 2050 REF QN AminCL. .... 32

Figure 27 – Net sand transport rates over a spring/neap tidal cycle for different transects along the Upper Sea Scheldt for the alternative VaG AplusCH and the reference simulation 2050 REF AplusCH..... 33

Figure 28 – Asymmetry of the over a transect averaged flow velocity to the power five integrated over a spring/neap tidal cycle for VaG alternative and reference simulation 2050 REF AplusCH..... 33

Figure 29 – top left: cross sectionally averaged flow velocities at transects 52, 53 and 54. .... 34

Figure 30 – Potential sedimentation erosion rates extrapolated from a spring/neap tidal cycle to one year for different polygons along the Upper Sea Scheldt for alternative VaG AplusCH and the reference simulation 2050 REF AplusCH..... 35

Figure 31 – Net sand transport rates over a spring/neap tidal cycle for different transects along the Upper Sea Scheldt for the alternative VaG AminCL and the reference simulation 2050 REF AminCL. .... 36

Figure 32 – Asymmetry of the over a transect averaged flow velocity to the power five integrated over a spring/neap tidal cycle for VaG alternative and reference simulation 2050 REF AminCL. .... 36

Figure 33 – Potential sedimentation erosion rates extrapolated from a spring/neap tidal cycle to one year for different polygons along the Upper Sea Scheldt for alternative VaG AminCL and the reference simulation 2050 REF AminCL..... 37

Figure 34 – Net sand transport rates over a spring/neap tidal cycle for different transects along the Upper Sea Scheldt for the alternative VaH AplusCH and the reference simulation 2050 REF AplusCH..... 38

Figure 35 – Asymmetry of the over a transect averaged flow velocity to the power five integrated over a spring/neap tidal cycle for VaH alternative and reference simulation 2050 REF AplusCH. .... 38

Figure 36 – Potential sedimentation erosion rates extrapolated from a spring/neap tidal cycle to one year for different polygons along the Upper Sea Scheldt for alternative VaH AplusCH and the reference simulation 2050 REF AplusCH..... 39

Figure 37 – Net sand transport rates over a spring/neap tidal cycle for different transects along the Upper Sea Scheldt for the alternative Chafing AplusCH and the reference simulation 2050 REF AplusCH. .... 40

Figure 38 – Asymmetry of the over a transect averaged flow velocity to the power five integrated over a spring/neap tidal cycle for Chafing alternative and reference simulation 2050 REF AplusCH. .... 40

Figure 39 – Potential sedimentation erosion rates extrapolated from a spring/neap tidal cycle to one year for different polygons along the Upper Sea Scheldt for alternative Chafing AplusCH and the reference simulation 2050 REF AplusCH..... 41

Figure 40 – Net sand transport rates over a spring/neap tidal cycle for different transects along the Upper Sea Scheldt for the alternatives Chafing, VaG, VaH and the reference simulation 2050 REF AplusCH. .... 42

Figure 41 – Asymmetry of the over a transect averaged flow velocity to the power five integrated over a spring/neap tidal cycle for alternatives Chafing, VaG, VaH and reference simulation 2050 REF AplusCH..... 42

Figure 42 – Potential sedimentation erosion rates extrapolated from a spring/neap tidal cycle to one year for different polygons along the Upper Sea Scheldt for alternatives Chafing, VaG, VaH and the reference simulation 2050 REF AplusCH..... 43

Figure 43 – Potential sedimentation/erosion rates for polygons along the Upper Sea Scheldt. Scenario QN 2013 REF AOCN. .... A2

Figure 44 – Potential Sedimentation/erosion rates for polygons along the Upper Sea Scheldt. Scenario QN 2050 REF AOCN. .... A2

Figure 45 – Potential Sedimentation/erosion rates for polygons along the Upper Sea Scheldt. Scenario QN 2050 REF AplusCH..... A3

Figure 46 – Potential Sedimentation/erosion rates for polygons along the Upper Sea Scheldt. Scenario QN 2050 REF AminCL..... A3

Figure 47 – Potential Sedimentation/erosion rates for polygons along the Upper Sea Scheldt. Scenario QN VaG AplusCH..... A4

Figure 48 – Potential Sedimentation/erosion rates for polygons along the Upper Sea Scheldt. Scenario QN VaH AplusCH..... A4

Figure 49 – Potential Sedimentation/erosion rates for polygons along the Upper Sea Scheldt. Scenario QN Chafing AplusCH. .... A5

Figure 50 – Potential Sedimentation/erosion rates for polygons along the Upper Sea Scheldt. Scenario QN VaG AminCL. .... A5

Figure 51 – Net sand transport over different cross sections along the Scheldt estuary calculated and plotted for a neap and spring tide and a full spring/neap tidal cycle. Scenario 2050 QN REF AOCN..... A8

Figure 52 – Net sand transport over different cross sections of the Upper Sea Scheldt calculated and plotted for a neap and spring tide and a full spring/neap tidal cycle. Scenario 2050 QN REF AOCN. .... A8

Figure 53 – Net sand transport over different cross sections along the Scheldt estuary calculated and plotted for a neap and spring tide and a full spring/neap tidal cycle. Scenario 2050 QN REF AminCL. .... A9

Figure 54 – Net sand transport over different cross sections of the Upper Sea Scheldt calculated and plotted for a neap and spring tide and a full spring/neap tidal cycle. Scenario 2050 QN REF AminCL. .... A9

Figure 55 – Net sand transport over different cross sections along the Scheldt estuary calculated and plotted for a neap and spring tide and a full spring/neap tidal cycle. Scenario 2050 QN REF AplusCH. .... A10

Figure 56 – Net sand transport over different cross sections of the Upper Sea Scheldt calculated and plotted for a neap and spring tide and a full spring/neap tidal cycle. Scenario 2050 QN REF AminCL. .... A10

Figure 57 – Net sand transport over different cross sections along the Scheldt estuary calculated and plotted for a neap and spring tide and a full spring/neap tidal cycle. Scenario VaG AplusCH. .... A11

Figure 58 – Net sand transport over different cross sections of the Upper Sea Scheldt calculated and plotted for a neap and spring tide and a full spring/neap tidal cycle. Scenario VaG AplusCH. .... A11

Figure 59 – Net sand transport over different cross sections along the Scheldt estuary calculated and plotted for a neap and spring tide and a full spring/neap tidal cycle. Scenario VaH AplusCH. .... A12

Figure 60 – Net sand transport over different cross sections of the Upper Sea Scheldt calculated and plotted for a neap and spring tide and a full spring/neap tidal cycle. Scenario VaH AplusCH. .... A12

Figure 61 – Net sand transport over different cross sections along the Scheldt estuary calculated and plotted for a neap and spring tide and a full spring/neap tidal cycle. Scenario Chafing AplusCH..... A13

Figure 62 – Net sand transport over different cross sections of the Upper Sea Scheldt calculated and plotted for a neap and spring tide and a full spring/neap tidal cycle. Scenario Chafing AplusCH..... A13

# 1 Introduction

## 1.1 project Integrated Plan Upper Sea Scheldt

The Sea Scheldt links the Port of Antwerp (2<sup>nd</sup> Port of Europe) with the Hinterland served by the inland navigation network of the Seine-Scheldt connection, a major axis of Trans European Network of canals and navigable waterways. The tides of the Sea Scheldt limit the access of deeper draught vessels to specific tide windows. Moreover infrastructure (bridges) and the sinuous nature limit the access to CEMT<sup>1</sup> class 4 vessels with a maximum of 2 layers of containers. In order to play a role in the Seine-Scheldt network an upgrade for larger vessels is necessary.

The project (Integrated Plan Upper Sea Scheldt) wants to evaluate different bathymetric (of the entire Upper Sea Scheldt) scenarios that resolve major bottle necks (bridges, shoals, narrow curves).

To evaluate the different scenarios for changes in sand transport a sand transport model was made (Smolders et al., 2018) using the module SISPYHE of the TELEMAC modeling software and this was coupled with the existing TELEMAC-3D hydrodynamic model Scaldis that was also created in the framework of this project (Smolders et al., 2016). Effects of different scenarios are quantified by comparing them to a reference case. For the sand transport model, sand transport over different transect along the entire Scheldt estuary will be evaluated.

This report will describe model results for sand transport of different scenarios with bathymetry alternatives for the Upper Sea Scheldt. These alternatives are called “B-alternatives” within this project and consist of:

- Chafing (Schaaf): accessibility for ships of 110 m long and 11.4 m wide but not following standard design rules and using fairway envelopes based on real time shipping simulations instead;
- VaG: Class Va standard design rules applied, mostly in the current channel (“G” for “Geul” or channel) leading to a single lane Va functionality upwards Wichelen (between Ghent and Dendermonde, uppermost part of Upper Sea Scheldt);
- VaH: Class Va standard design rules applied with Hybrid (“H”) properties, specifically the “Chafing” alternative downstream Wichelen, and “VaG” upstream Wichelen.

The comparison of modelled results from different scenarios/alternatives are analyzed with a focus on the Upper Sea Scheldt, where most of these future scenarios/alternatives are located. More information about the alternatives and scenarios, model sequence and an overview of the data flow are given in the memo ‘Afstemming Modelinstrumentarium’ (IMDC, INBO, UA, WL, 2015). In the course of the present study, these “B-alternatives” will be evaluated and further developed to the final alternatives that will be considered in the final Integrated Plan, termed the “C-alternatives”.

---

<sup>1</sup> In 1992 Europe decided to divide the hinterland canals and navigable rivers into classes depending on the size of the ships that can pass. This was agreed in the Conférence Européenne des Ministres de Transport, hence the name CEMT-class.

## 1.2 Evaluation framework

An evaluation framework is applied to assess the environmental impact related to the different project alternatives (environmental impact assessment, EIA). The EIA disciplines Water and Fauna & Flora can be evaluated on the basis of the output of model instruments. The evaluation framework is largely based on the Evaluation Method for the Scheldt Estuary (EMSE) (Holzhauer *et al.*, 2011; Maris *et al.*, 2014) because it is a tailor-made method that has been designed for the evaluation of the state of the estuary (based on monitoring data), starting from the Long Term Vision (Directie Zeeland *et al.*, 2001) and the ecosystem functioning and “seeking as much concertation as possible with the existing legal evaluation frameworks and criteria” (Maris *et al.*, 2014).

Based on the current understanding of the estuarine system (system knowledge), specific parameters are considered as having a main signaling function. According to EMSE, in case it is also possible to interpret and evaluate the evolution of such a parameter, it is presented as an **evaluation parameter**. For such parameters, the evaluation will be made explicit. Other variables will be presented as **explanatory parameters** because the significance of the evolution of the parameter depends on the interpretation at a higher level in the estuarine functioning or ecosystem (e.g. an increasing high water level might be beneficial for navigation windows or under keel clearance. However, it can also be considered negative for safety).

For the Sand transport model only the theme “Sediment and morphology” in the evaluation framework is important. Table 1 gives an overview of the evaluation and explanatory parameters in this theme. The sand model models sand transport on the short term and can't be used to assess morphological evolutions on the long term. Moreover, the sand model models rather transport capacity of sand because of the unlimited supply of sand on the bottom. Therefore the sand transport model can give information on increasing or decreasing erosion or sedimentation capacity in certain areas in the estuary. This is one of the explanatory variables that is desired in the evaluation framework (see Table 1 text in red). This explanatory variable can be translated into the evaluation parameter “maintenance dredging volumes”. If an alternative shows more erosion capacity in a current dredging zone in the estuary, less maintenance dredging volume can be expected for that zone.

Table 1 – The Evaluation parameters in the framework of the “Sediment and morphology” theme. (from IMDC et al., 2018)

Indicator	Evaluation parameter	EIA indicator
Sediment management	Risk for hyperturbidity Maintenance dredging volumes	V V
Geometry and bathymetry	Average depth	V
Explanatory parameters	Long term vertical changes Meandering Sedimentation/erosion (polygons) Bottom shear stress Suspended sediment fluxes Long-term sediment balance	

This report will show results of reference situations in 2013 and 2050 and results of different alternative scenarios. It will show calculated sand transport rates over cross sections of the Scheldt estuary. These transport rates are then used to make mass balances for different areas (shown as polygons) in the Scheldt estuary. A mass balance over a spring/neap tide indicate if these areas accumulate sediments or erode. Knowledge of current dredging efforts in specific areas combined with the erosion/sedimentation polygons can result in an evaluation on the maintenance dredging efforts of these areas.

## 2 Units and reference plane

Time is expressed in CET (Central European Time).

Depth, height and water levels are expressed in meter TAW (Tweede Algemene Waterpassing).

Bathymetry and water levels are positive above the reference plane.

The horizontal coordinate system is RD Paris.

## 3 Summary of Scaldis sand transport model

### 3.1 Scaldis HD 2013

The Scaldis model was developed within the framework of the project 13\_131 Integrated Plan for Upper Sea Scheldt. There was a need for a numerical model with higher mesh resolution in the upstream part of the Scheldt estuary. An unstructured mesh has the advantage to be very flexible in changing mesh resolution in specified areas. Therefore the Scaldis model was developed in the TELEMAC software, which is based on a finite element method.

The computational grid includes the Belgian coastal zone, extended to Dunkirk in France and Westenschouwen in the Netherlands. The grid includes the Eastern Scheldt as well. The mesh resolution varies between 400 and 150 m in this part of the model. In the Western Scheldt and estuary mouth area the grid resolution increases towards 120 to 80 m. The grid includes all tributaries reaching as far as the tidal influence. The grid resolution keeps increasing all the way till the upstream boundary in Merelbeke where it is 5-7 m. All flood control areas of the Sigma Plan are included in the grid. The 2D grid consists of 459,692 nodes. The 3D mesh consists of prisms eventually cut into tetrahedrons and is automatically constructed from the 2D mesh. A sigma transformation is used for the vertical location of these 5 layers. Layer 1 is the bottom layer and the following layers are always situated on 0.12, 0.30, 0.60 and 1.00 fraction of the water depth.

The bathymetry is interpolated from measured data from 2013 or the closest date available. For more detailed information we refer to the calibration report of the Scaldis model from Smolders et al. (2016).

There are 9 liquid boundaries in the Scaldis model. The downstream boundary is located in the North Sea. A water level is imposed on this boundary. This boundary contains 469 nodes. On every node a water level time series with 10 minute interval is imposed. These time series are extracted from the regional ZUNO model of the southern North Sea. A correction of the harmonic components was calculated based on the comparison of the harmonic components of the ZUNO results and measurements over a period of 1 year (Maximova et al., 2015). Differences in harmonic components (ZUNO vs. measurements) are found for stations in the Belgian and Dutch Coastal zone for the  $M_2$ ,  $M_4$ ,  $S_2$  phases and the  $Z_0$  component. After extraction of time series from the ZUNO model the time series of the boundary conditions of the Scaldis model are “harmonically corrected” with the obtained correction terms (+4° for  $M_2$ , -6° for  $M_4$ , +7° for  $S_2$  phase and -21 cm for  $Z_0$ ). This means that the time series are decomposed in harmonic components and a residual term. The harmonic components are corrected, and the signal is resynthesized. The subroutine BORD3D.f was changed to read and impose the appropriate time series for each boundary node.

There are 8 upstream liquid boundaries with prescribed discharges. Measured daily average discharges are available as upstream boundary conditions for Merelbeke (Melle), Dender, Zenne, Dijle, Kleine Nete, Grote Nete, and channel Ghent – Terneuzen. The values for the channel Ghent-Terneuzen were taken downstream the weir of Evergem. This location was used as a proxy. For the channel of Bath hourly discharge measurements were available. In this time series the small negative values were set to zero for stability reasons. All the other daily averaged discharge values for the other upstream discharge boundaries were then hourly interpolated. So all discharge boundaries have hourly discharge values. For each simulation these time series per upstream boundary are given in a liquid boundary file.

Wind influence is not included in the hydrodynamic model. It is assumed to be incorporated in the boundary conditions downstream.

Salinity is applied as an active tracer. This means that density effects are taken into account in the model. time series with 10 minute interval are imposed on the downstream boundary. The salinity values are generated from the CSM-ZUNO model train. Salinity boundary values in the Scaldis model were corrected based on the comparison of the simulated and measured salinity time series at Vlake van de Raan (located

in the larger mouth area of the Scheldt Estuary). The ZUNO model underestimates the salinity values in the area of interest and a salinity correction at the boundaries was necessary. The correction is specific for a specific time period. The difference between the daily averaged measured and modelled values was used for correction of the salinity time series for the downstream boundary condition. No tracer (Salinity) values are set for the upstream boundary conditions. No salinity is entering the domain through these boundaries in the Scaldis 3D HD model. The model starts from an initial salinity field: a map is made based on a combination of salinity measurements (Western Scheldt) and corrected model results from ZUNO (coastal area). This initial salinity map is read at the start of a simulation by a modified subroutine FONSTR.f. The values of the 2D map are copied to the other four layers in the model.

The model runs with a time step of 4 seconds. A cold start is done with a constant water level throughout the entire model domain and the boundary imposed water levels and discharges are smoothed for the first tidal cycle. Manning's equations is used for the bottom roughness and these values vary along the estuary and were used to calibrate the hydrodynamic model. Negative depths are clipped to zero with flux control to keep the model stable. The RANS equations are solved also on the tidal flats with corrections. As a vertical turbulence model the mixing length model of Nezu and Nakagawa was used. The horizontal turbulence model is a Smagorinski model. Coriolis is activated with a coefficient value of 1.13522E-04.

## 3.2 Sand transport model in SISYPHE

### 3.2.1 model parameters

The sediment module SISYPHE is coupled with the 3D hydrodynamic module TELEMAC-3D. No parameter changes were done in the hydrodynamic model Scaldis, described in Smolders et al. (2016).

In SISYPHE, the module is coupled with the hydrodynamics every time step. Engelund and Hansen (1967) was chosen as the transport equation. The formula is used in the sediment grain size range of  $D_{50} = [0.2 - 1]$  mm. This formula is derived for river flow (Engelund and Hansen, 1967). The formula given by Engelund and Hansen estimates the total transport,  $\vec{Q}_0$ , in the direction of the flow velocity,  $\vec{v}$ :

$$|\vec{Q}_0| = \frac{0.05\alpha|v|^5}{\sqrt{g}s^2C^3d_{50}} \quad 3.1$$

where  $\alpha$  is a calibration coefficient (order 1);  $|v| = \sqrt{u^2 + v^2}$  is the magnitude of the flow velocity [m/s];  $s = (\rho_s - \rho)/\rho$  is the relative density with  $\rho_s$  and  $\rho$  the sediment and water density, respectively [-];  $C$  is the Chézy friction coefficient [ $m^{1/2}/s$ ]; and  $d_{50}$  is the median grain size [m]. Furthermore, to account for the bed slope effects, the correction method of Flokstra and Koch (1981) is available in Sisyphé (keyword: FORMULA FOR DEVIATION = 1) and multiplies the above equation by a factor:

$$|\vec{Q}| = |\vec{Q}_0| \left(1 - \beta \frac{\partial z_b}{\partial s}\right) \quad 3.2$$

where  $\beta$  is a bed slope coefficient (keyword: BETA = 1.3);  $s$  is the coordinate in the flow direction and  $z_b$  is the bed level.

This formula is implemented in Sisyphé in the subroutine bedload\_engel.f. The formula is implemented as follows:

$$\Phi_b = C_{engel} \sqrt{(C_1 * TOB)^5 / \max(CF, 1.E - 6)} \quad 3.3$$

whit

$$C_{engel} = 0.1 \sqrt{s * g * d^3} \quad 3.4$$

and

$$C_1 = \frac{1}{(s * \rho * g * d)} \quad 3.5$$

and

$$CF = \frac{2n^2g}{h^{1/3}} \quad 3.6$$

and

$$TOB = 0.5 * \rho * CF * |v|^2 \quad 3.7$$

where  $\Phi_b$  is the dimensionless current induced sediment transport rate; TOB is the bed shear stress [Pa]; CF is the quadratic friction coefficient;  $s = (\rho_s - \rho) / \rho$  is the relative density [-]; g is the gravitational acceleration constant [m/s<sup>2</sup>]; d is the sediment grain size [m];  $|v| = \sqrt{u^2 + v^2}$  is the magnitude of the flow velocity [m/s]; n is the Manning friction coefficient [m<sup>1/3</sup>/s]; h is the water depth [m]; and  $\rho$  is the water density [kg/m<sup>3</sup>]. CF can have a different formula depending on the type of friction coefficient that was chosen in the model. For Scaldis a Manning bottom friction coefficient was chosen and the corresponding formula for CF is given here (equation 3.6).

Suspended load transport is not activated in SISYPHE because the Engelund and Hansen transport equation is a total load equation. The morphological factor is set to 1. The sediment grain size is equal to 150  $\mu$ m. Only a single sediment fraction is taken into account over the entire model domain. There is an unlimited amount of sediment available in the model (= 100 m of sediment layer thickness).

The simulation will run for 15 days (a full spring-neap tidal cycle) and graphical output is written to a results file every half hour. the time step is four seconds.

Slope effects are taken into account by default. Secondary currents is not active when coupled with a 3D hydrodynamic model. The 3D flow patterns are given to the SISYPHE module in a depth averaged way. SISYPHE is a 2D module.

### 3.2.2 Boundary conditions

No sediment will enter the model domain through the boundaries because only 15 days are simulated. Sediment can leave the domain freely. To prevent the model from resulting into unwanted erosion at the inflow boundaries, a fixed bed elevation (zero evolution) was defined in the boundary conditions file (.cli). This can be achieved by assigning LIEBOR=5 for the inflow nodes (8th column in .cli file).

### 3.2.3 Initial conditions

The hydrodynamic model has two days to spin up. After these two days the model is started again from the last time step of the spin up simulation and the sediment module SISYPHE is coupled. A uniform sediment layer is available throughout the entire model domain. By default the initial sediment layer thickness is 100 m.

### 3.2.4 Bottom friction coefficient

In the hydrodynamic model a Manning bottom friction coefficient was spatially varied to calibrate the water levels and flow velocities in the model. By default the sediment module uses the bottom friction coefficient of the hydrodynamic module to calculate the bed shear stresses to estimate sediment motion. But during calibration of the hydrodynamic model the variation in bottom friction coefficient is used to compensate also for non-physical properties of the model, like numerical diffusion. Taking these values of the bottom friction coefficient would not be correct for sediment transport. Therefore a fixed value for the Manning bottom friction coefficient was used for the entire model domain for the sediment transport. In the subroutine `coefro_sisyphe.f` a fixed value for the bottom friction coefficient was introduced. The Manning coefficient was set to 0.02 m/s<sup>1/3</sup>. In the subroutine `tob_sisyphe.f` changes were made to make sure the fixed bottom friction coefficient was used in the calculations of the bed shear stress.

The difference in sand transport between using a fixed Manning value for the entire model domain or using the Manning coefficient spatially varying from the hydrodynamic model is part of the sensitivity analysis that follows.

### 3.2.5 Bottom update in hydrodynamic model switched off

The sediment module calculates a certain sand transport and the related bottom changes. By default these bottom changes are updated in the bottom file of the hydrodynamic model every time step. But the focus of the sand transport model is on sand transport and not on morphology. Therefore the update of the bottom in the hydrodynamic model is switched off in the code. The mass balance and bottom changes are still recorded in the sediment module and are given as output, but the sand transport is always calculated based on the hydrodynamics with a fixed initial bathymetry.

## 4 Alternatives and Scenarios

The calibrated sand transport model is used to evaluate the effects of different alternatives (specified morphology of the Scheldt estuary in a specific state and at a specific time), under different scenarios (a range of boundary conditions to take into account climate change, sea level rise, increasing or decreasing tidal amplitude, high or low river discharge). This chapter will give an overview of all scenarios that will be analyzed with the sand transport model.

### 4.1 Alternatives

This section describes the different specified morphologies of the Scheldt estuary in a specific state and at a specific time, also called different alternatives to improve the navigability in the Upper Sea Scheldt. These alternatives are situated in the future in the year 2050. Therefore the bathymetry of the current hydrodynamic model Scaldis 2013 needs to be updated to a future state. This 2050 state will serve as a reference to compare the different alternatives with. The different changes in bathymetry to go from the 2013 reference bathymetry to the 2050 reference bathymetry are listed first. Then the different changes in bathymetry off the different alternatives are described.

#### 4.1.1 Bathymetry Updates from Scaldis 2013 to Scaldis 2050

An overview of all bathymetry updates that were implemented in the Scaldis 2013 model to make the 2050 model are presented in the next subsections. This information is already described in full length in the report of Scaldis 2050 (Smolders et al., 2017) and is repeated here briefly. Five major differences can be listed and shown in the bathymetry (an overview is given in Figure 1):

1. **Sustainable bathymetry** – a sustainable bathymetry for the Upper Sea Scheldt was developed to maintain the fairway with respect for the tidal nature. The designed bathymetry takes into account the needs for navigation and the characteristics of the river. The impact on the tidal nature is limited to specific areas. The hydrodynamic and morphological processes can develop to the extent that the safety and tidal nature are not endangered. The Management Plan aims to optimize the existing management efforts for navigation and protection of the riverbanks (IMDC, 2015). The changes in bathymetry are limited to the deeper parts of the main channel. The largest changes are located near Uitbergen (location see Figure 9) and are shown in Figure 2.
2. **Tidal tributary Durme** – The tributary Durme had no upstream discharge in 2013 and acted as a large sediment trap. This tributary will be dredged and maintained again in the future (when writing this report these changes have been executed). The new dredged bathymetry will be taken into account in the Scaldis 2050 model. The location of the Durme within the estuary can be seen in the overview in Figure 1. A detail of the bathymetry changes is given in Figure 3.
3. **New sluice at Heusden** - Just north of the de-embankment of Heusden (location see overview in Figure 1), a new sluice will prevent the full tide from penetrating further upstream. This sluice will get bypass culverts to allow part of the tide to pass and to encourage the development of fresh water tidal nature upstream in this tidal arm. In Figure 4 the difference in bathymetry with the 2013 bathymetry is given and the location of the new sluice is shown.
4. **groynes at Fort Filip** – At this inner bend at Fort Filip in the Lower Sea Scheldt (location in overview Figure 1) two groynes will slow down the estuarine flow creating a low dynamic area. These groynes and the expected elevation of the bottom around them is implemented in the 2050 bathymetry.
5. **Full Sigma plan active** – In 2050 all Sigma areas to ensure safety against flooding will be active. These areas were already foreseen in the 2013 model but were given an high elevation so that they would not interfere with the flow. In the 2050 bathymetry these areas were given proper

topographies and the appropriate culverts were assigned to them to ensure water exchange between the areas and the Scheldt estuary. A full and detailed list of all areas is given in Smolders et al. (2017). Most of these activated areas are shown in blue in Figure 1. Areas that were already active were adapted to future expected topography.

Figure 1 – Changes in bathymetry going from 2013 to 2050.

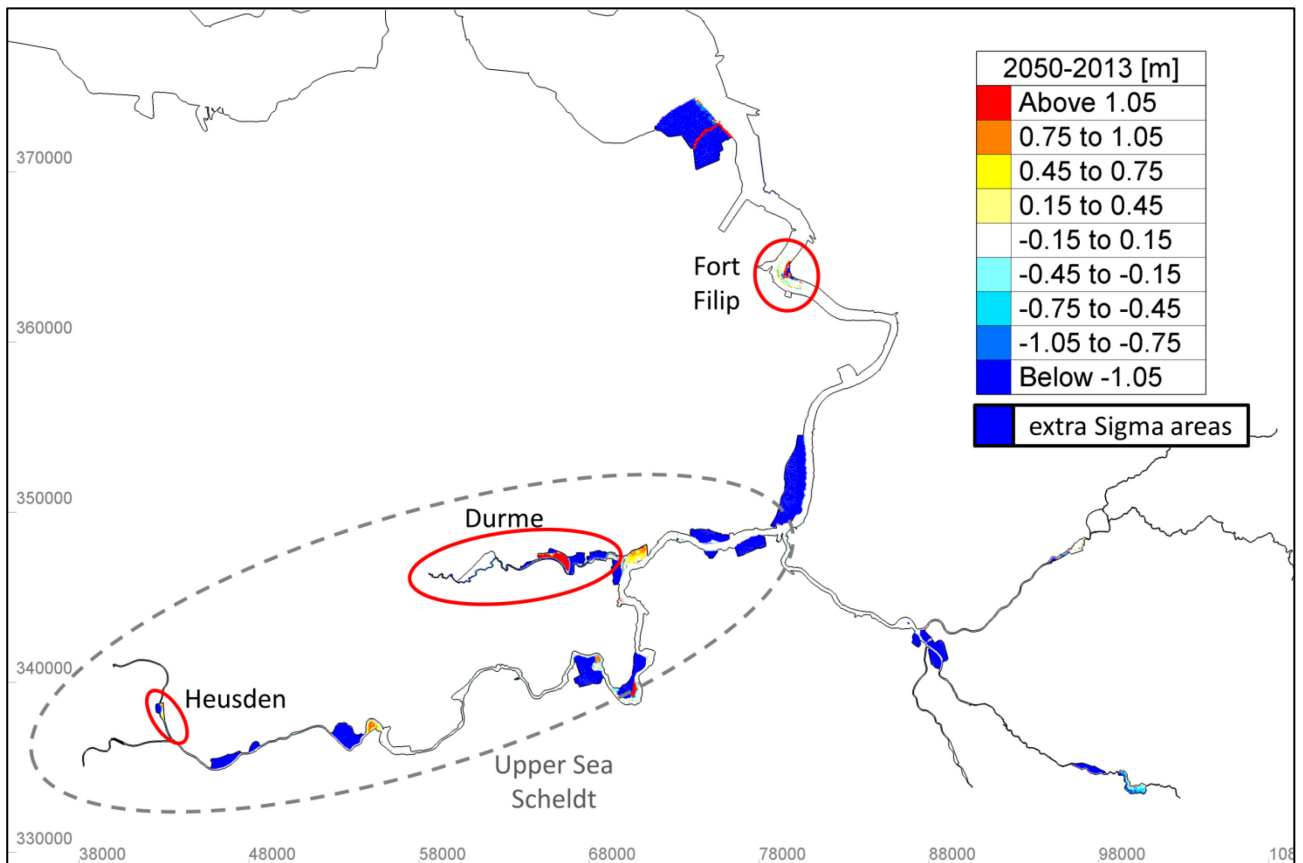


Figure 2 – Biggest changes in bathymetry in the sustainable bathymetry (circled in red) for the Upper Sea Scheldt compared to the 2013 situation.

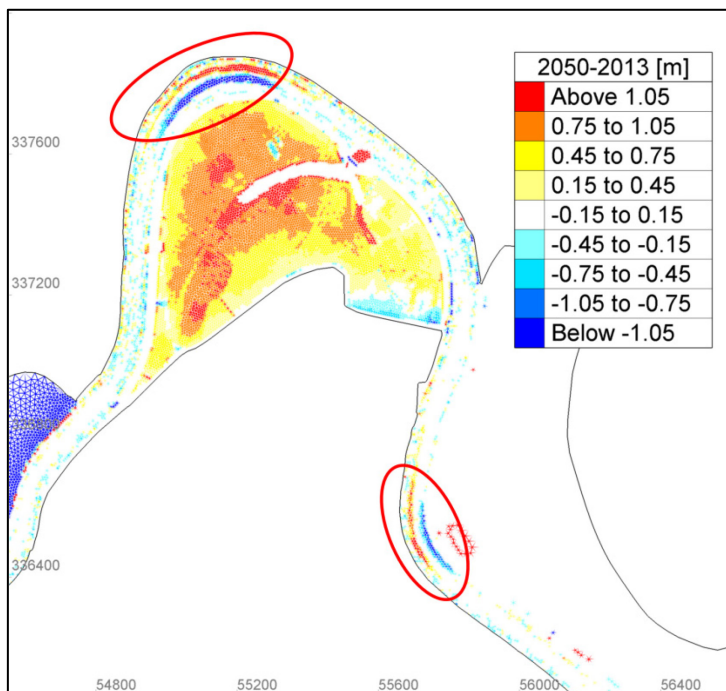


Figure 3 – Future bathymetry of the tidal tributary Durme

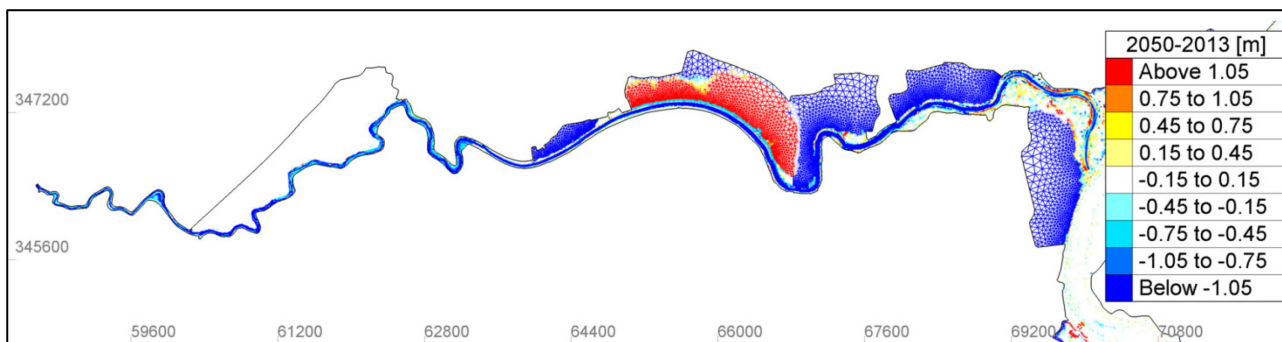
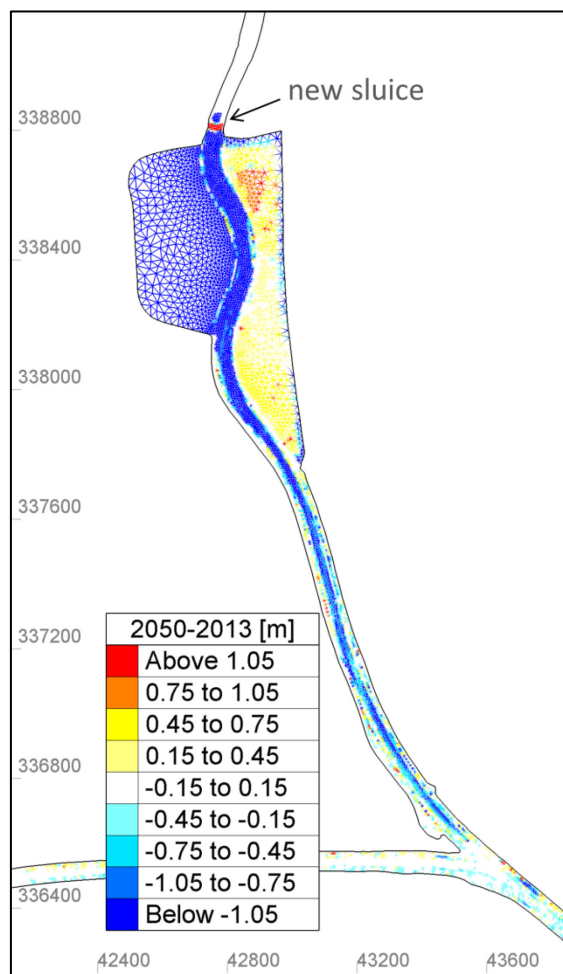


Figure 4 – Future development of the Heusden are with a new sluice.



#### 4.1.2 The B alternatives: Chafing

Chafing (Schaaf): accessibility for ships of 110 m long and 11.4 m wide but not following standard design rules but using fairway envelopes based on real time shipping simulations. This means that some bends are chafed a little bit to make them easier to pass by the ships (Figure 5 and Figure 6).

Figure 5 – Difference in bathymetry (Chafing – Reference 2050) part 1 of 2

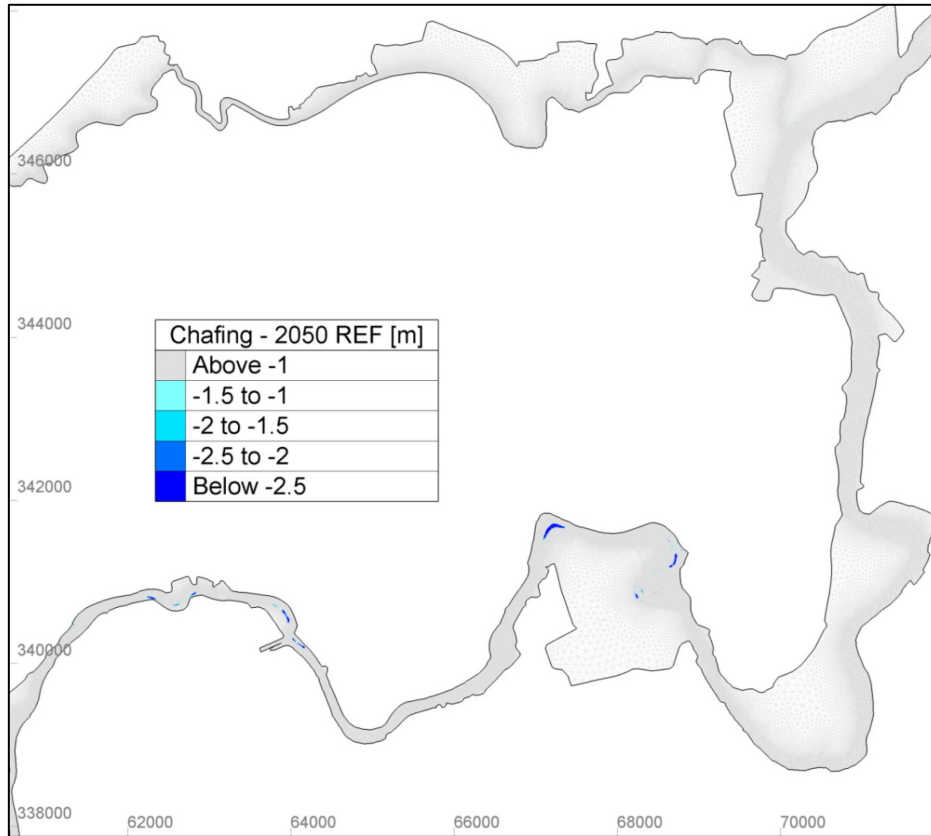
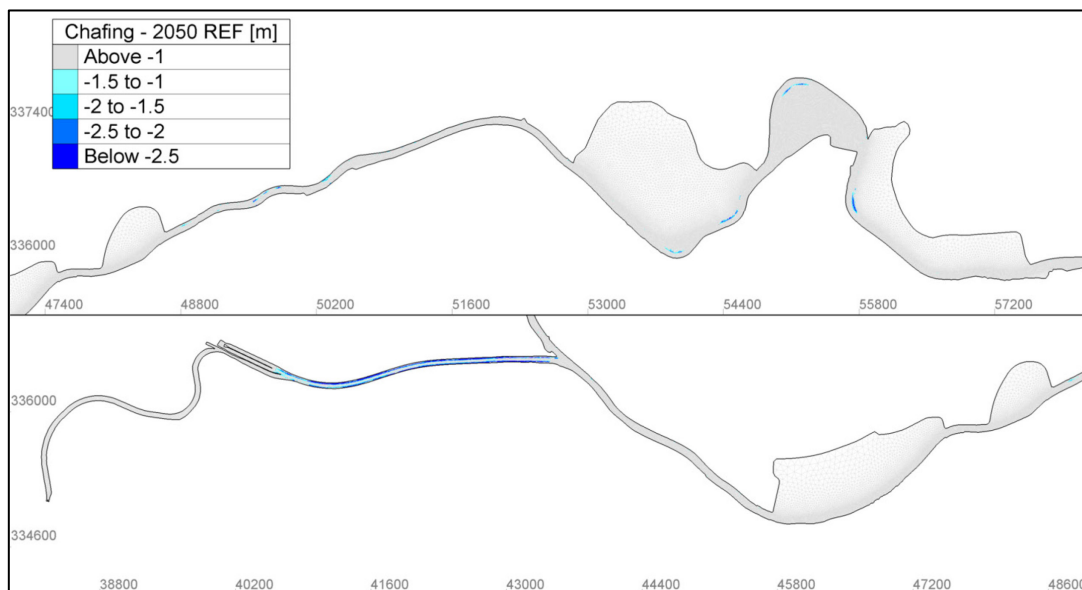


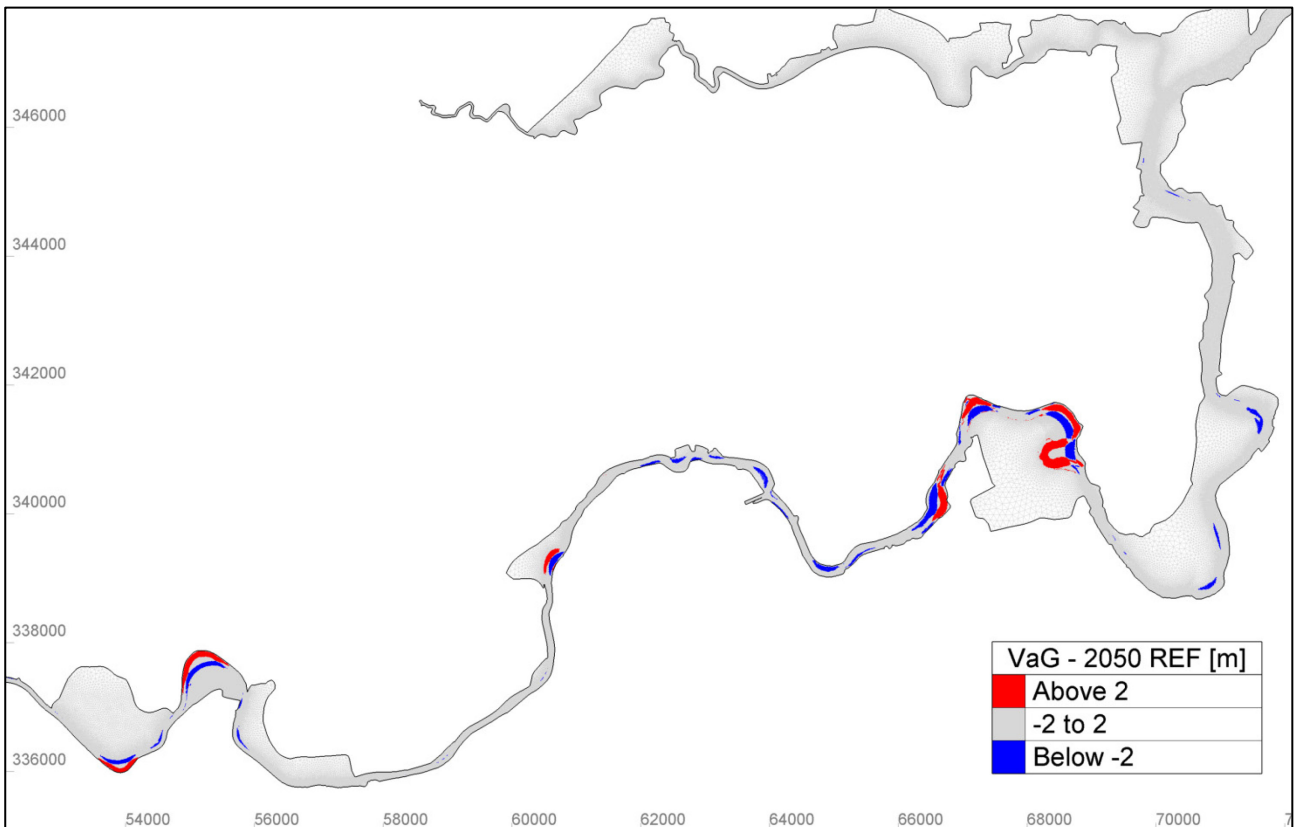
Figure 6 – Difference in bathymetry (Chafing – Reference 2050) part 2 of 2



### 4.1.3 The B alternatives: VaG

VaG: Class Va standard design rules applied, mostly in the current channel (“G” for “Geul” or channel) leading to a single lane Va functionality upwards Mariekerke (uppermost part of Upper Sea Scheldt). This is the alternative with the biggest changes to the reference bathymetry. The difference in bathymetry between the VaG alternative and the 2050 reference bathymetry is shown in Figure 7.

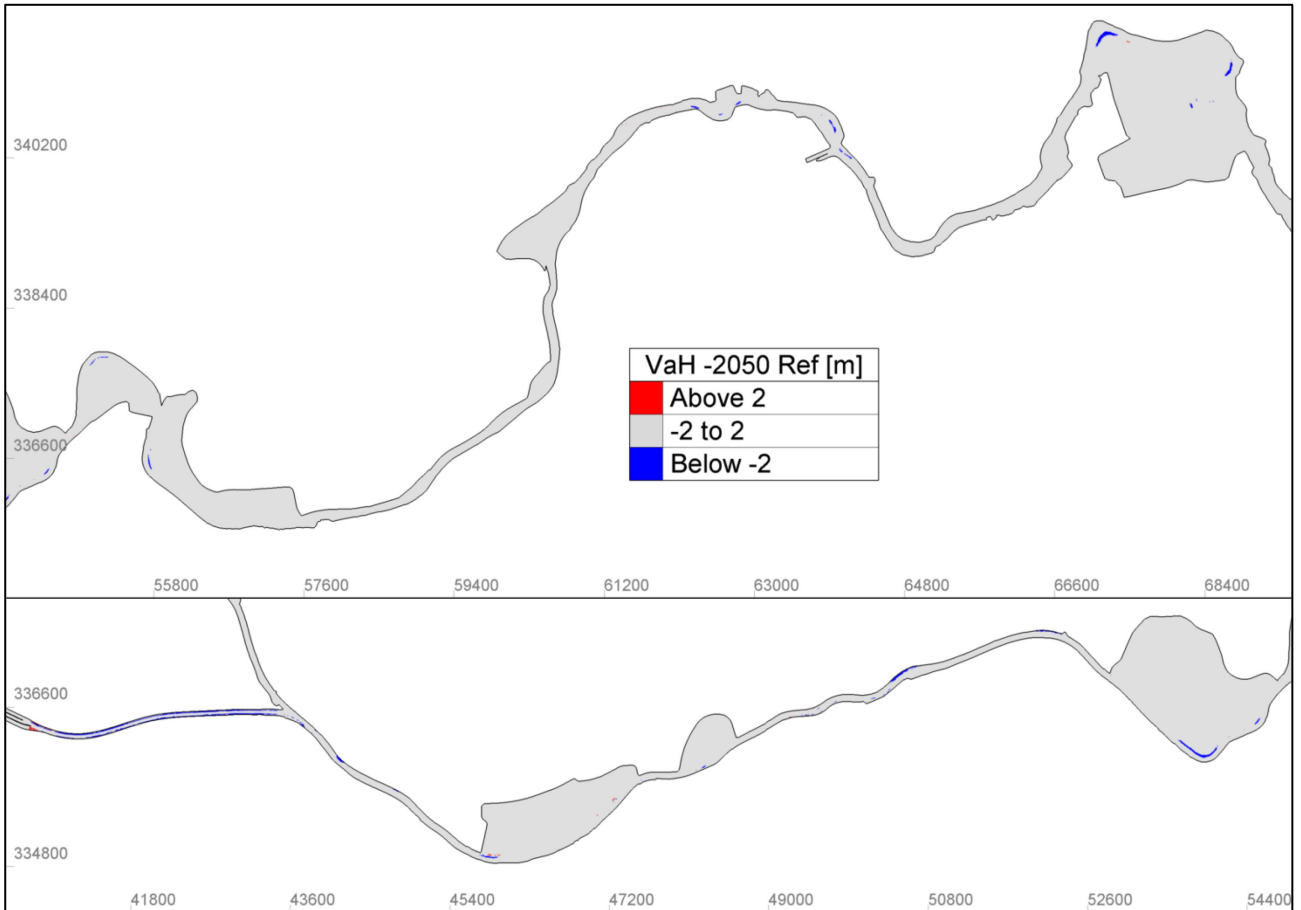
Figure 7 – Difference in bathymetry (VaG – Reference 2050)



4.1.4 The B alternatives: VaH

VaH: Class Va standard design rules applied with Hybrid (“H”) properties, specifically the “Chafing” alternative downstream Wichelen (Wichelen is located just upstream of Schoonaarde, see Figure 9), and “VaG” upstream Wichelen (Figure 8).

Figure 8 – Difference in bathymetry (VaH – Reference 2050)



## 4.2 Scenarios

### 4.2.1 Normal and events discharge scenarios

**QN** is a normal discharge scenario. The downstream boundary is a harmonic boundary without a storm surge. The upstream boundary is a synthetic discharge boundary containing events with a return period equal to or smaller than 1/6 year (combined with QE (T1 & T1/2) this results in 6 exceedances of this discharge). The simulation period is 40 days.

**QE** is an events discharge scenario. The downstream boundary is a harmonic signal plus a storm surge signal. The upstream boundary is a discharge time series that contain 2 discharge events with return periods of 1 year and 1/2 year. The simulation period is 40 days.

### 4.2.2 Tidal range scenarios

The 3D hydrodynamic Scaldis model is used to evaluate the effect of increased and reduced tidal amplitude near Schelle and further upstream in the Upper Sea Scheldt. The increase and decrease of the amplitude is enforced by changing the roughness in the Western Scheldt. By changing the roughness, the tidal propagation will be influenced, without simulating specific measures in the downstream parts of the estuary (e.g. creating additional flooding areas, deepening, etc.) (IMDC/INBO/UA/WL, 2015).

Tidal range scenarios **A+**, **A0** and **A-** have been modeled. In these three scenarios, the tidal amplitude at Schelle is equal to 5.70, 5.40 and 5.00 m, respectively (Table 2).

Table 2 – Tidal range scenarios

Scenario	Bottom friction	Tidal amplitude at Schelle (m)
<b>A+</b>	<i>The bottom friction for hydrodynamics in the Western Scheldt is lowered.</i>	5.70
<b>A0</b>	<i>The bottom friction for hydrodynamics in the Western Scheldt remains as in HD model.</i>	5.40 (current tidal range)
<b>A-</b>	<i>The bottom friction for hydrodynamics in the Western Scheldt is increased.</i>	5.00

### 4.2.3 Sea level rise scenarios

The following sea level rise scenarios are modeled for 2050:

- The “low” scenario (**CL**, +15 cm in 2050);
- The “high” scenario (**CH**, +40 cm in 2050).

The downstream boundary conditions for year 2050 are increased with these values.

The tidal range scenario **A+** is combined with the sea level rise **CH**. The tidal range scenario **A-** is combined with the sea level rise **CL**. More information about the scenarios is given in IMDC/INBO/UA/WL (2015).

### 4.3 Simulation period

All the runs listed in Table 4 have a simulation period of 15 days and a spin up period of 4 days. The details are shown in Table 3.

Table 3 – List of the simulation periods

Code	Start date	End of spin up	End date
<b>QN_2013_REF_A0CN (CAL_007)</b>	<i>2013/07/29 22:20:00</i>	<i>2013/08/02 22:20:00</i>	<i>2013/08/17 22:20:00</i>
<b>QN_2050_REF_A0CN</b>	<i>2013/07/29 22:20:00</i>	<i>2013/08/02 22:20:00</i>	<i>2013/08/17 22:20:00</i>
<b>QN_2050_REF_AminCL</b>	<i>2050/08/09 22:00:00</i>	<i>2050/08/13 22:00:00</i>	<i>2050/08/28 22:00:00</i>
<b>QN_2050_REF_AplusCH</b>	<i>2050/08/09 22:00:00</i>	<i>2050/08/13 22:00:00</i>	<i>2050/08/28 22:00:00</i>
<b>QN_Chafing_AplusCH</b>	<i>2050/08/09 22:00:00</i>	<i>2050/08/13 22:00:00</i>	<i>2050/08/28 22:00:00</i>
<b>QN_VaG_AplusCH</b>	<i>2050/08/09 22:00:00</i>	<i>2050/08/13 22:00:00</i>	<i>2050/08/28 22:00:00</i>
<b>QN_VaG_AminCL</b>	<i>2050/08/09 22:00:00</i>	<i>2050/08/13 22:00:00</i>	<i>2050/08/28 22:00:00</i>
<b>QN_VaH_AplusCH</b>	<i>2050/08/09 22:00:00</i>	<i>2050/08/13 22:00:00</i>	<i>2050/08/28 22:00:00</i>

## 4.4 Overview of Model Runs

The overview table of model runs is listed in Table 4.

Table 4 – List of the different scenarios/alternatives runs

Code	Year	Bathymetry (alternatives)	Discharge Type	Amplitude correction	Climate Scenario	Duration of run [days]
QN_2013_REF_A0CN	2013	Reference	QN	A0	CN	15
QN_2050_REF_A0CN	2050	Reference	QN	A0	CN	15
QN_2050_REF_AminCL	2050	Reference	QN	A-	CL	15
QN_2050_REF_AplusCH	2050	Reference	QN	A+	CH	15
QN_Chafing_AplusCH	2050	Chafing	QN	A+	CH	15
QN_VaG_AplusCH	2050	VaG	QN	A+	CH	15
QN_VaG_AminCL	2050	VaG	QN	A-	CL	15
QN_VaH_AplusCH	2050	VaH	QN	A+	CH	15

**QN:** normal discharge scenario.

**QE:** events discharge scenario.

**(A0, A+, A-):** Different tidal range scenarios.

**(CL, CH):** Sea level rise scenarios.

## 5 Methodology of scenario analysis

The first step consists of going from the 2013 model to the 2050 model. Both models act as a reference for their specific time period. Sand transport will be calculated over transects and mass balances between transects will be made. The results of different scenarios will be compared with the reference simulation. Differences in sand transport are tried to be explained by looking at flow velocity differences. In the case of the 2013 and 2050 model, the 2013 model will be the reference to see how much sand transport changes when using the 2050 model. When comparing different alternatives, the 2050 model will act as a reference.

### 5.1 Calculating sand transport

For every time step of the model output (= every 30 minutes) the sand transport over different transects along the Scheldt estuary is calculated. When these transports are summarized over a specific time, e.g. a full spring/neap tidal cycle, a net sand transport over this period is the result. Plots will be made with on the x-axis the distance of the transect from the estuary mouth (Vlissingen) and on the y-axis the net sand transport for the specific transect. An overview map of the estuary is given in Figure 9 with the most common locations and their distance along the navigation channel to the mouth of the estuary (Vlissingen).

The lines that separate the boxes from the UA ecosystem model (Van Engeland et al., 2018) were chosen as transects. These transects are used and mentioned in different reports within this project. The polygons representing the UA boxes are shown in Figure 10, Figure 11, Figure 12, and Figure 13. the transect downstream in the polygon or box gets the same number as the polygon.

When for the B alternatives the planform of the estuary changes too much so that the polygons don't fit around the navigation channel anymore, small changes were made to the transects to let them fit again. For the VaG alternative the planform changes too much in two locations: around km 130-131 (Figure 14) and around km 152 (Figure 15). For the VaH an Chafing alternative the planform changed too much around km 130-131 (Figure 16). Polygons and transects were changed only for these locations.

Every transect line is cut in matlab to fit exactly within the model boundaries. The line is then resampled with a 5 m interval. For every time step at these 5 m interval nodes on the transect a value for sand transport is interpolated from the model results. To get the total transport over the entire transect for a specific time step the sand transport values were integrated over the transect line.

Net transport magnitude and direction over a full spring/neap tidal cycle is calculated by integrating the cross sectional transport over this time period. The same was done for a spring/neap tide. The results are plotted in function of their distance from the Estuary mouth at Vlissingen (Figure 9). A negative transport means the transport is directed upstream or is flood dominated. A positive transport means its direction is downstream or is ebb dominated.

Figure 9 – Map of the Scheldt estuary with main tributaries and most important locations

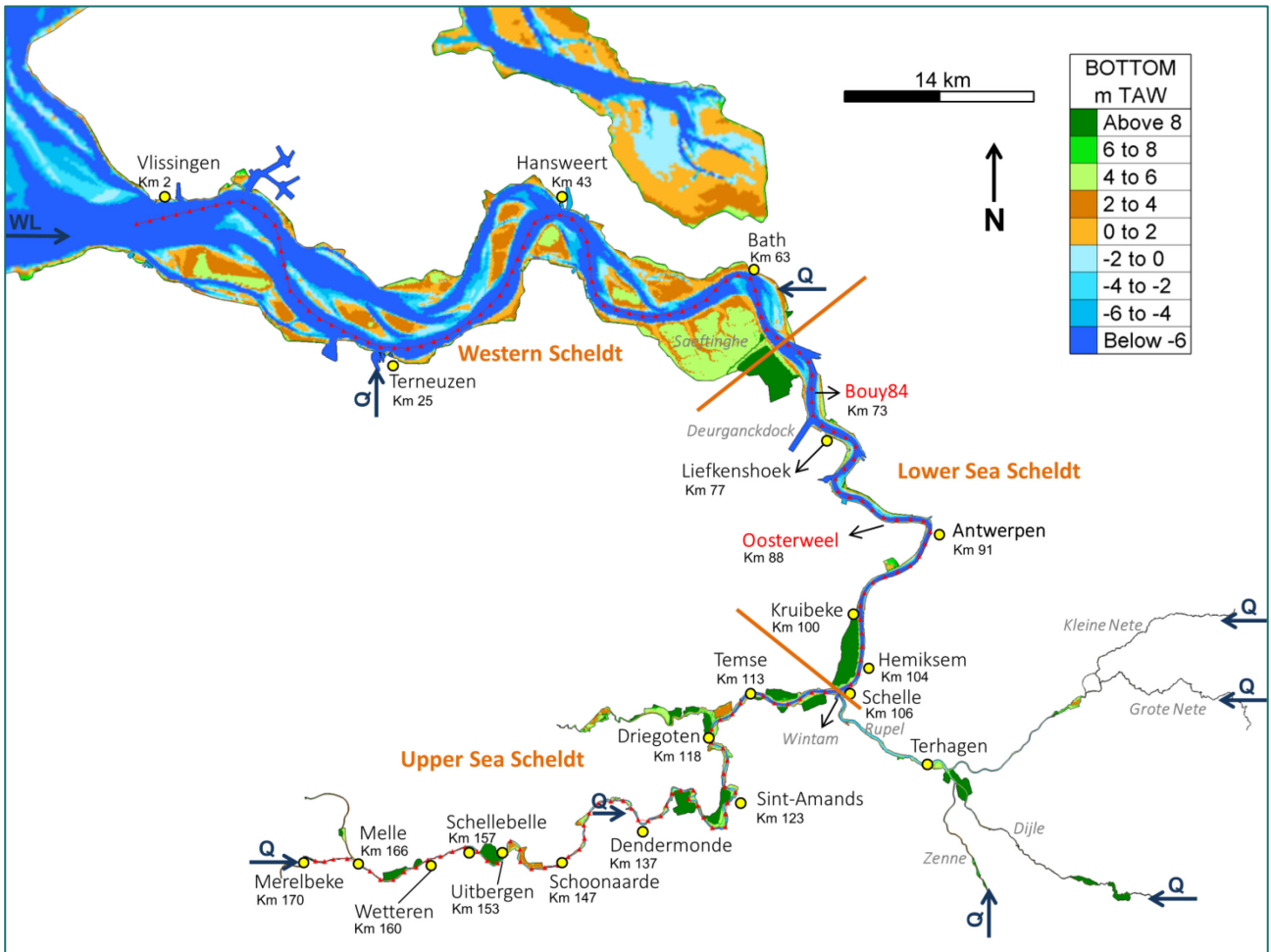


Figure 10 – boxes of the ecosystem model used in the calculation of the sand transport (Western Scheldt)

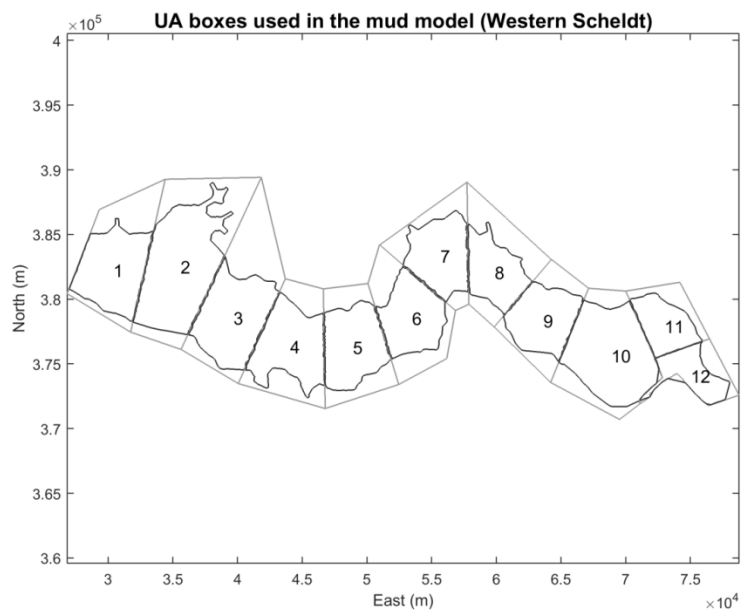


Figure 11 – boxes of the ecosystem model used in the calculation of the sand transport (Lower Sea Scheldt)

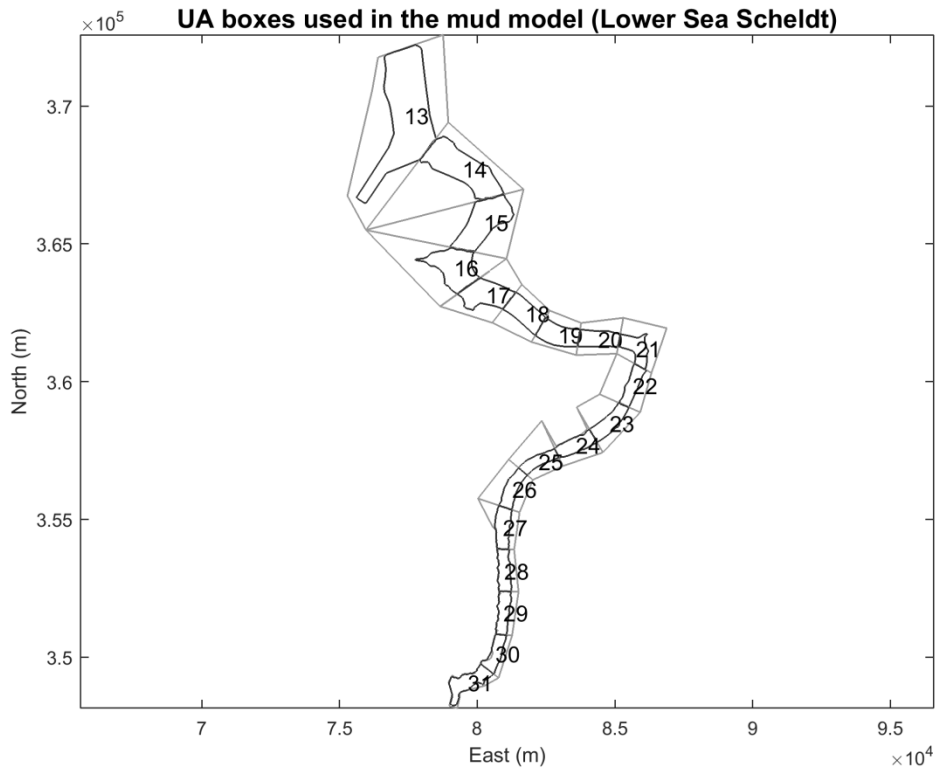


Figure 12 – boxes of the ecosystem model used in the calculation of the sand transport (Upper Sea Scheldt Part 1)

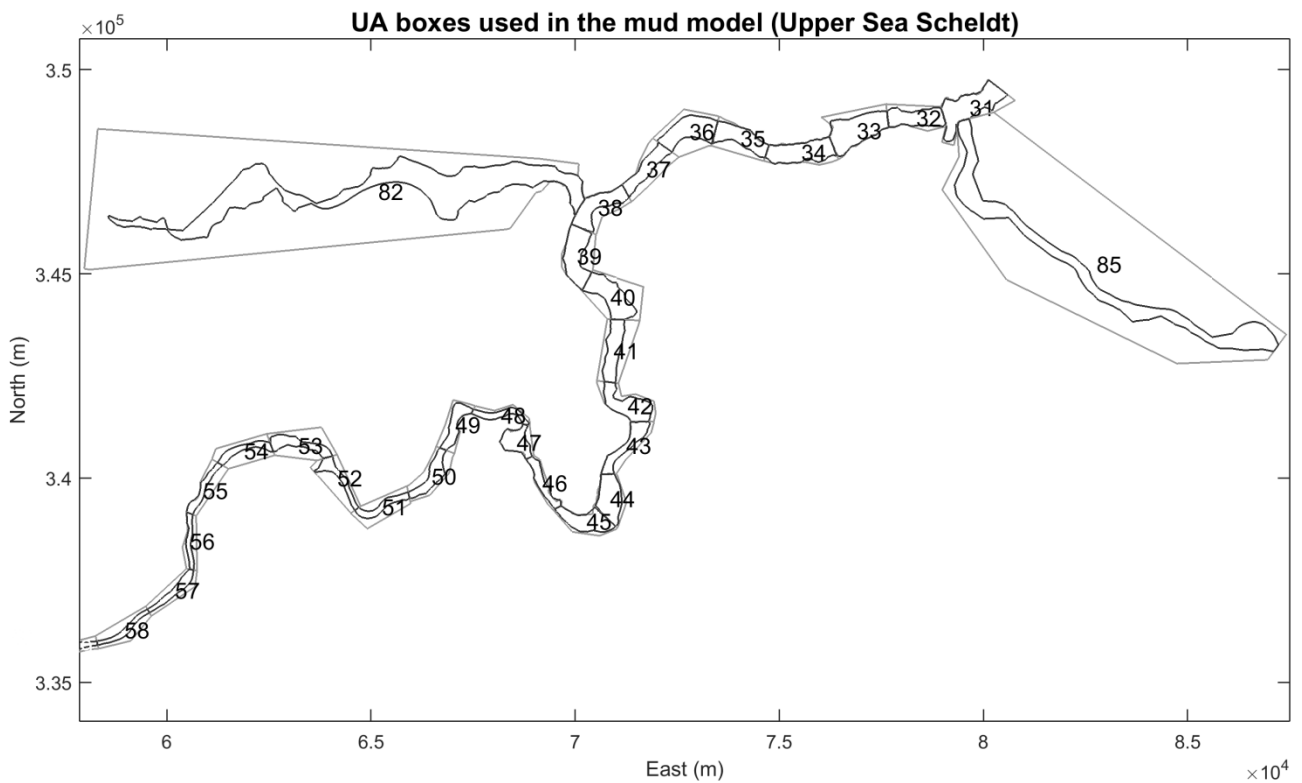


Figure 13 – boxes of the ecosystem model used in the calculation of the sand transport (Upper Sea Scheldt Part 2)

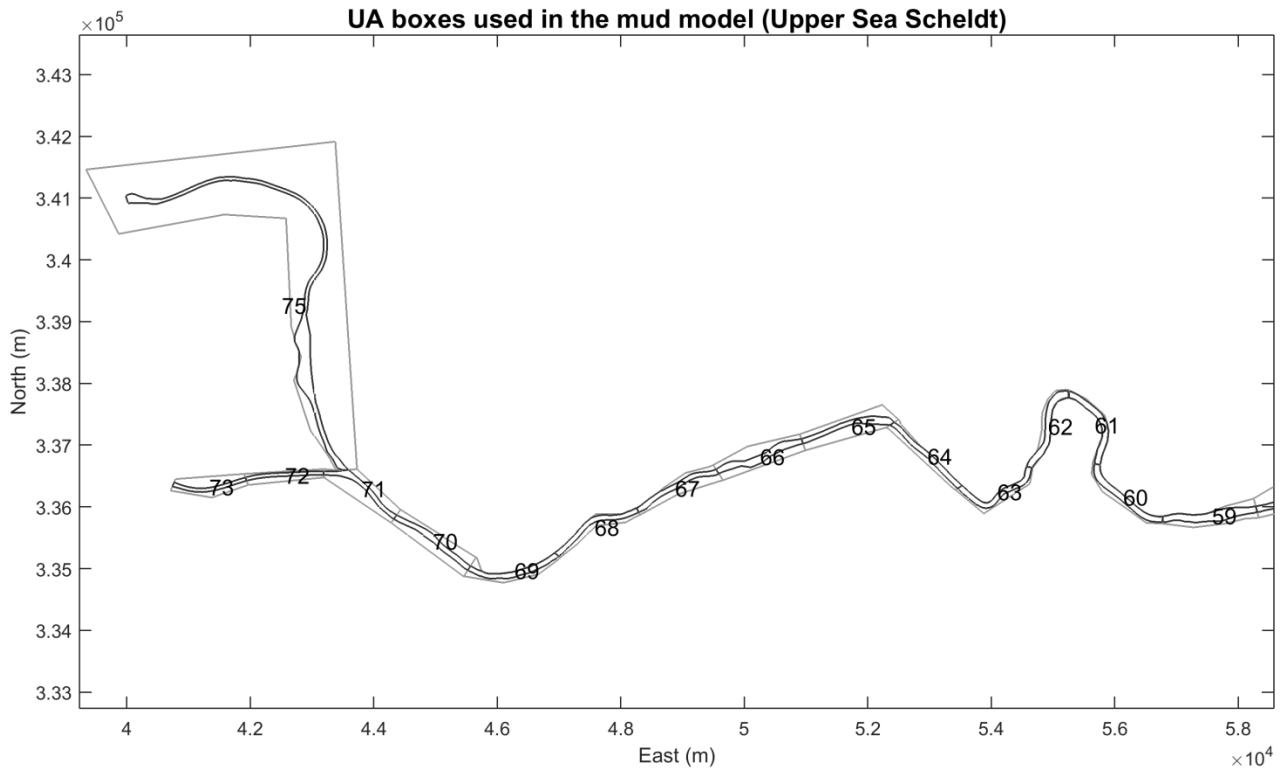


Figure 14 – Difference in transects (transect 48) between the 2050 REF and VaG alternative for location around km 130-131 (Uitbergen)

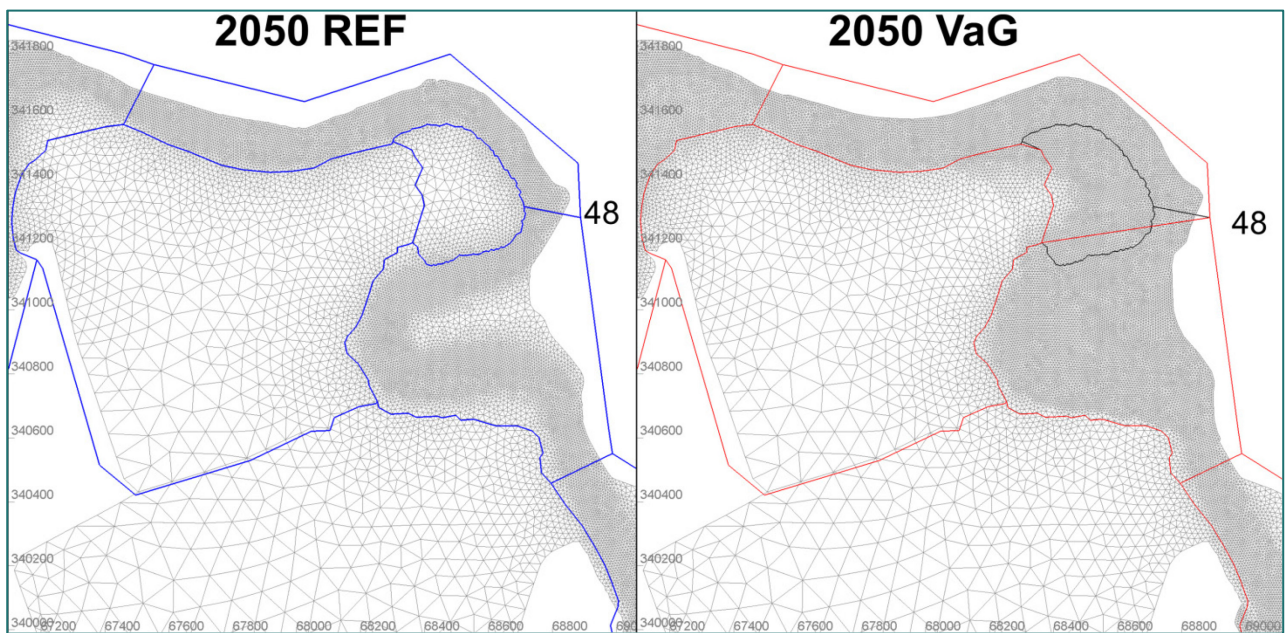


Figure 15 – Difference in transects (transect 62) between the 2050 REF and VaG alternative for location around km 152 (Bergenmeersen)

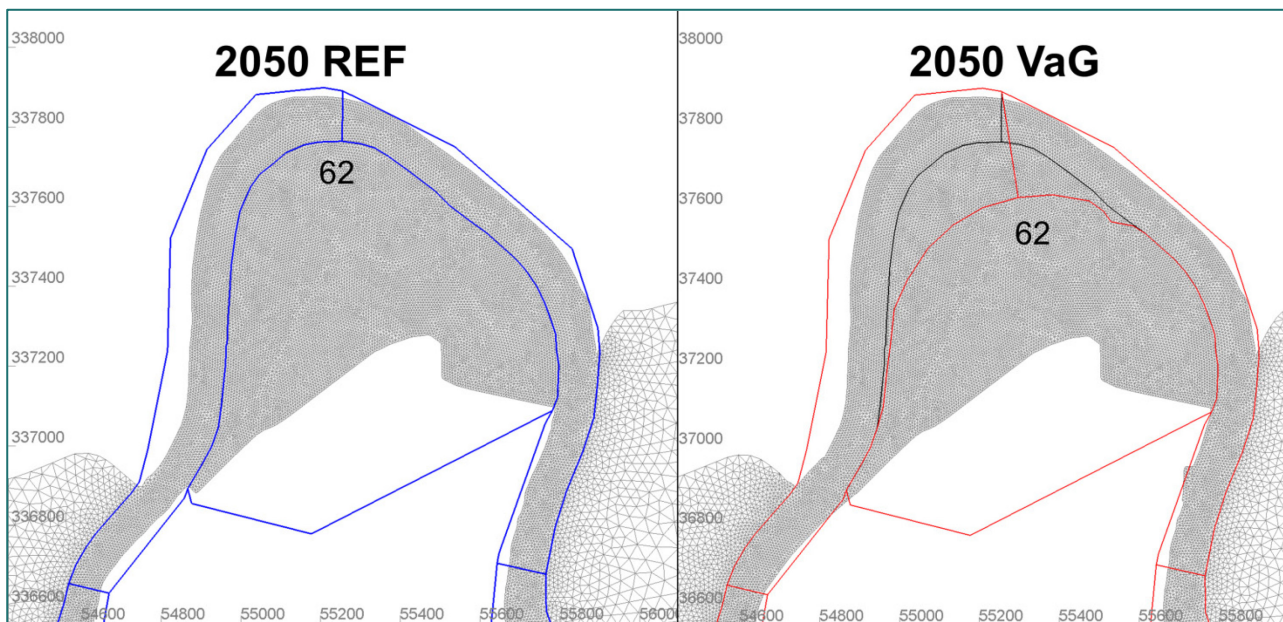
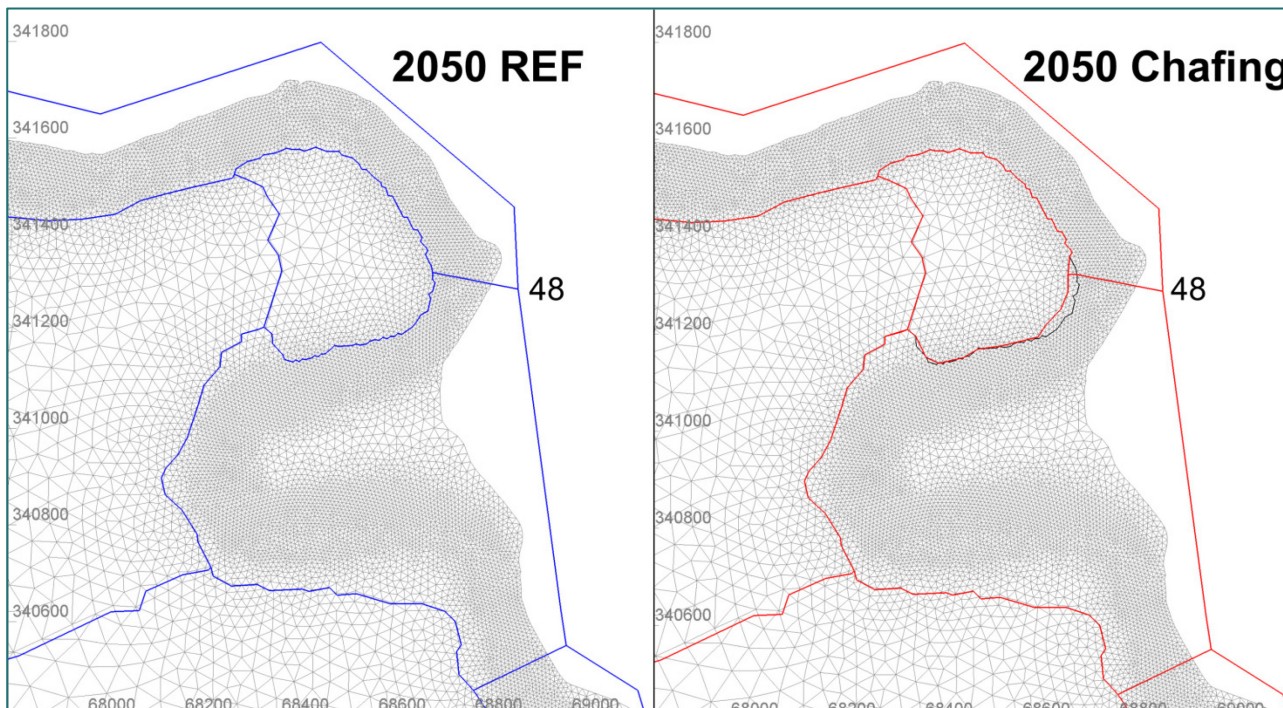


Figure 16 – Difference in transects (transect 48) between the 2050 REF and Chafing alternative for location around km 130-131 (Uitbergen)



## 5.2 Tidal asymmetry effects on sand transport

Flow velocity is the most important explanatory variable for sand transport. Trying to explain changes in sand transport between different scenarios/alternatives, the cross sectional averaged flow velocity is used. In the Engelund and Hansen equation (equation 3.1) flow velocity to the power five is located in the nominator, impacting directly the amount of sediment transport. In trying to explain the net transport directions and magnitude a plot will be made of the ratio between the integrated flood flow velocity to the power five over the integrated ebb flow velocity to the power five:

$$\frac{\int (V_{flood})^5}{\int (V_{ebb})^5} \tag{5.1}$$

If this ratio is higher than one, a flood dominated transport is expected. If it is smaller than one the cross sectional averaged flow is ebb dominated.

## 5.3 Erosion and sedimentation patterns

There is no feedback loop of the sediment transport module SISYPHE to the hydrodynamic simulation. So the water motion is modelled with a fixed bottom and time varying boundary conditions. Based on this water motion sediment transport is calculated. SISYPHE keeps a mass balance of eroded and deposited sand in the entire model, but this is not fed back to the bottom of the hydrodynamic model. Sedimentation and erosion plots will show a pattern only based on the hydrodynamics without the feedback of sand transport on the bottom of these hydrodynamics. This is important to take into account. Mass balance plots will be shown to indicate net sedimentation or net erosion in a box or polygon after a full spring/neap tidal cycle. This value will be extrapolated to a one year sedimentation or erosion rate. Positive values indicate sedimentation and negative values indicate erosion.

## 6 Scenario Results

First the results of the reference simulation for 2013 will be repeated again (Smolders et al., 2018). Then the results of the reference simulation for 2050, called 2050 REF QN AOCN, will be discussed and differences with the 2013 simulation will be shown. Next, two different scenarios for 2050 are given: AplusCH and AminCL are compared with the 2050 (and 2013) reference simulation. Finally the different alternatives will be compared with the corresponding 2050 reference scenario.

### 6.1 Scaldis 2013 REF QN AOCN

The net sand transport over different transects along the Scheldt estuary is given in Figure 17. The yellow dots give the net sand transport over a full spring/neap tidal cycle expressed in kg per second, whereas the red and blue triangles give the net transport over two spring and two neap tides respectively. In general the net sand transport in the Western Scheldt is flood dominated (negative values) and the net transport in the Sea Scheldt is ebb dominated (positive values).

Figure 17 – Net sand transport over different cross sections along the Scheldt estuary calculated and plotted for a neap and spring tide and a full spring/neap tidal cycle. Scenario 2013 QN REF AOCN. A positive value means transport in downstream direction.

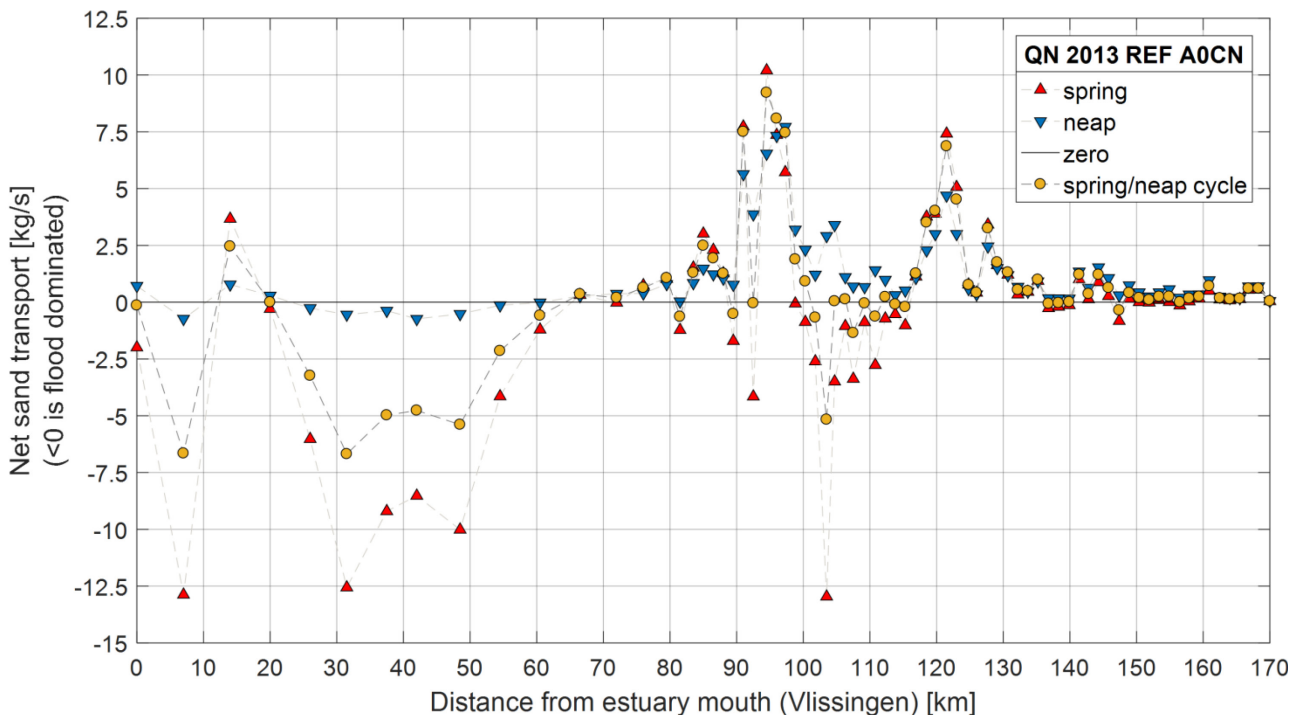
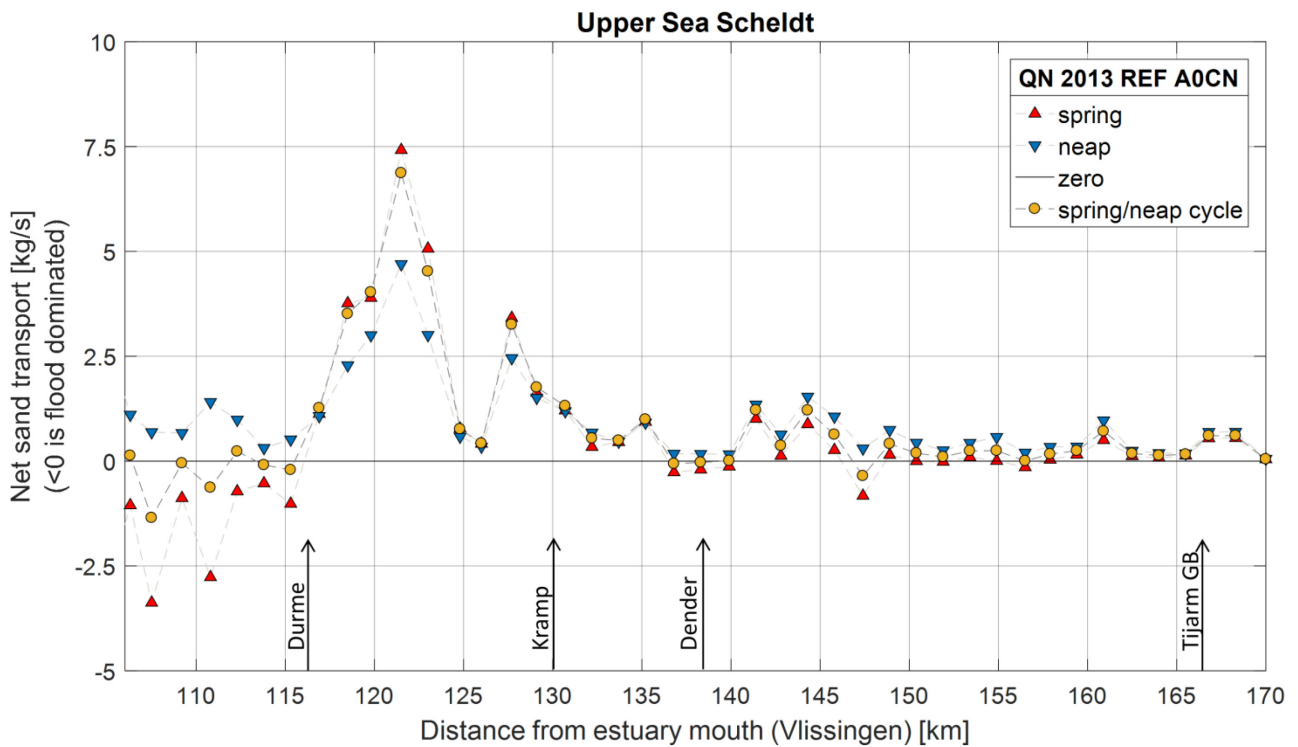


Figure 18 shows the same results as Figure 17 but focusses on the Upper Sea Scheldt. From km 105 to km 116 the net sand transport is slightly flood dominated (negative value). For neap tides, when the flood flow is weaker, it is slightly ebb dominated (positive value). Then from km 116 to km 125 and between km 127 and km 136 the net sand transport is larger and clearly ebb dominated. This is upstream of the tributary Durme. Further upstream the net sand transport remains ebb dominated and is smaller. At km 137 and km 147 by exception the net sand transport becomes flood dominant again for average and spring tides, whereas it remains ebb dominant for neap tides.

Figure 18 – Net sand transport over different cross sections of the Upper Sea Scheldt calculated and plotted for a neap and spring tide and a full spring/neap tidal cycle. Scenario 2013 QN REF A0CN. A positive value means transport in downstream direction.



The ebb or flood dominance in sand transport is partly explained in Figure 19 where the ratio of the cross sectional averaged flow velocities to the power five, integrated over two spring tides or two neap tides or a full spring/neap tidal cycle, for flood and ebb direction is shown. Values above 1 suggest a more flood dominated sand transport due to the more dominance of the cross sectional averaged flood velocity values to the power five. Figure 19 shows that the Western Scheldt is mainly flood dominated. Upstream from km 65 the sand transport becomes more ebb dominated. Neap tides are always more ebb dominated (or less flood dominated) than spring tides. Figure 20 shows the same results as Figure 19 but focusses on the Upper Sea Scheldt. Between km 105 and km 115 the values for a full spring/neap tidal cycle are lying around 1, with more values just above 1. This explains the small flood dominated sand transport in this section as seen in Figure 18. Upstream from km 115 Figure 20 shows a clear ebb dominance with exceptions around km 138 and km 147. It is at these last two locations that the net sand transport becomes slightly flood dominant again in the Upper Sea Scheldt. Figure 19 and Figure 20 show that a spring tide always results in a more flood dominant or less ebb dominance in the cross sectional averaged flow velocities to the power five. So it is expected that at spring tide the net sand transport is higher flood dominated or less ebb dominated. Figure 18 shows that this is not the case between km 117 and km 131. In this region the spring tide increases the ebb dominated sand transport. In Figure 20 it can be seen that in this region also spring tide is very ebb dominated in terms of flow velocity and thus resulting in a larger ebb dominated sand transport. In the rest of the Upper Sea Scheldt (until km 160) at spring tide the dominance between ebb and flood in terms of flow velocity is more equal.

Figure 19 – Asymmetry between flood and ebb over time integrated cross sectional averaged flow velocity to the power five for scenario 2013 QN REF A0CN.

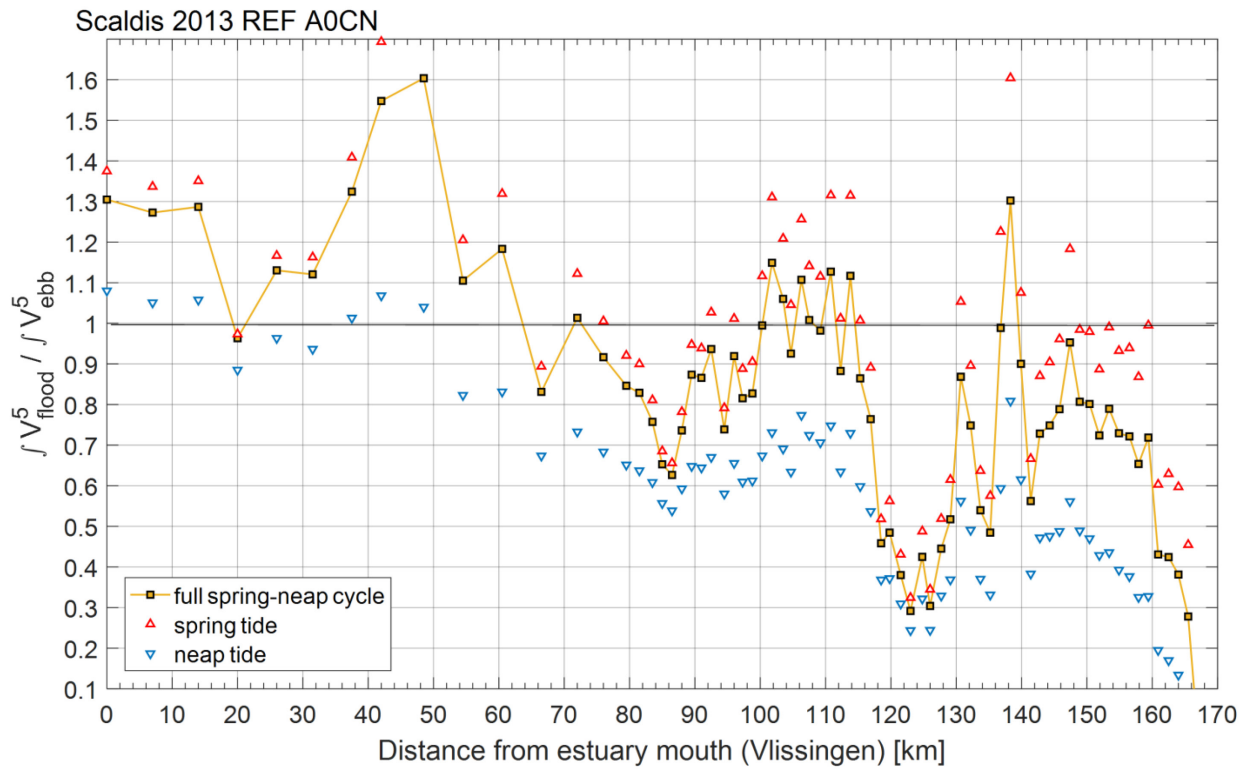


Figure 20 – Asymmetry between flood and ebb over time integrated cross sectional averaged flow velocity to the power five for scenario 2013 QN REF A0CN focused on the Upper Sea Scheldt.

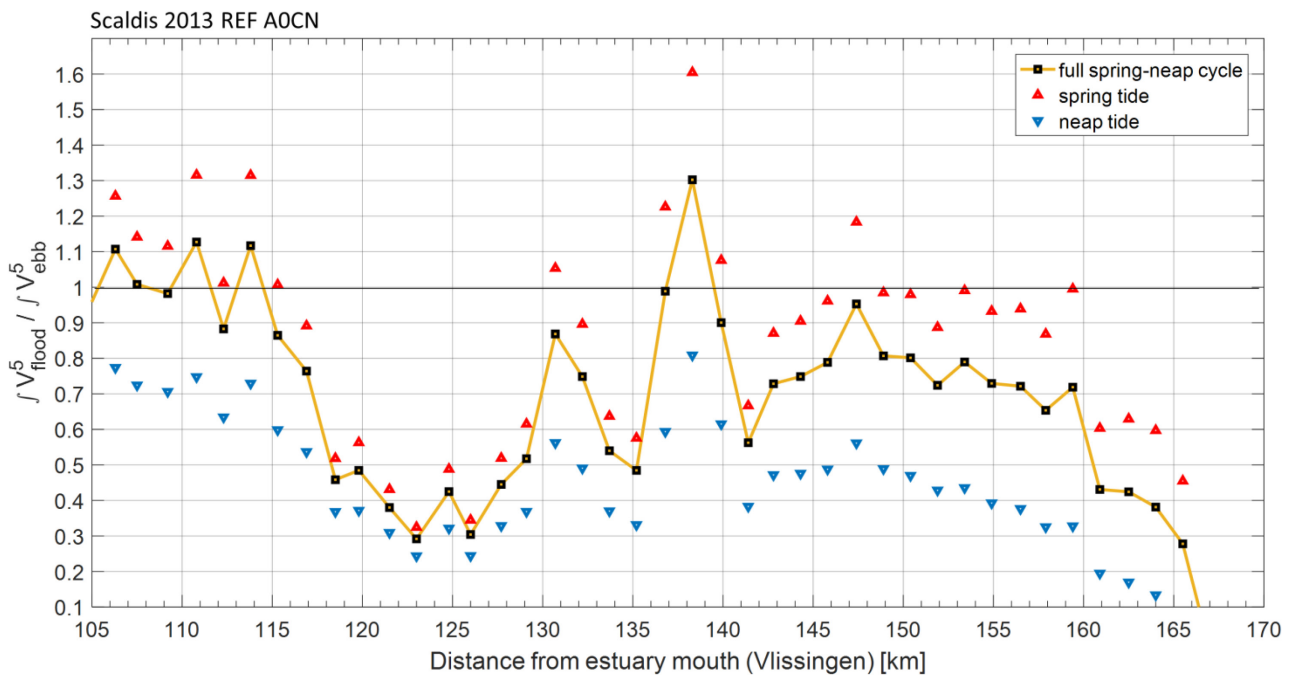
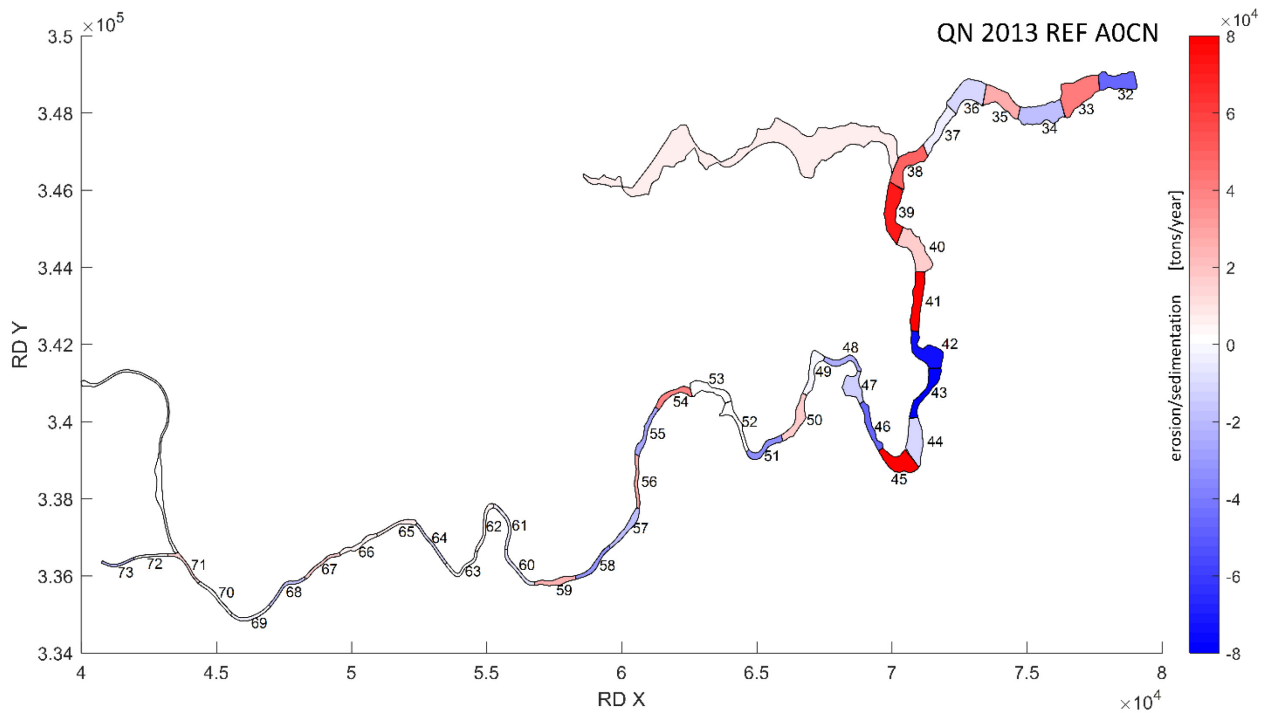


Figure 21 shows for different polygons in the Upper Sea Scheldt the mass balance of the potential sand transport after a full spring/neap tidal cycle (15 days). The red color indicates sedimentation and the blue color indicates erosion or loss of sand in that polygon. The tidal arm to Gentbrugge is importing sand at a modelled rate of 61 tons per year. The Durme is importing sand in the model at a rate of 7130 tons per year. The ratio of the cross sectional averaged flow velocity to the power five for the transect at the entrance of the Durme for a complete spring/neap tidal cycle was 1.91; indicating a very strong flood dominance, explaining the sedimentation in the Durme. In the red polygons more maintenance dredging can be expected keeping in mind that the model predicts transport capacities and that in the real estuary in some locations no abundance of sand might be available for transport. By comparing different alternatives and scenarios with a reference situation, some areas (polygons) may need more maintenance dredging than in the reference situation and if in the current situation these areas already need frequent maintenance dredging, this can be seen as an undesired evolution. The mass balance maps of all following scenarios are given in Appendix A together with a table listing the exact numbers of erosion or sedimentation in tons per year for each polygon for each scenario.

Figure 21 – Mass balance of potential sand transport over spring/neap tidal cycle for polygons along the Upper Sea Scheldt. Scenario QN 2013 REF A0CN. Erosion in blue and sedimentation in red.



## 6.2 Scaldis 2050 REF QN: A0CN, AplusCH and AminCL

Scaldis 2050 REF QN AplusCh or Scaldis 2050 REF QN AminCL will be the reference to compare the alternatives with. In order to see how these scenarios differ from the 2013 reference, discussed here above, a two-step approach was taken to see the effect of a changed bathymetry and changed boundary conditions separately. Figure 22 shows that to go from Scaldis 2013 to Scaldis 2050, first only the bathymetry was changed. In a second step the boundary conditions were changed. The result of this first step is Scaldis 2050 REF QN A0CN and the results and differences with Scaldis 2013 REF QN A0CN will be discussed. In step 2 the boundary conditions will be changed from QN A0CN to QN AminCL and QN AplusCH. These results will be compared with the QN A0CN results of Scaldis 2050 mainly, but Scaldis 2013 results are also shown.

Figure 22 – Schematic view of the two step path from Scaldis model 2013 to Scaldis model 2050

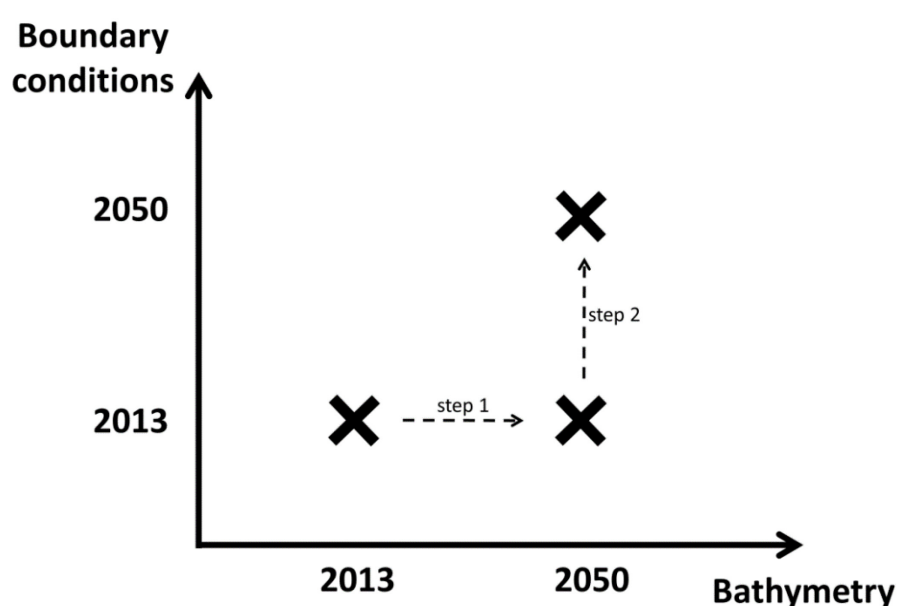


Figure 23 shows in a bar graph the net sand transport over different transects along the Upper Sea Scheldt derived from a spring/neap tidal cycle for the scenarios 2013 REF QN A0CN, 2050 REF QN A0CN, 2050 REF AplusCH and 2050 REF AminCL. The difference between 2013 REF QN A0CN and 2050 REF QN A0CN is small and the direction of the net transport remains the same everywhere, except around km 111 where the flood dominated transport in the 2013 model changes to an ebb dominated transport in the 2050 model. The changes in bathymetry between the 2013 and 2050 model are rather small. One of the biggest changes is the deepening of the Durme tributary. This deepening causes more flood dominance in the Durme and more sand is transported to the Durme: from 7130 ton per year in 2013 to 21570 ton per year in 2050. Also the tidal arm towards Gentbrugge was shortened by the implementation of a sluice. This change reduced the import of sand from 61,5 ton per year in 2013 to 15,3 ton per year in 2050. Concerning the tidal asymmetry over the transect of flow velocity to the power five the differences between 2013 REF QN A0CN and 2050 REF QN A0CN remain small. Up to km 137 (Figure 24 and Figure 25) the 2050 simulation is slightly more ebb dominant than the 2013 simulation. Upstream from the Dender the 2050 simulation becomes slightly more flood dominant than the 2013 simulation.

Figure 23 – Bar graph of net potential sand transport over different transects along the Upper Sea Scheldt calculated over a full spring/neap tidal cycle for scenarios 2013 REF QN A0CN, 2050 REF QN A0CN, 2050 REF QN AplusCH and 2050 REF QN AminCL.

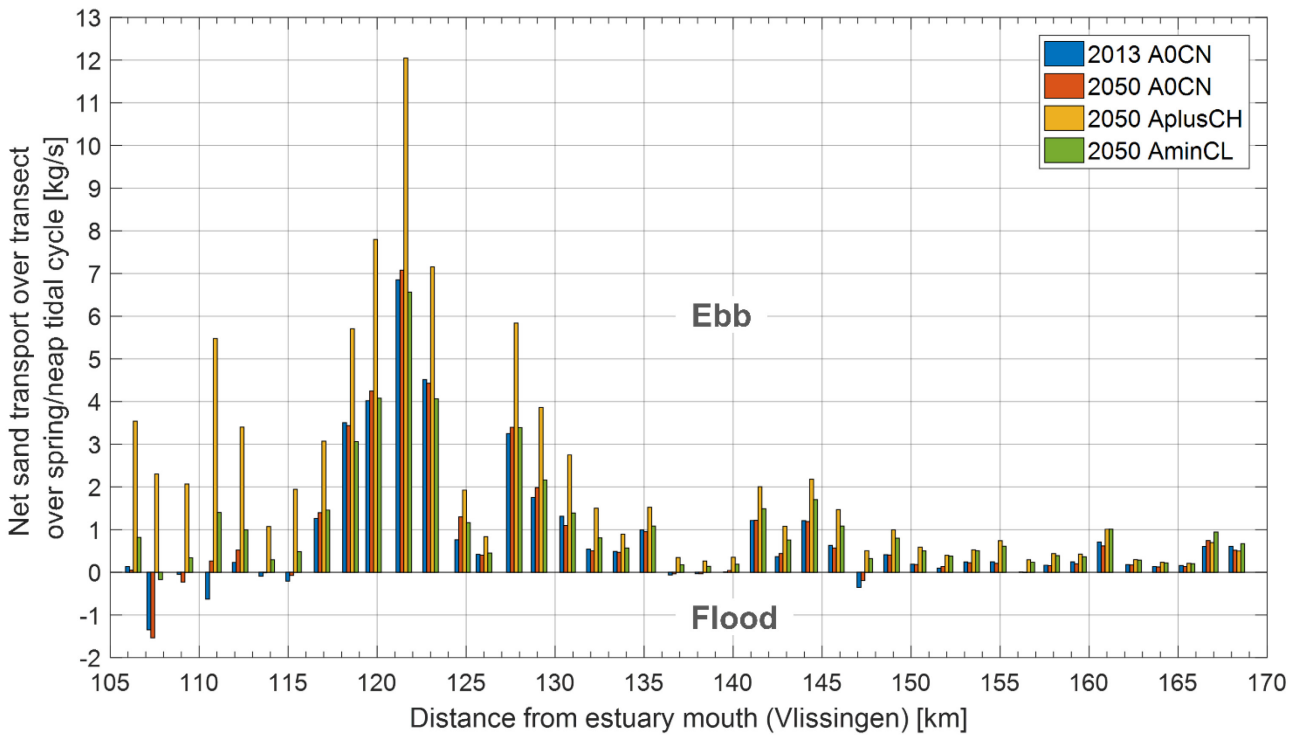


Figure 24 – Asymmetry between flood and ebb over time integrated cross sectional averaged flow velocity to the power five for scenario 2013 QN REF A0CN, 2050 QN REF A0CN, 2050 REF QN AplusCH and 2050 REF QN AminCL.

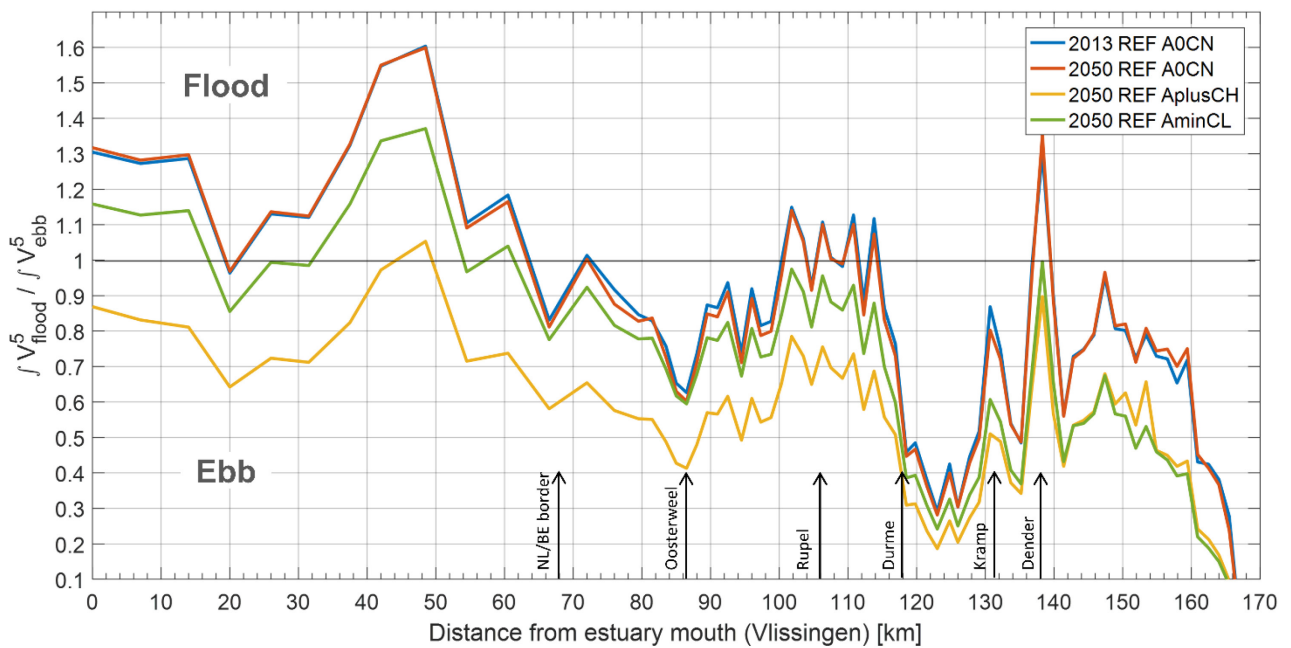
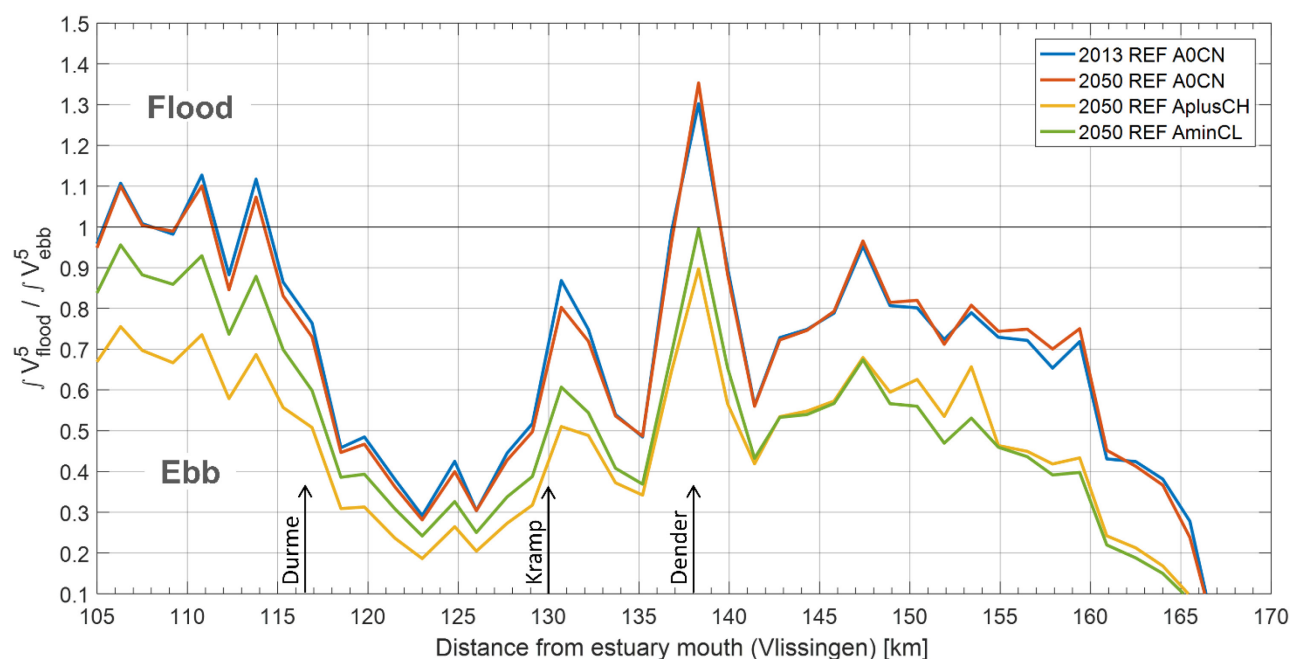


Figure 25 – Asymmetry between flood and ebb over time integrated cross sectional averaged flow velocity to the power five for scenario 2013 QN REF A0CN, 2050 QN REF A0CN, 2050 REF QN AplusCH and 2050 REF QN AminCL. Focus on the Upper Sea Scheldt.

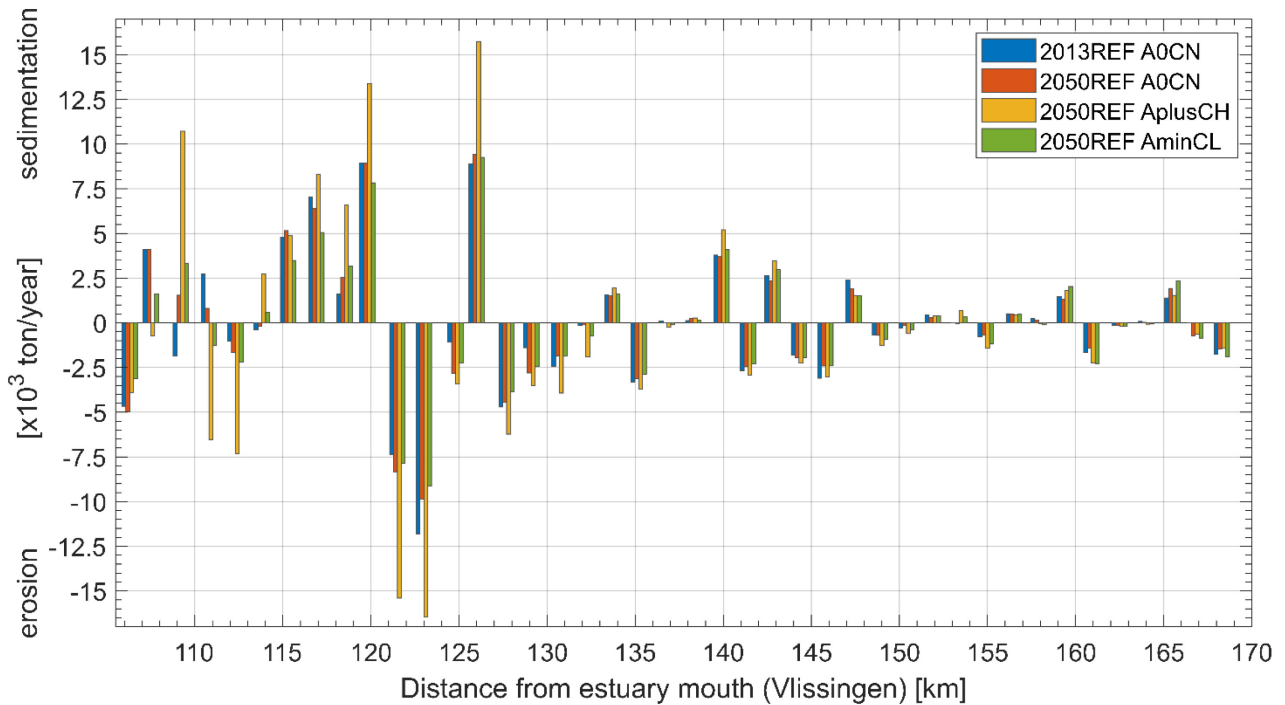


When the boundary conditions are changed with a low and high sea level rise and a change in tidal amplitude the differences with the A0CN simulations become much larger. With the AplusCH boundary conditions the net sand transport becomes ebb dominant in the entire Upper Sea Scheldt. Transport rates are also much higher: double or more than double the values of 2050 REF A0CN. For boundary conditions AminCL the net sand transport also becomes ebb dominant in the entire Upper Sea Scheldt except around km 107 (Figure 23), and transport rates are usually lower than for the AplusCH simulation. The sand transport rates in the simulation with AminCL boundary are more similar to the 2050 REF QN A0CN transport rates. All the way upstream (> km 166) the transport rates of 2050 REF AminCL are higher than all other scenarios. In terms of velocity asymmetry Figure 25 shows that the AplusCH scenario becomes much more ebb dominant than the 2050 REF QN A0CN scenario. From km 105 to km 140 the AplusCH scenario is more ebb dominant than the AminCL scenario. Upstream km 142 the AminCL scenario becomes more ebb dominant than the AplusCH scenarios and this shows in the net sand transports in Figure 23: upstream km 142 the difference in net sand transport becomes much smaller between the AplusCH and AminCL scenarios. The larger ebb dominance is explained by an increased ebb velocity over the transects while the flood velocity remains the same or decreases a little. This results in a larger ebb transport capacity and in most locations thus in a larger ebb dominance of the net transport of sand. For the Durme the import of sand increases from 21570 ton per year in the 2050 REF A0CN scenario to 34180 ton per year in the 2050 REF AplusCH scenario. With the AminCL boundary conditions it decreases to 16330 ton per year compared to 2050 REF A0CN. This big difference in sand transport into the Durme is due to the big difference in tidal amplitude (which is largest around Schelle which is relatively close to the Durme) for the AplusCH and AminCL boundary conditions. For the tidal arm towards Gentbrugge the net sand import further decreases towards 9,6 ton per year in the AplusCH scenario and changes to a net export of 2,8 ton per year for the AminCL scenario.

The potential sedimentation erosion rates of the scenarios 2013 REF QN A0CN, 2050 REF QN A0CN, 2050 REF QN AplusCH and 2050 REF QN AminCL are given in Figure 26. This bar graph shows the impact of changes in the local sedimentation or erosion rates of sand calculated after a spring/neap tidal cycle and extrapolated to one year. For most of the Upper Sea Scheldt the erosion sedimentation pattern is the same and only the amounts differ between the different boundary conditions. Between km 106 and 115 the erosion sedimentation pattern changes between different boundary conditions. The AplusCH scenario

showed the largest transport rates for sand and so this scenario also shows the largest values in accumulated sand or eroded amounts of sand in certain areas. In some areas these values can increase or decrease up to more than double the amount of the other scenarios.

Figure 26 – Potential sedimentation erosion rates extrapolated from a spring/neap tidal cycle to one year for different polygons along the Upper Sea Scheldt for scenarios 2013 REF QN A0CN, 2050 REF QN A0CN, 2050 REF QN AplusCH and 2050 REF QN AminCL.



### 6.3 VaG alternative

Because the VaG alternative has the largest changes in bathymetry and on the hydrodynamics it was decided to show both the impact of the AplusCH and AminCL scenario on sand transport. For the other alternatives only the AplusCH scenario will be simulated and shown.

#### 6.3.1 AplusCH scenario

The general trend in the AplusCH scenario for VaG is a more and larger ebb dominant transport. This is shown in Figure 27. However at the locations with the biggest bathymetrical changes, like channel straightening, the sand transport becomes less ebb dominant and at km 138 it even becomes flood dominant. The channel straightening between km 123 and km 126 and the more severe straightening at the Kramp around km 130 leads to diminished ebb dominated transport. This can also be seen in Figure 28 where the integrated cross sectional averaged velocity to the power five also indicates a loss in ebb dominance at these locations. From km 133 to km 150 the transport is clearly more ebb dominated (Figure 27) and this can also be seen in the graph with the cross sectional averaged velocities to the power five.

Figure 27 – Net sand transport rates over a spring/neap tidal cycle for different transects along the Upper Sea Scheldt for the alternative VaG AplusCH and the reference simulation 2050 REF AplusCH.

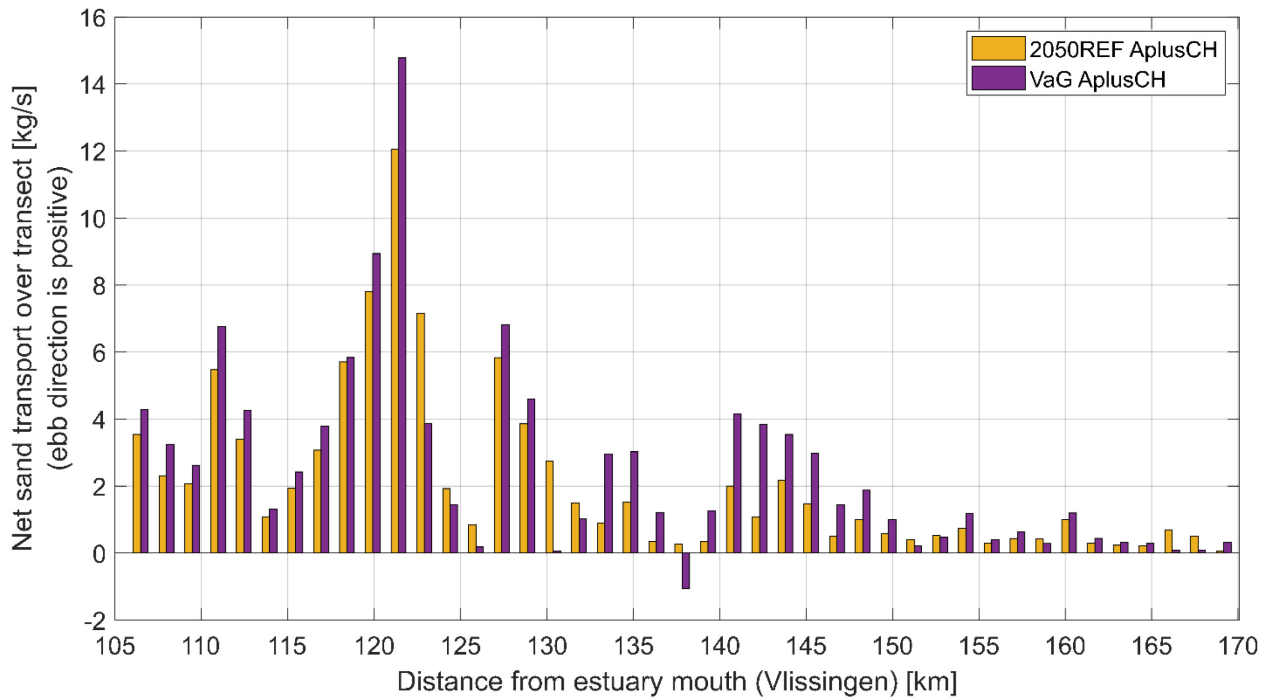
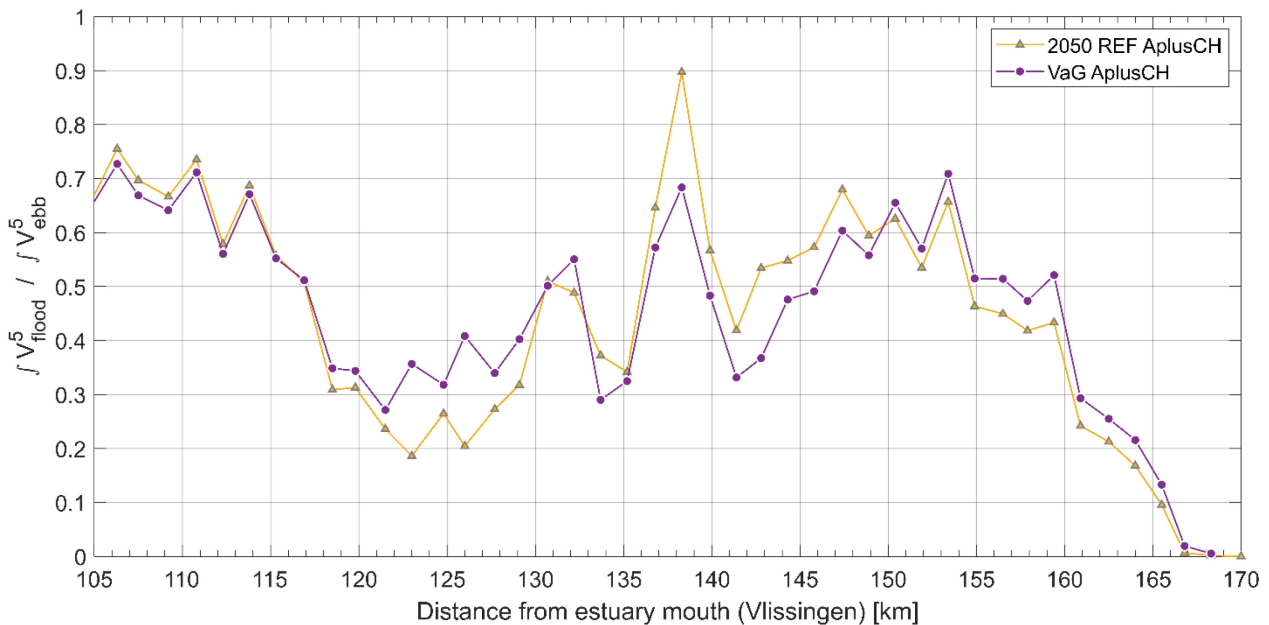


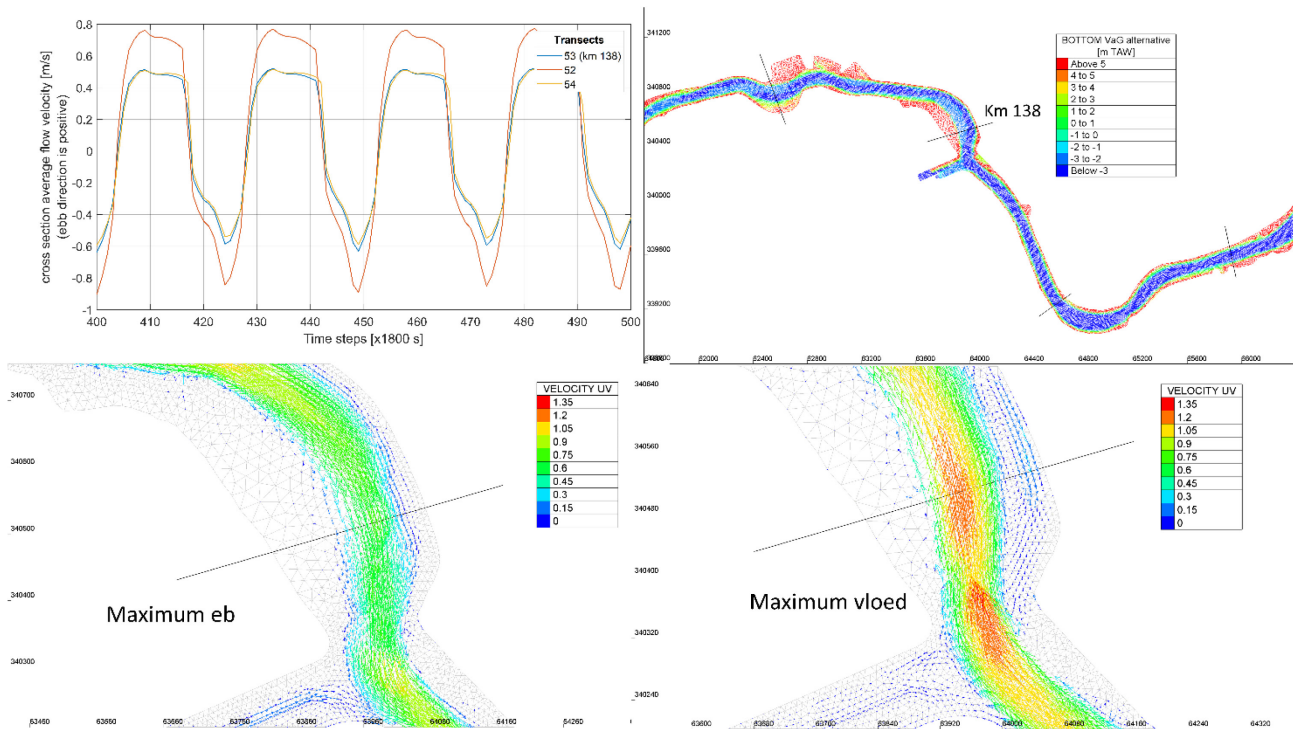
Figure 28 – Asymmetry of the over a transect averaged flow velocity to the power five integrated over a spring/neap tidal cycle for VaG alternative and reference simulation 2050 REF AplusCH.



There is one exception in the ebb dominance between km 133 to km 150 and that is around km 138, just upstream the Dender mouth. This was already a location where the ebb dominance in flow velocities had a local minimum (i.e. becomes less ebb dominant), and by deepening the inner bend, it created the ideal conditions for flood flow to pass this section in the newly deepened part. The deepening actually widened

the river locally and the cross sectional averaged flood velocity does not significantly increase. The ebb flow over this cross section is nicely divided over the entire width of the section, keeping its maximum flow velocity (around 0,8 m/s) much lower than the maximum flood velocity (around 1,25 m/s). Examples of the ebb and flood flow conditions are given in Figure 29. This figure also shows the exact location of this transect (number 53) and shows in the top left panel that the cross sectionally averaged flow velocities don't differ a lot from the ones at a transect downstream (number 52). In this case the cross sectionally averaged doesn't explain what really occurs.

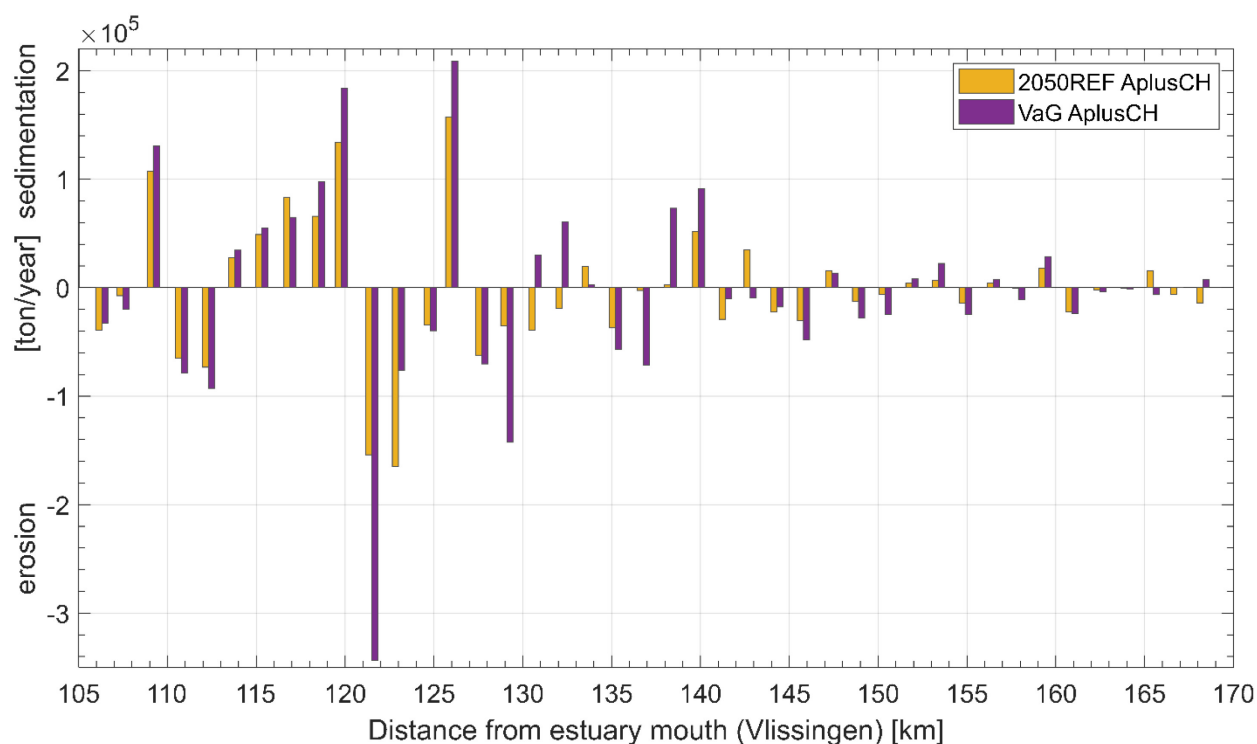
Figure 29 – top left: cross sectionally averaged flow velocities at transects 52, 53 and 54. The locations are shown in the top right panel. Bottom left shows the local ebb flow velocities in the model at transect 53 and the bottom right panel shows the flood flow velocities at transect 53.



When making the mass balances of all polygons in the Upper Sea Scheldt the AplusCH scenario shows in general an increase in erosion and sedimentation patterns, but the local changes in the bathymetry in the VaG alternative have a huge influence on the local sedimentation erosion patterns. At those locations where the ebb dominance was increased or decreased or even changed to flood dominance, the effects on the sedimentation erosion patterns are the largest. For example around km 130 where the channel was severely straightened, the ebb dominance decreased. The erosion in these polygons decreased and changed to a net sedimentation compared to the reference simulation. If in a polygon less sediment is transported downstream and in the polygon upstream more sediment is transported downstream, this will lead to a net sedimentation in the current polygon.

For the Durme the net sand import rate decreased from 34180 ton per year for the reference simulation to 30360 ton per year for the VaG alternative. For the tidal arm to Gentbrugge the sand export rate increased from 9,5 ton per year to 20,3 ton per year for the VaG alternative compared to the reference simulation.

Figure 30 – Potential sedimentation erosion rates extrapolated from a spring/neap tidal cycle to one year for different polygons along the Upper Sea Scheldt for alternative VaG AplusCH and the reference simulation 2050 REF AplusCH.



### 6.3.2 AminCL scenario

This section describes the differences between the VaG alternative and the reference simulation for AminCL boundary conditions. Figure 31 shows the net transport rate for sand for both VaG AminCL and 2050 REF AminCL. The small flood dominated transport rate at km 107 in the reference simulation changes to an ebb dominated transport rate. The opposite happens around km 138 (entering of the Dender into the Upper Sea Scheldt) where a small ebb dominated transport rate changes into a larger flood dominated transport rate. The reason of this shift was already explained in the previous section. From km 105 to km 122 the VaG alternative is more ebb dominant than the reference, then more upstream the sand transport becomes less ebb dominant because of changes in high water levels during flood and low water levels during ebb, caused by the large straightening measures around km 130. The explanation is similar to the one above of the VaG AplusCh scenario. Upstream from km 138 transport rates increase again until km 150. The patterns in transport rates of AminCL are similar to the ones in the AplusCH scenario, but the absolute values are lower for the lower climate scenario AminCL.

For the Durme the change in import rate between the reference and the VaG alternative is minimal, i.e. from 16330 ton per year to 15570 ton per year. For the tidal arm to Gentbrugge the difference is significant because for the reference simulation there is a net import rate of 2,8 ton per year. In the VaG alternative this changes to a net export rate of 1,1 ton per year.

Figure 32 shows the asymmetry in the integral of the cross sectionally averaged flow velocity to the power five. The patterns are very similar to the AplusCh scenario.

Figure 33 shows the net sedimentation erosion per polygon for the Upper Sea Scheldt and also here the patterns are very similar as for the AplusCH scenario. The absolute numbers are lower compared with the AplusCH scenario.

Figure 31 – Net sand transport rates over a spring/neap tidal cycle for different transects along the Upper Sea Scheldt for the alternative VaG AminCL and the reference simulation 2050 REF AminCL.

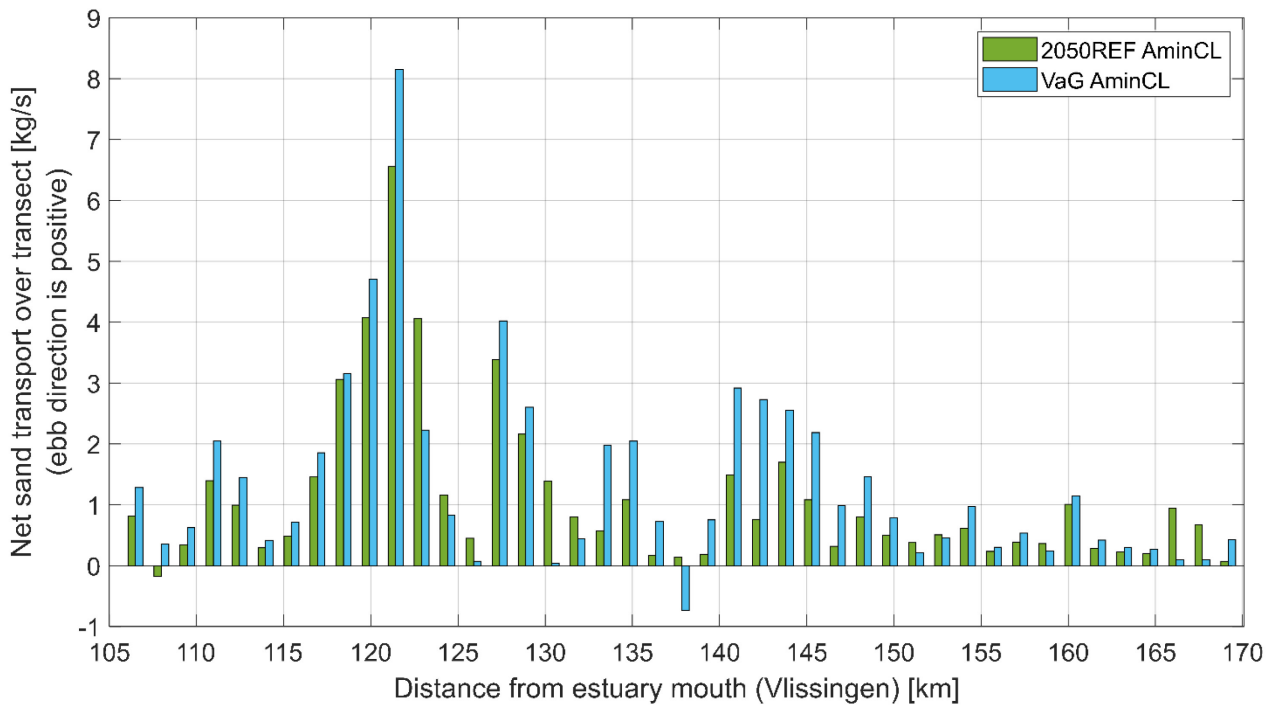


Figure 32 – Asymmetry of the over a transect averaged flow velocity to the power five integrated over a spring/neap tidal cycle for VaG alternative and reference simulation 2050 REF AminCL.

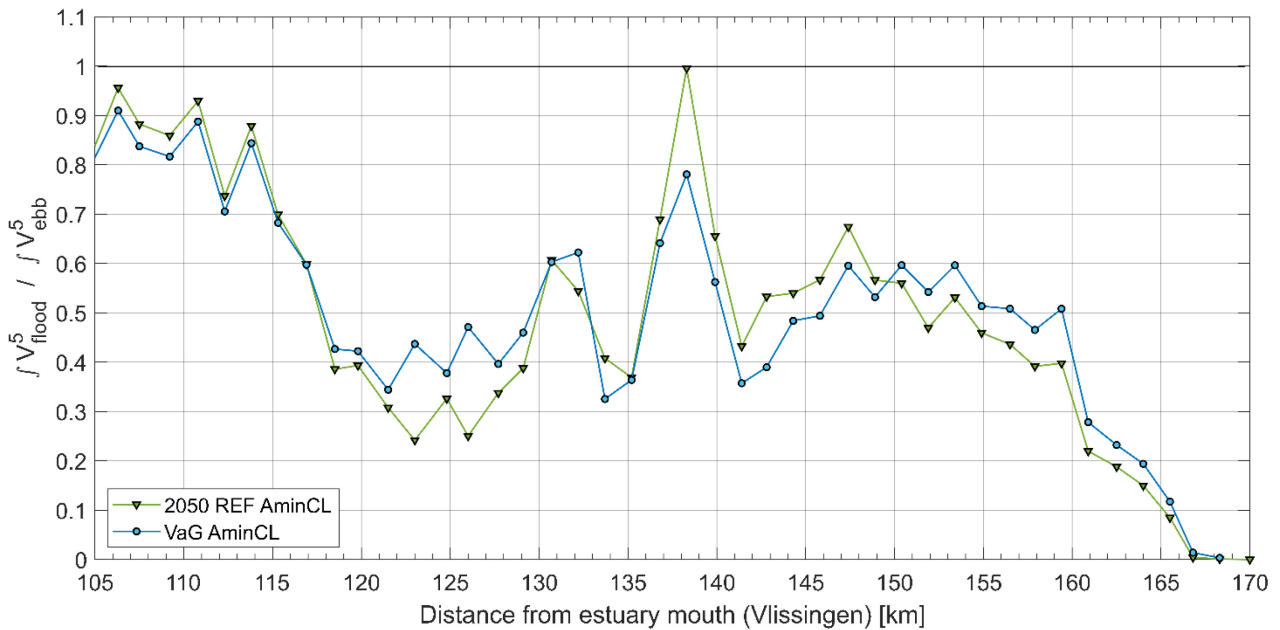
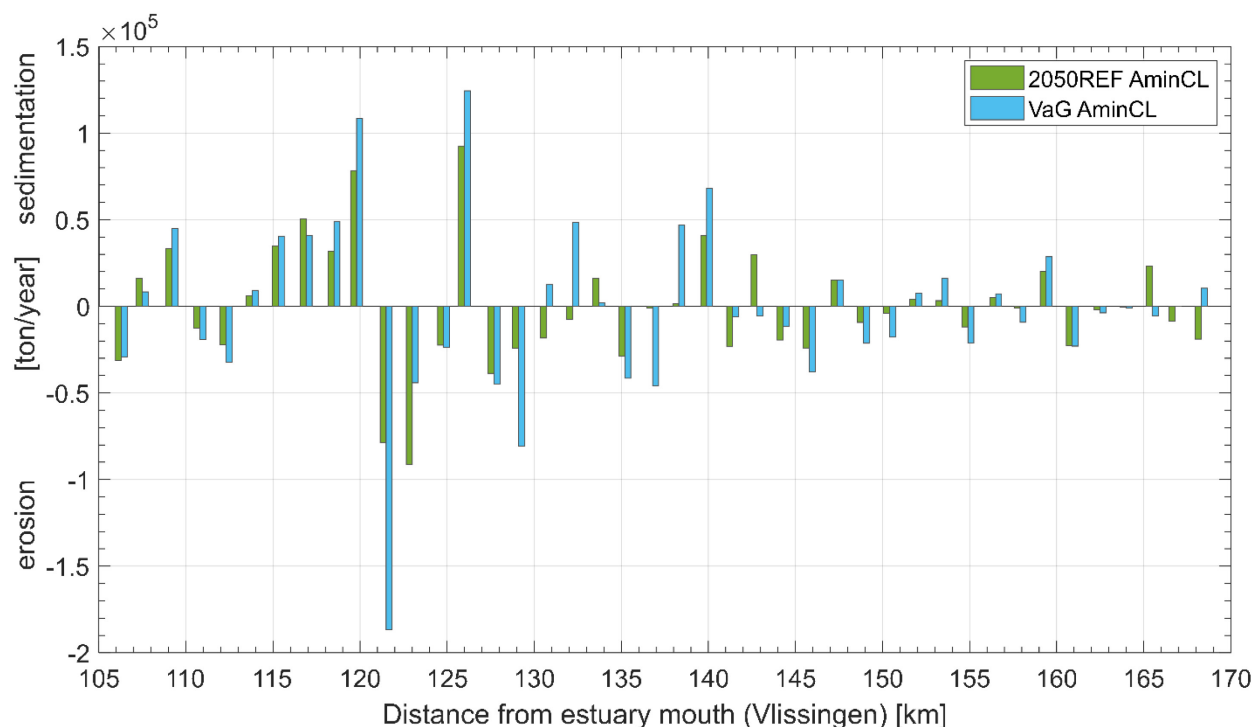


Figure 33 – Potential sedimentation erosion rates extrapolated from a spring/neap tidal cycle to one year for different polygons along the Upper Sea Scheldt for alternative VaG AminCL and the reference simulation 2050 REF AminCL.



## 6.4 VaH alternative

The changes in bathymetry in the VaH alternative are rather small compared to the VaG. In general a small increase in ebb dominated sand transport can be seen along the Upper Sea Scheldt for the VaH alternative compared to the reference simulation (Figure 34). At the locations where the bathymetry was changed the changes in sand transport rates coincide well with the specific changes that were made. Like in the VaG alternative around km 138 the channel was widened and this makes it easier for the flood flow to travel upstream, resulting in a net decrease in ebb dominated sand transport rates at this location. At locations where the inside of sharper bends was widened for better ship traffic, generally the flood flow can also travel better upstream, resulting in a decrease in ebb dominated transport. In Figure 35 this can be seen clearly between km 145 and km 160. In sedimentation erosion patterns in polygons in the Upper Sea Scheldt the effect of the VaH alternative is rather small in the downstream section. In the upstream section the absolute values are much smaller than in the downstream section, but then the relative changes become bigger. For example around km 160 the relative changes are large. There is a more than 50 % decrease in sedimentation and erosion in those polygons (Figure 36)

For the Durme the VaH alternative shows a slight decrease of sand import rate, i.e. from 34,180 ton per year in the reference simulation to 33600 ton per year for the VaH alternative. For the tidal arm to Gentbrugge the sand export rate decreases from 9,6 ton per year in the reference simulation to 7,1 ton per year in the VaH alternative.

Figure 34 – Net sand transport rates over a spring/neap tidal cycle for different transects along the Upper Sea Scheldt for the alternative VaH AplusCH and the reference simulation 2050 REF AplusCH.

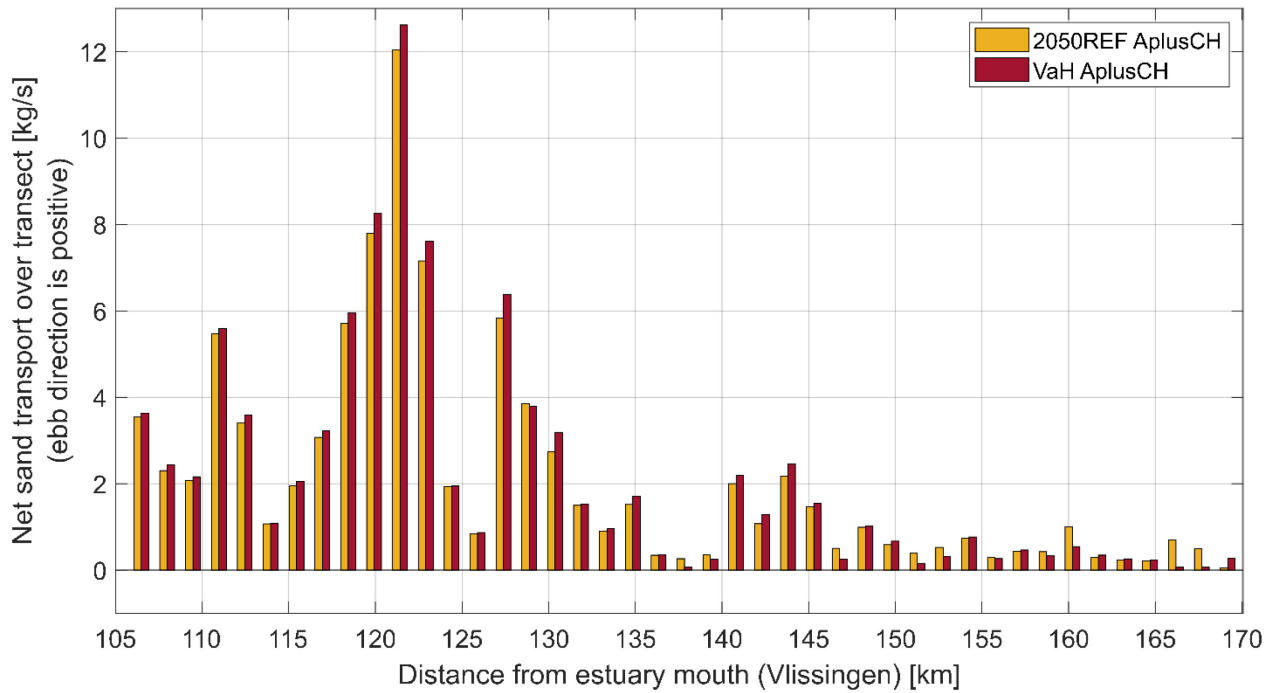


Figure 35 – Asymmetry of the over a transect averaged flow velocity to the power five integrated over a spring/neap tidal cycle for VaH alternative and reference simulation 2050 REF AplusCH.

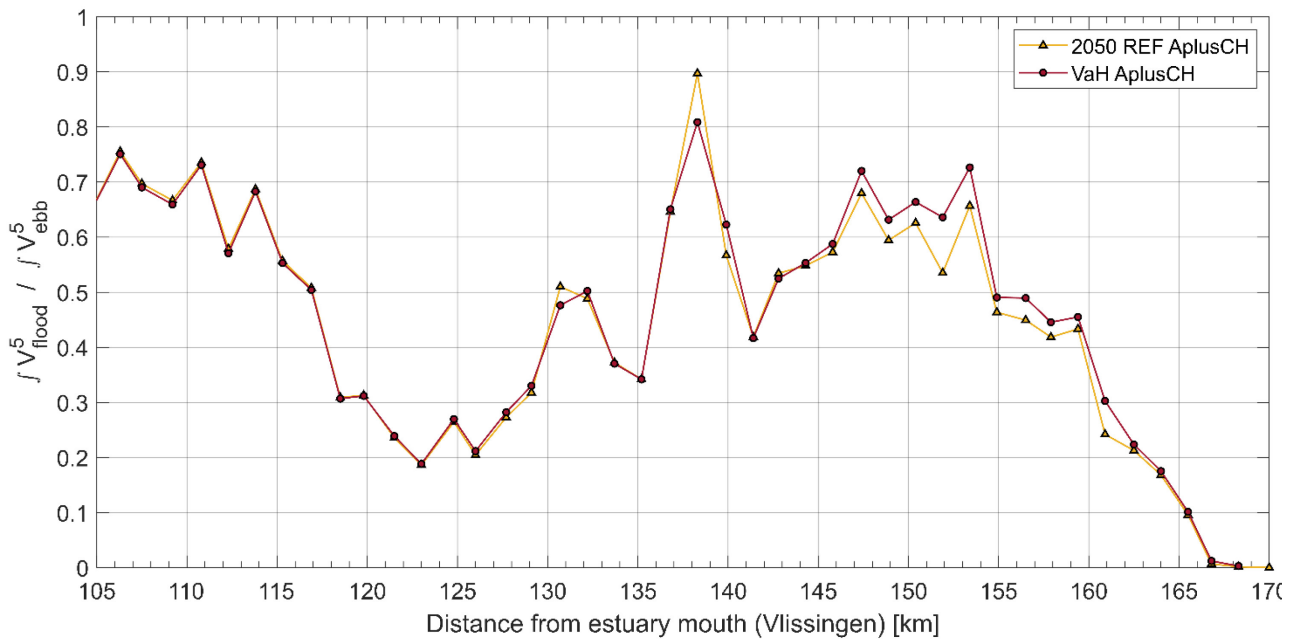
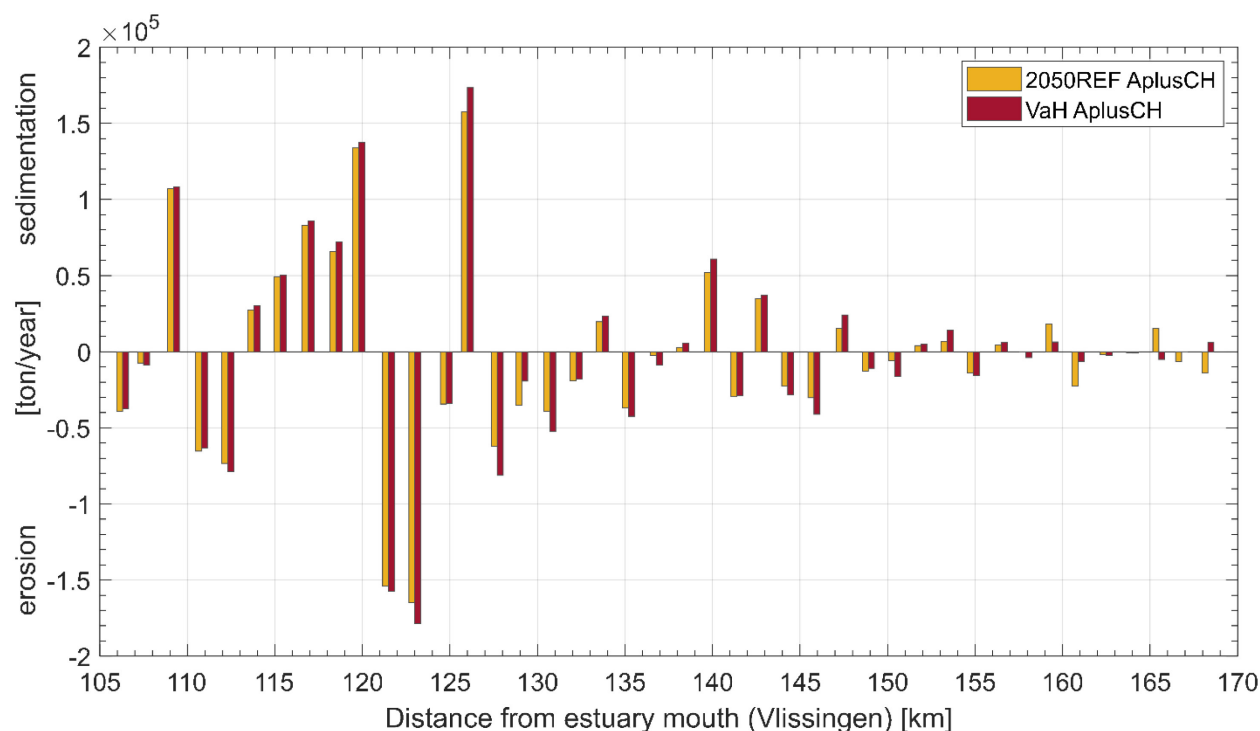


Figure 36 – Potential sedimentation erosion rates extrapolated from a spring/neap tidal cycle to one year for different polygons along the Upper Sea Scheldt for alternative VaH AplusCH and the reference simulation 2050 REF AplusCH.



## 6.5 Chafing alternative

The changes in bathymetry in the Chafing alternative are rather small compared to the VaG. In general a small increase in ebb dominated sand transport can be seen along the Upper Sea Scheldt for the Chafing alternative compared to the reference simulation (Figure 37). At the locations where the bathymetry was changed the changes in sand transport rates coincide well with the specific changes that were made. Like in the VaG alternative around km 138 the channel was widened and this makes it easier for the flood flow to travel upstream, resulting in a net decrease in ebb dominated sand transport rates at this location. At locations where the inside of sharper bends was widened for better ship traffic, generally the flood flow can also travel better upstream, resulting in a decrease in ebb dominated transport. However in this Chafing alternative the impact of the measures on the sand transport seems smaller compared to the VaH alternative. This can also be seen in Figure 38 where the differences in the integrated cross sectionally averaged flow velocities to the power five are rather small. In sedimentation erosion patterns in polygons in the Upper Sea Scheldt the effect of the Chafing alternative is small in the entire Upper Sea Scheldt. The biggest differences are the ones upstream of km 165. They are caused by the deepening of the ringvaart and cause the same effect in all alternatives (Figure 39).

For the Durme the Chafing alternative shows a slight decrease of sand import rate, i.e. from 34,180 ton per year in the reference simulation to 33,720 ton per year for the Chafing alternative. For the tidal arm to Gentbrugge the sand export rate increases from 9,6 ton per year in the reference simulation to 11,3 ton per year in the Chafing alternative.

Figure 37 – Net sand transport rates over a spring/neap tidal cycle for different transects along the Upper Sea Scheldt for the alternative Chafing AplusCH and the reference simulation 2050 REF AplusCH.

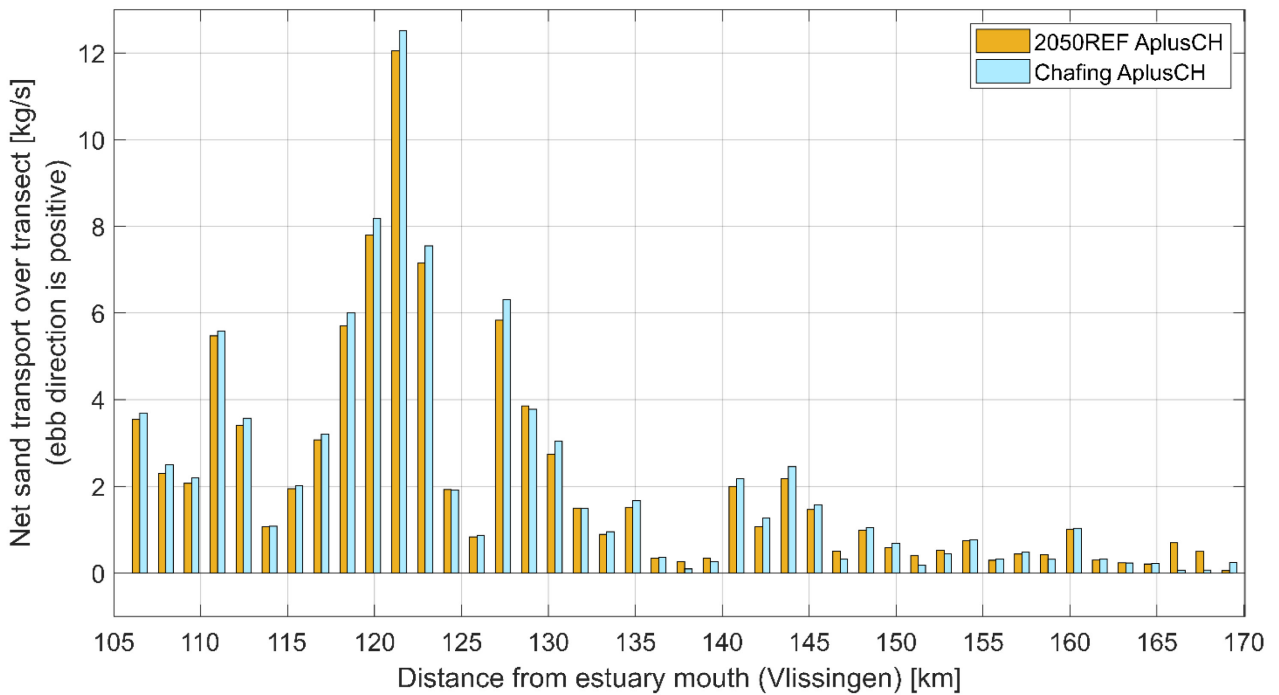


Figure 38 – Asymmetry of the over a transect averaged flow velocity to the power five integrated over a spring/neap tidal cycle for Chafing alternative and reference simulation 2050 REF AplusCH.

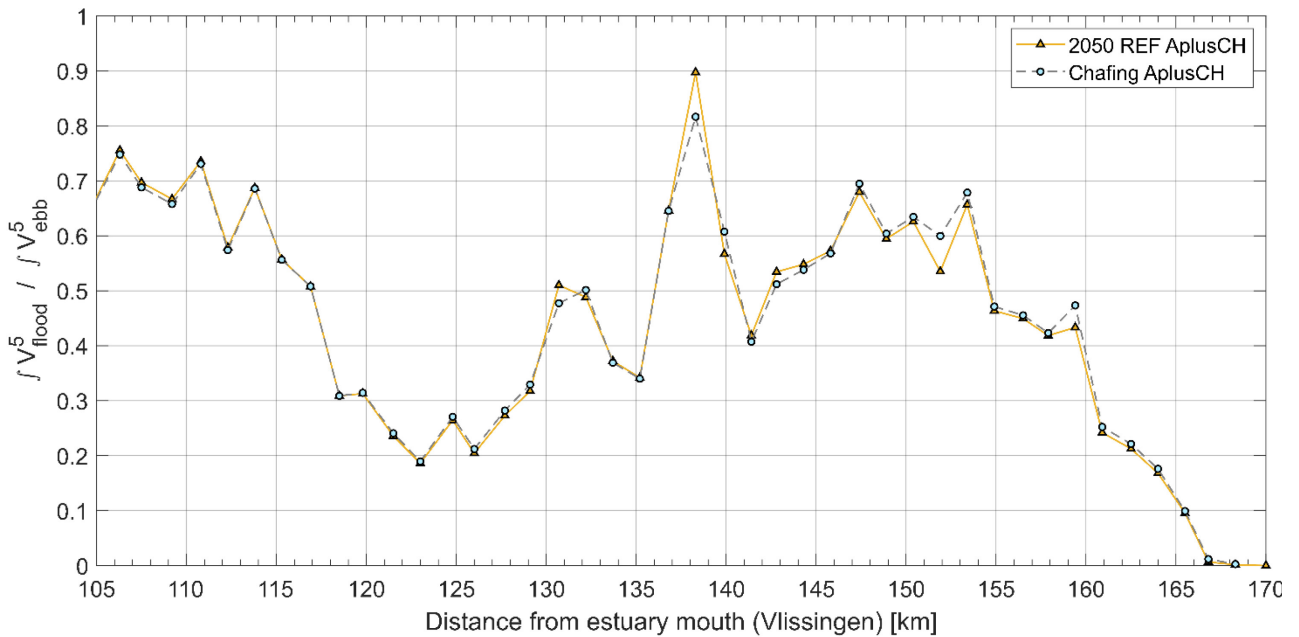
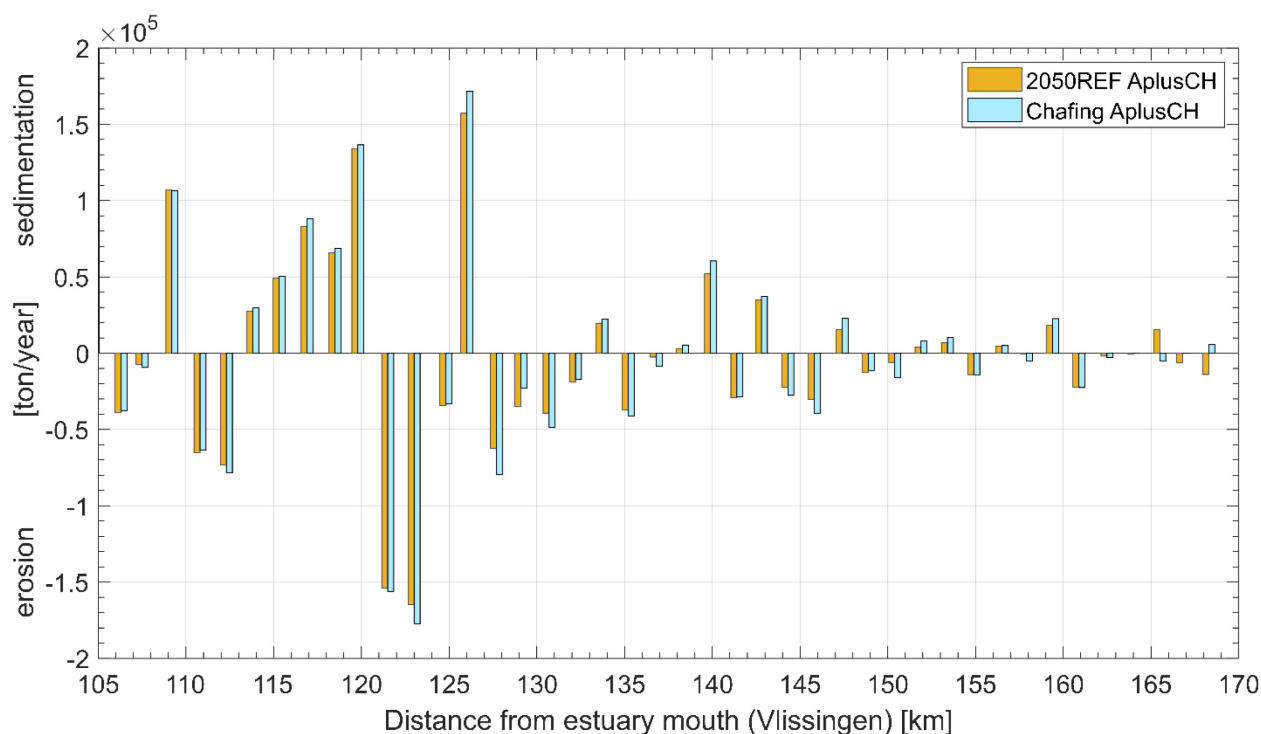


Figure 39 – Potential sedimentation erosion rates extrapolated from a spring/neap tidal cycle to one year for different polygons along the Upper Sea Scheldt for alternative Chafing AplusCH and the reference simulation 2050 REF AplusCH.



## 6.6 Synthesis of alternatives with AplusCH boundary condition

In this section the results of all alternatives with the AplusCH boundary condition are compared with each other and with the 2050 REF results. It combines the results of the above sections and adds the comparison of the different alternatives with each other.

In terms of sand transport rates over the different transects Figure 40 shows the results combined for the three alternatives and the reference simulation. This graph shows that the transport rates of VaH and Chafing differ only a little bit from the 2050 REF results and that the transport rates of the VaG scenario differ much more from all other results. This is automatically translated into the sedimentation erosion of the different polygons in the Upper Sea Scheldt, seen in Figure 42 and partly explained by the change in ebb dominance in the asymmetry between the integral of the cross sectionally averaged flow velocities to the power five for flood and ebb in Figure 41. The bathymetric changes in the VaG alternative are much bigger than the VaH or Chafing alternative and so it is logical that these measures have a bigger effect. This bigger effect however causes significantly larger sand transport rates and thus sedimentation and erosion rates along the Upper Sea Scheldt. This would imply a larger maintenance or better protection of the current navigation channel compared to the assumed 2050 Reference situation. So from the sand transport capacity point of view the VaG alternative has the largest impact on the estuary. It will change transport patterns significantly and implies a larger effort to maintain a reference situation. The VaH and Chafing alternative show fewer differences with the 2050 reference situation and cause minimal additional sand transport and as such will require much less maintenance of the navigation channel compared to the VaG alternative.

Figure 40 – Net sand transport rates over a spring/neap tidal cycle for different transects along the Upper Sea Scheldt for the alternatives Chafing, VaG, VaH and the reference simulation 2050 REF AplusCH.

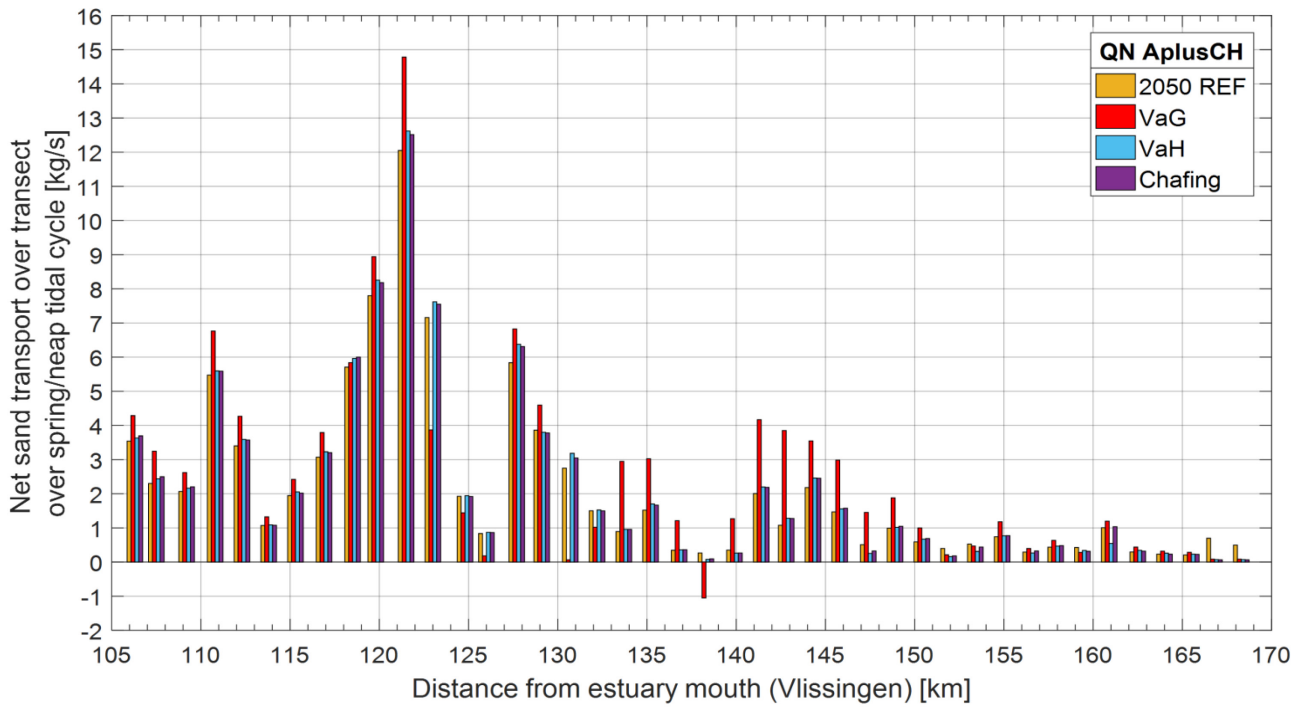


Figure 41 – Asymmetry of the over a transect averaged flow velocity to the power five integrated over a spring/neap tidal cycle for alternatives Chafing, VaG, VaH and reference simulation 2050 REF AplusCH. Above the figure, the grey areas indicate for each alternative the largest changes in bathymetry.

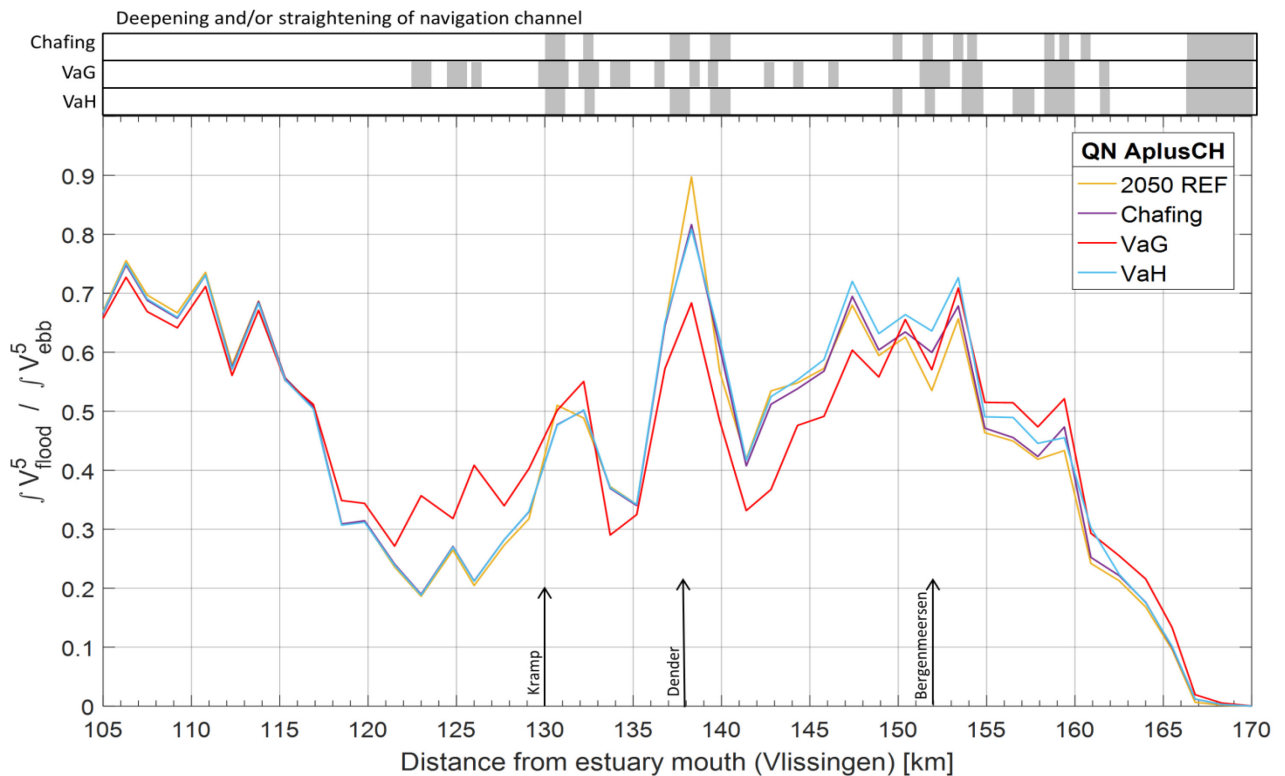
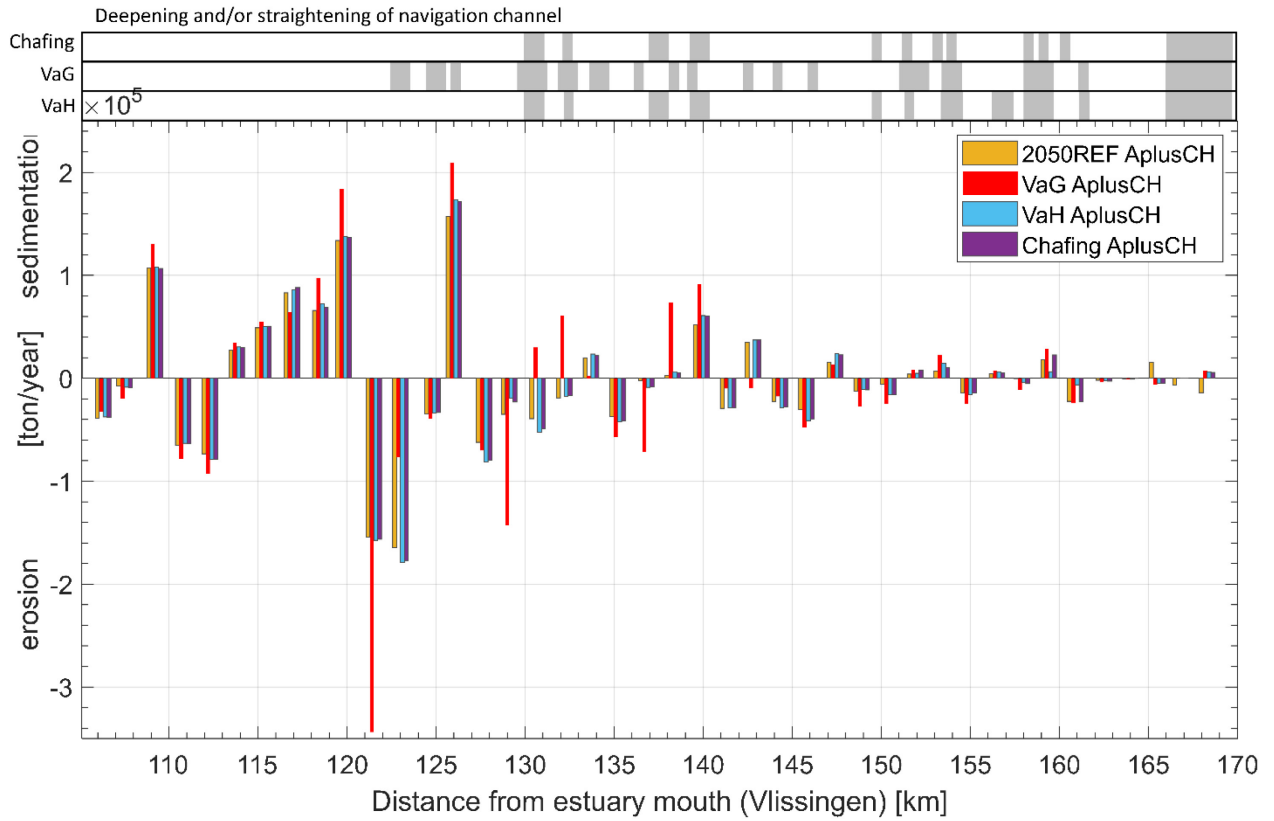


Figure 42 – Potential sedimentation erosion rates extrapolated from a spring/neap tidal cycle to one year for different polygons along the Upper Sea Scheldt for alternatives Chafing, VaG, VaH and the reference simulation 2050 REF AplusCH.



## 7 Conclusions

### 7.1 Autonomous development from 2013 to 2050

The autonomous development of the estuary, i.e. the bathymetry change in the model going from 2013 to 2050, results in only minor differences in sand transport rates, which increase in most parts of the Upper Sea Scheldt.

The asymmetry in the cross sectionally averaged flow velocity indicates a small increase ebb dominance downstream from Dendermonde (km 138) and a small decrease upstream of Dendermonde.

### 7.2 Climate scenarios in 2050: AplusCH and AminCL

The net sand transport rate increases largely and becomes more ebb dominant in the entire Upper Sea Scheldt. The AplusCH has a much larger effect than the AminCL scenario, as could be expected.

The tidal asymmetry increases strongly to more ebb dominance. The effect for AplusCH is much larger and differs from the AminCL scenario from downstream up till the Durme (km 117). Upstream from this point the difference between the two climate scenarios becomes smaller, but the difference with the reference stays large.

In terms of potential sedimentation erosion patterns the AplusCH scenario shows significant increases in sedimentation and erosion rates. Compared with these large differences the AminCL scenario does not differ that much from the reference.

### 7.3 Alternatives: Chafing, VaG and VaH

For the VaG alternative both the AplusCH and AminCL climate scenario were compared and they showed similar effects on the sand transport rates and direction, but differed strongly in absolute values. Therefore to compare all alternatives with each other only the AplusCH scenario was used.

The effects of VaH and Chafing on sand transport rates and potential sedimentation erosion patterns are small compared to the effects of the VaG alternative. This was also clearly visible in the asymmetry of the cross sectionally averaged flow velocities.

The results of all alternatives show that channel straightening improves the flood flow and locally decreases the ebb dominance. The climate scenarios and a general deepening of the navigation channel improve the ebb flow and make the estuary more ebb dominant. The larger the measures or changes made to the bathymetry, the larger the local response of the system and the larger the sand transport capacity differs from the reference state.

The VaG alternative has the most intrusive measures taken into the bathymetry and these cause large changes in sand transport rates and large changes in potential sedimentation and erosion rates throughout the entire Upper Sea Scheldt. With this scenario it is expected that more maintenance and navigation channel protection works will be necessary.

The effect on sand transport rates of the VaH and Chafing alternative is in the same order of magnitude as the effect of the autonomous development of the estuary (2013 → 2050).

## 8 References

**Directie Zeeland, Ministerie van de Vlaamse Gemeenschap & Administratie Waterwegen en Zeewezen** (2001). Langetermijnvisie Schelde-estuarium.

**Engelund, F. and Hansen, E.**, 1967. A Monograph on Sediment Transport in Alluvial Streams. Teknisk Forlag, Copenhagen, Denmark.

**IMDC** (2015). Bepalen van randvoorwaarden voor de referentiesituatie (2050) m.b.t. debiet en waterstand. I/NO/11448/15.128/TFR/

**IMDC/INBO/UA/WL** (2015). Modelling instruments for Integrated Plan Upper Sea Scheldt. I/NO/11448/14.165/DDP.

**IMDC in cooperation with WL, INBO, UA & Tractebel.** 2018. Evaluation method for Integrated Plan Upper Sea Scheldt. Memo I/NO/11448/15.185/DDP.

**Flokstra, C.; Koch, F.** (1981). Numerical aspects of bed level predictions for alluvial river bends. Delft Hydraulics Laboratory. Netherlands, Publication 258

**Holzauer H., Maris T., Meire P., Van Damme S., Nolte A., Kuijper K., Taal M., Jeuken C., Kromkamp J., van Wesenbeeck B., Van Ryckegem G., Van den Bergh E. & Wijnhoven S.** (2011). Evaluatiemethodiek Schelde-estuarium. Fase 2. Vlaams Nederlandse Schelde Commissie (VNSC). Projectnummer Deltares: 1204407.

**Maris T., Bruens A., van Duren L., Vroom J., Holzauer H., De Jonge M., Van Damme S., Nolte A., Kuijper K., Taal M., Jeuken C., Kromkamp J., van Wesenbeeck B., Van Ryckegem G., Van den Bergh E., Wijnhoven S. & Meire P.** (2014). Evaluatiemethodiek Schelde-estuarium Update 2014. VNSC.

**Smolders, S.; Maximova, T.; Vanlede, J.; Plancke, Y.; Verwaest, T.; Mostaert, F.** (2016). Integraal Plan Bovenzeeschelde: Subreport 1 – SCALDIS: a 3D Hydrodynamic Model for the Scheldt Estuary. Version 5.0. WL Rapporten, 13\_131. Flanders Hydraulics Research: Antwerp, Belgium.

**Smolders, S.; Maximova, T.; Vandenbruwaene, W.; Coen, L.; Vanlede, J.; Verwaest, T.; Mostaert, F.** (2017). Integraal Plan Bovenzeeschelde: Deelrapport 5 – Scaldis 2050. Version 4.0. FHR Reports, 13\_131\_5. Flanders Hydraulics Research: Antwerp.

**Smolders, S.; Vanlede, J.; Mostaert, F.** (2018). Integraal Plan Boven-Zeeschelde: Sub report 10 – Scaldis Sand: a sand transport model for the Scheldt estuary. Version 4.0. FHR Reports, 13\_131\_10. Flanders Hydraulics Research: Antwerp.

**Van Engeland T., T.J.S. Cox, K. Buis, S. Van Damme, P. Meire** (2018). 1D Ecosystem model of the Schelde estuary: model calibration and validation. Report 018-R217.



# Appendix A: Mass balance for USS for different scenarios

Overview of mass balances for different scenarios with results given as sedimentation/erosion rates per polygon in the Upper Sea Scheldt

Figure 43 – Potential sedimentation/erosion rates for polygons along the Upper Sea Scheldt.  
Scenario QN 2013 REF A0CN.

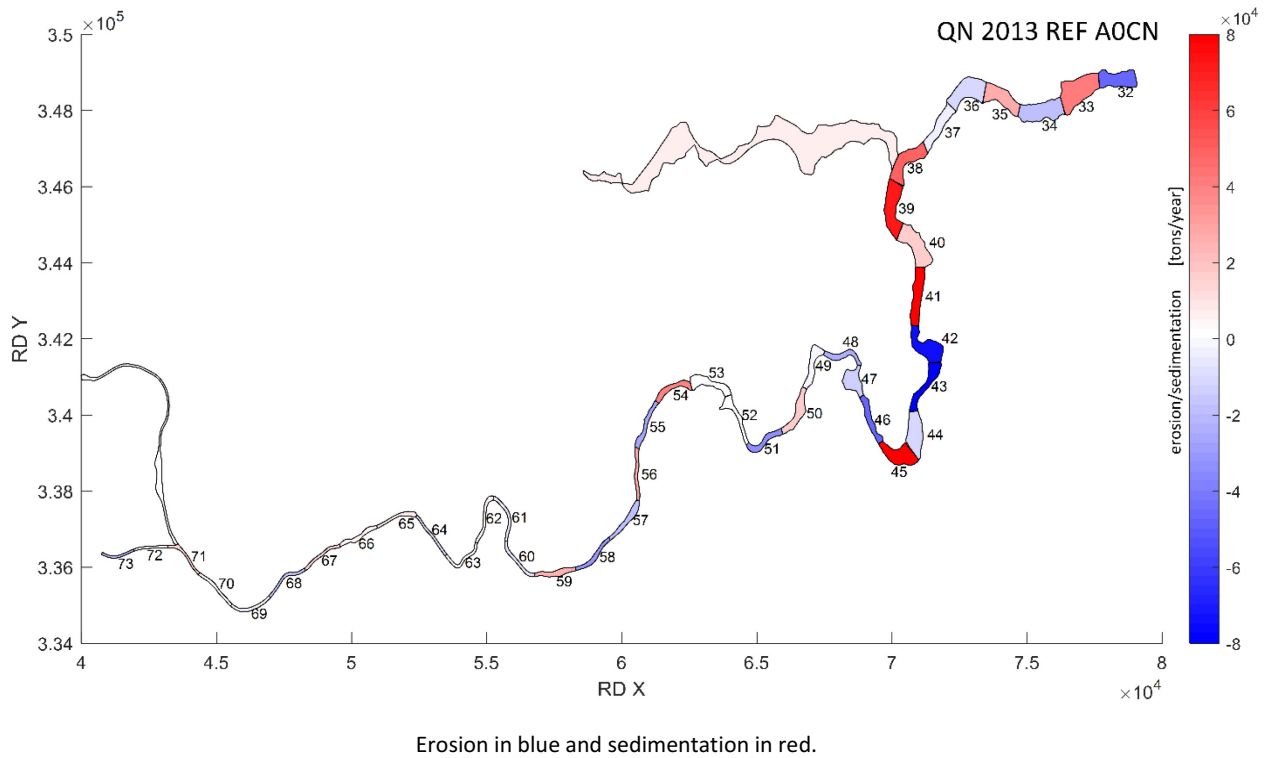


Figure 44 – Potential Sedimentation/erosion rates for polygons along the Upper Sea Scheldt.  
Scenario QN 2050 REF A0CN.

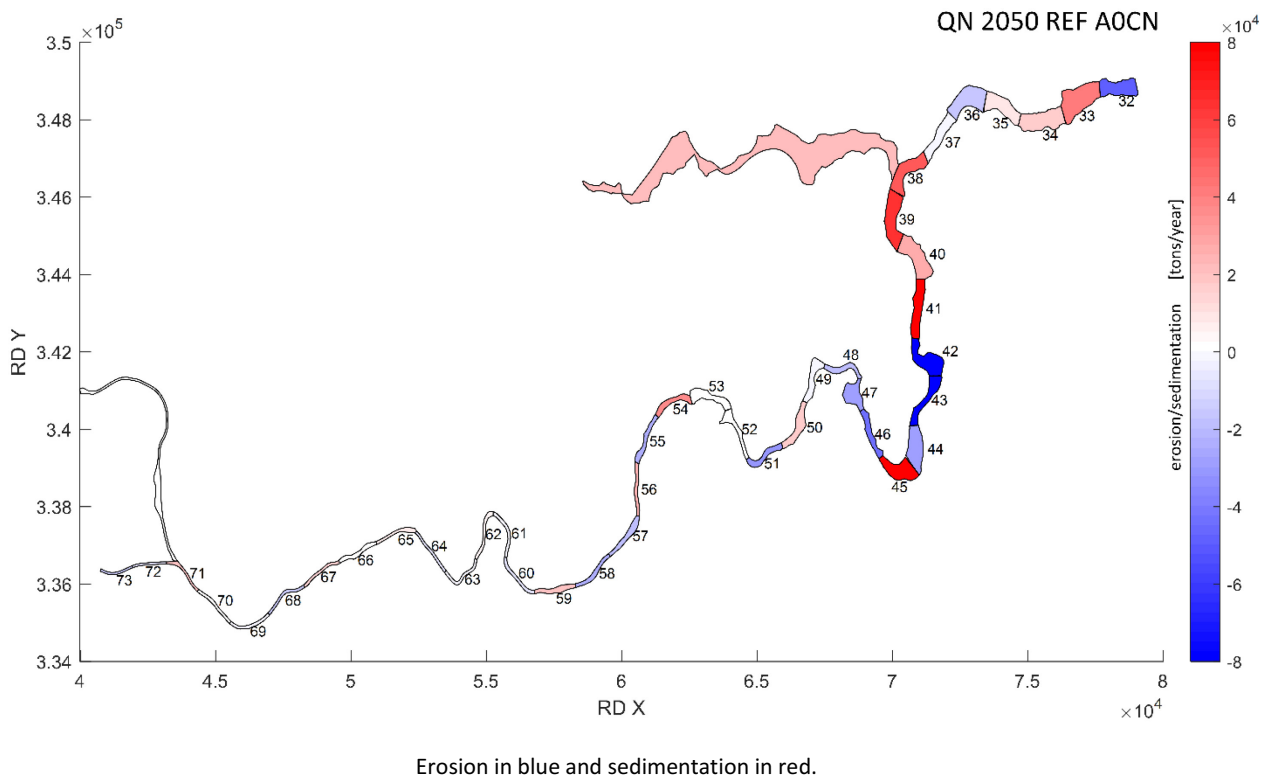


Figure 45 – Potential Sedimentation/erosion rates for polygons along the Upper Sea Scheldt.  
Scenario QN 2050 REF AplusCH.

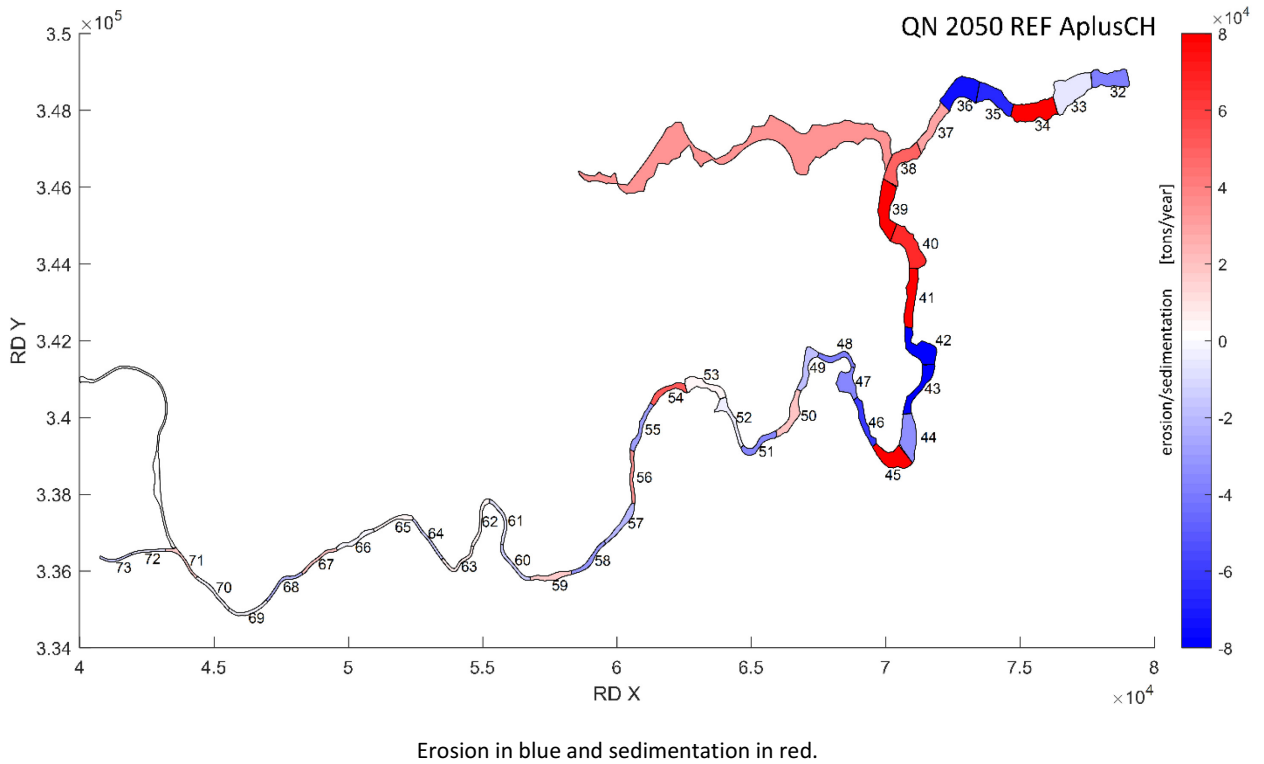


Figure 46 – Potential Sedimentation/erosion rates for polygons along the Upper Sea Scheldt.  
Scenario QN 2050 REF AminCL.

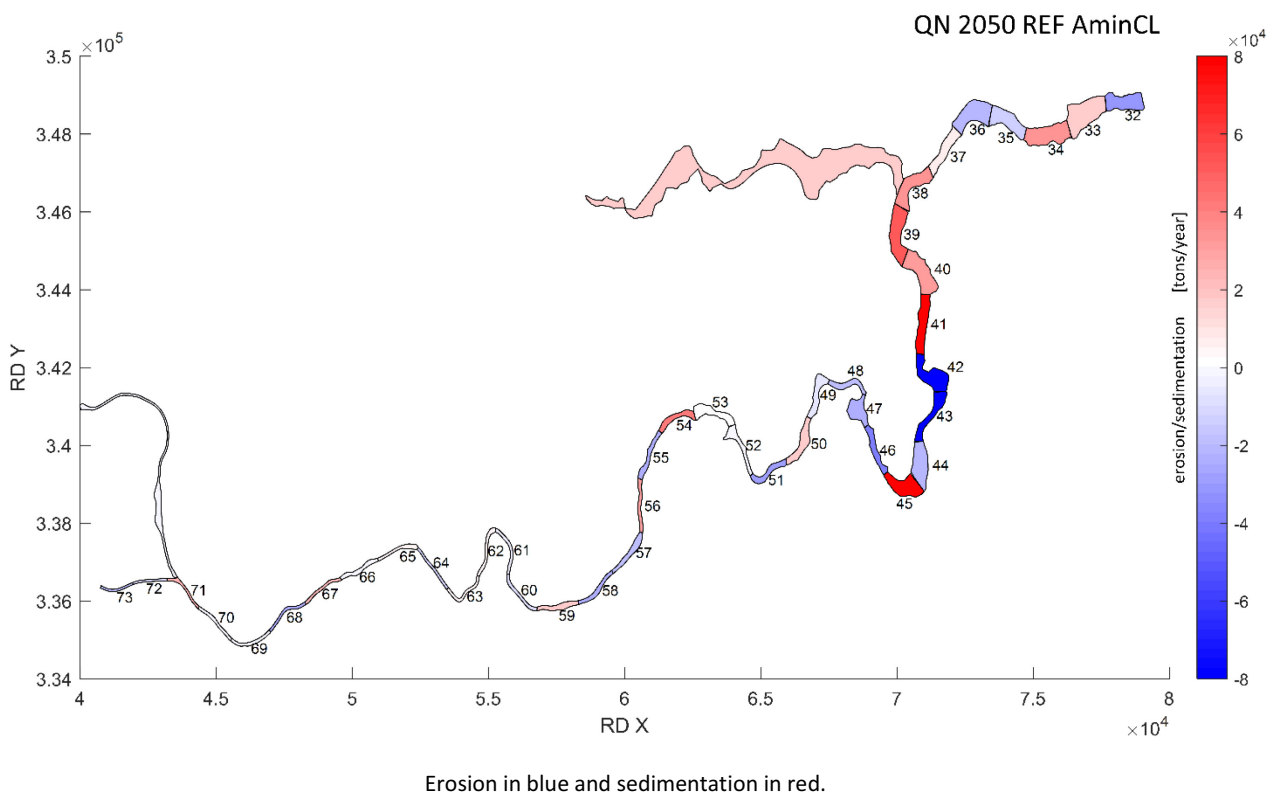
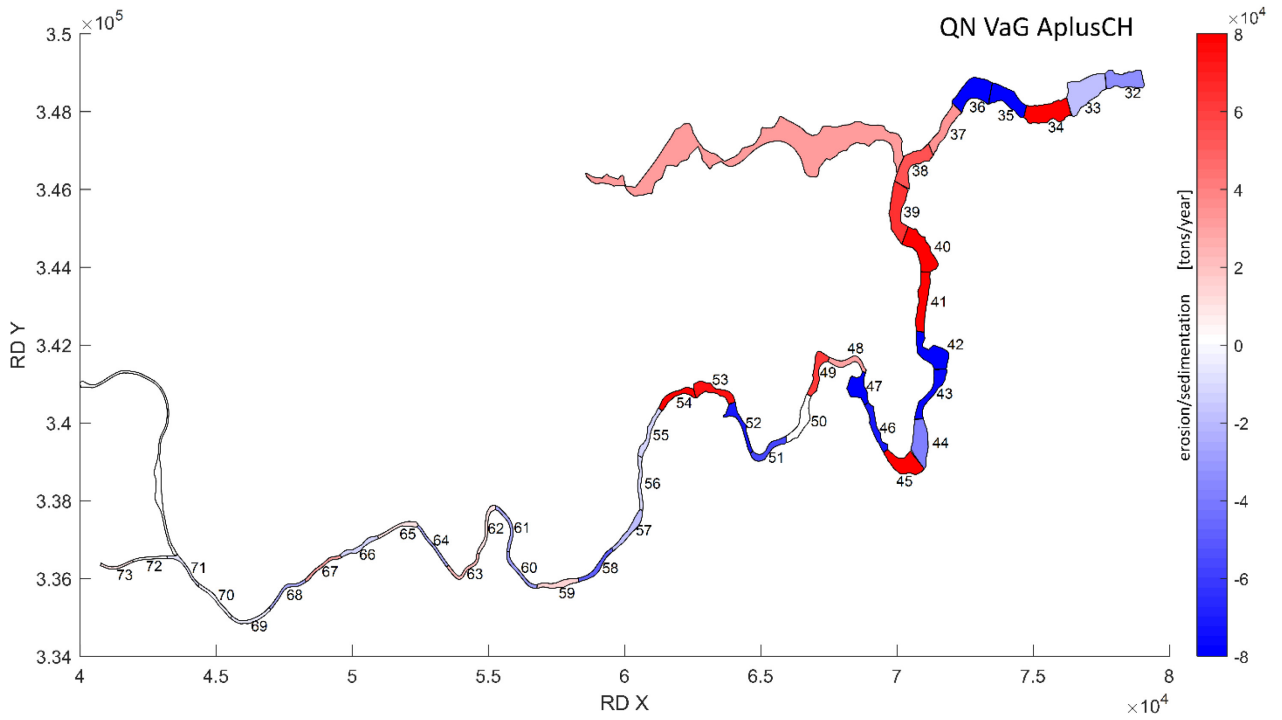
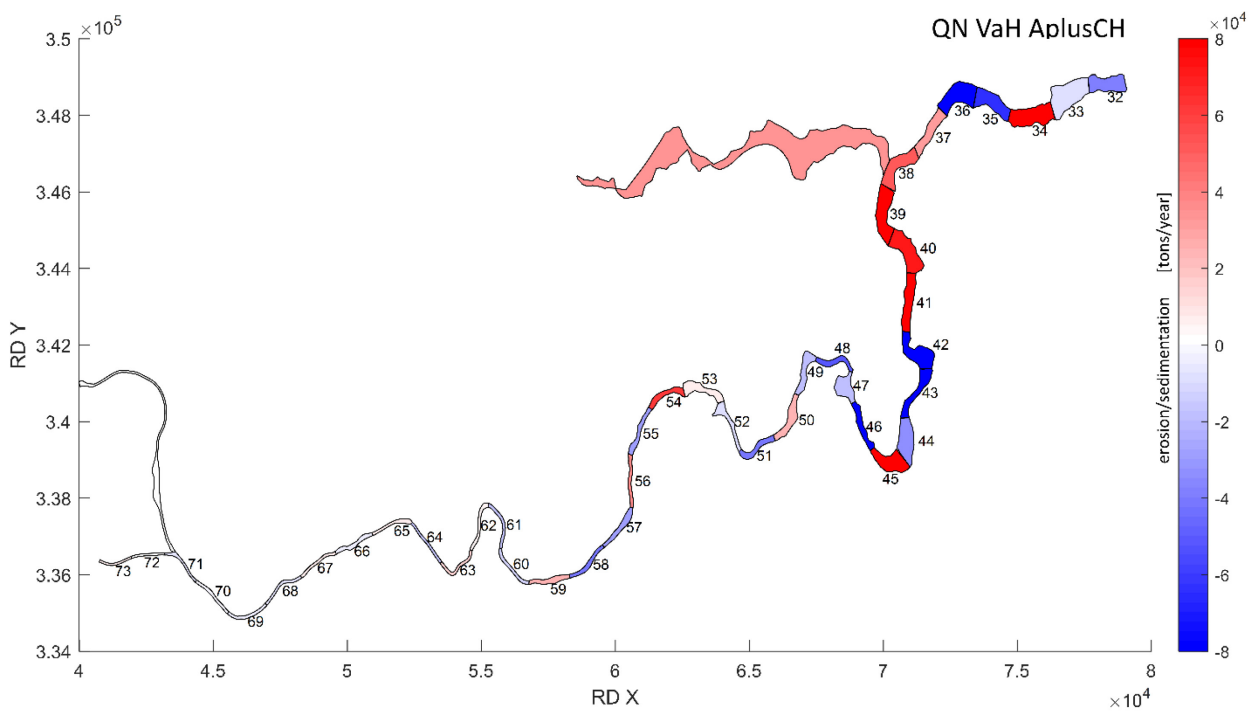


Figure 47 – Potential Sedimentation/erosion rates for polygons along the Upper Sea Scheldt.  
Scenario QN VaG AplusCH.



Erosion in blue and sedimentation in red.

Figure 48 – Potential Sedimentation/erosion rates for polygons along the Upper Sea Scheldt.  
Scenario QN VaH AplusCH



Erosion in blue and sedimentation in red.

Figure 49 – Potential Sedimentation/erosion rates for polygons along the Upper Sea Scheldt.  
Scenario QN Chafing AplusCH.

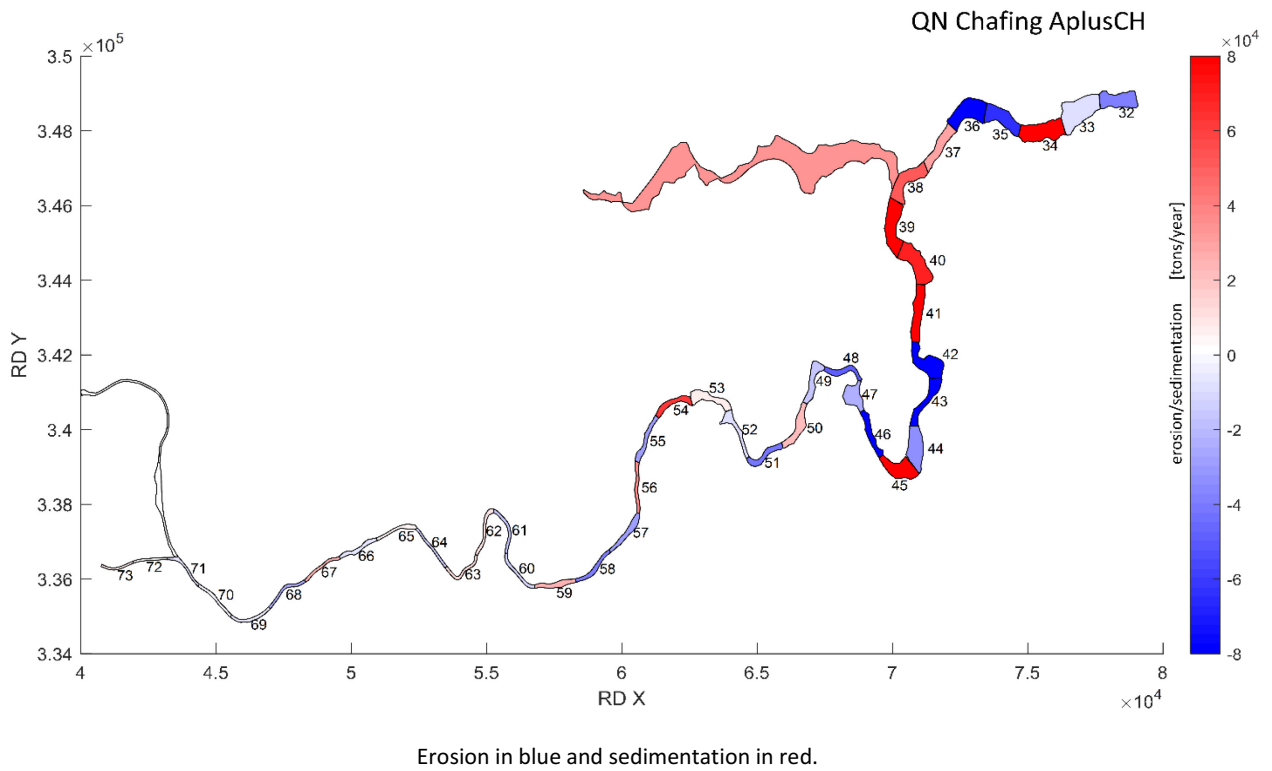


Figure 50 – Potential Sedimentation/erosion rates for polygons along the Upper Sea Scheldt.  
Scenario QN VaG AminCL.

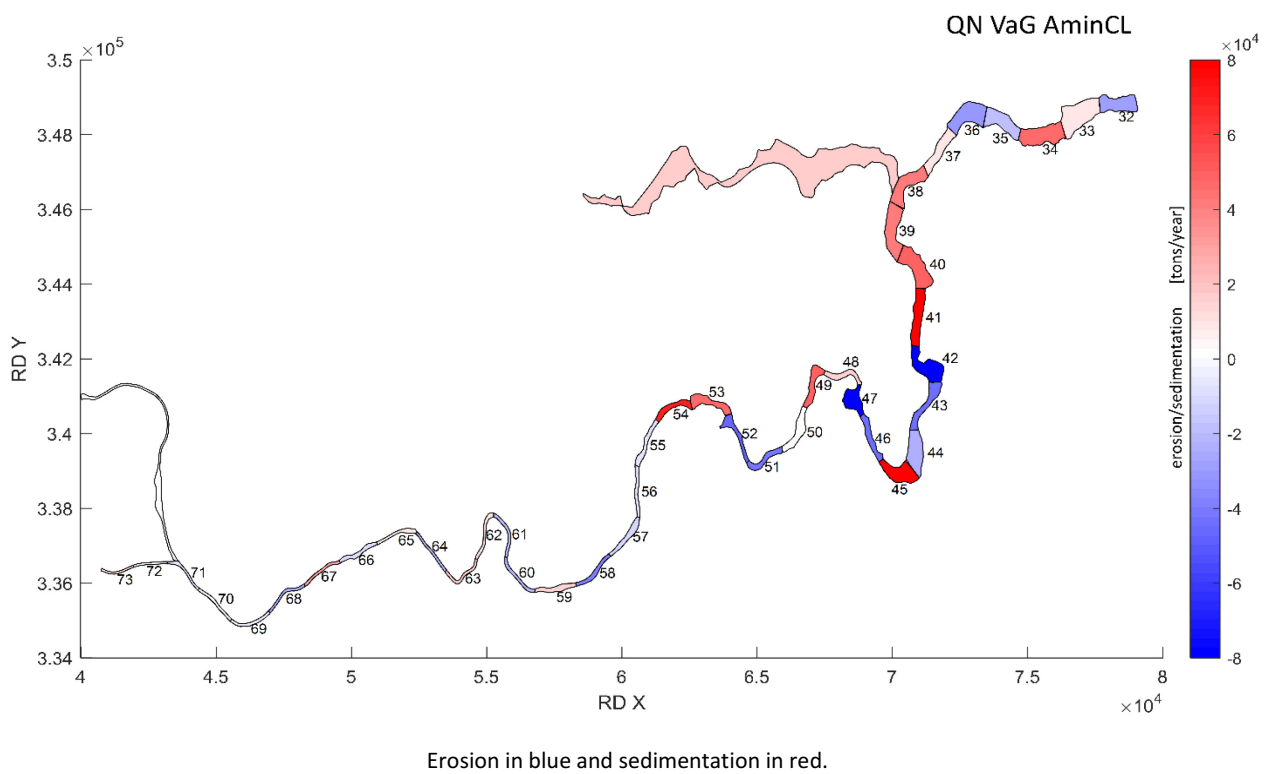


Table 5 – Cumulative potential sand transport per polygon extrapolated from a spring/neap tidal cycle to one year [x 10<sup>3</sup> tons/year]

polygon	2013 REF AOCN	2050 REF AOCN	2050 REF AplusCH	2050 REF AminCL	VaG AplusCH	VaH AplusCH	Chafing AplusCH	VaG AminCL
32	-46,66	-49,90	-39,01	-31,15	-32,86	-37,59	-37,70	-29,13
33	41,02	41,25	-7,38	16,14	-19,65	-8,68	-9,36	8,33
34	-18,45	15,43	107,23	33,25	130,44	108,13	106,64	45,05
35	27,21	8,07	-65,26	-12,67	-78,53	-63,15	-63,42	-19,19
36	-10,14	-16,65	-73,36	-22,08	-92,79	-78,79	-78,57	-32,33
37	-3,70	-2,07	27,51	5,98	34,57	30,39	29,60	9,24
38	47,98	51,58	49,03	34,90	54,96	50,16	50,51	40,22
39	70,53	64,20	82,97	50,55	64,44	86,02	88,08	40,86
40	16,05	25,36	65,86	31,87	97,65	72,17	68,62	48,84
41	89,34	89,22	133,84	78,36	183,98	137,46	136,54	108,58
42	-73,58	-83,30	-154,04	-78,69	-343,67	-157,44	-156,38	-186,57
43	-118,09	-98,50	-164,75	-91,36	-76,45	-178,70	-177,29	-44,12
44	-10,74	-28,20	-34,34	-22,44	-39,63	-33,85	-33,25	-23,72
45	88,98	94,22	157,46	92,54	209,10	173,41	171,49	124,38
46	-47,07	-44,51	-62,24	-38,67	-70,22	-81,24	-79,66	-44,72
47	-13,89	-28,03	-35,06	-24,31	-142,53	-19,31	-23,09	-80,82
48	-24,24	-18,57	-39,27	-18,37	29,95	-52,30	-48,83	12,76
49	-1,58	-1,03	-19,02	-7,42	60,75	-17,80	-16,99	48,32
50	15,76	15,21	19,68	16,15	2,43	23,49	22,39	2,15
51	-33,19	-31,14	-37,02	-28,71	-57,08	-42,36	-41,17	-41,58
52	1,00	0,10	-2,54	-0,94	-71,38	-8,83	-8,42	-45,92
53	1,23	2,41	2,70	1,48	73,18	5,79	5,40	46,80
54	37,90	36,94	52,05	40,89	91,17	60,88	60,43	68,22
55	-26,64	-24,50	-29,21	-23,01	-10,00	-28,85	-28,68	-5,90
56	26,49	23,55	34,71	29,71	-9,58	37,12	37,14	-5,49
57	-18,16	-19,43	-22,43	-19,44	-17,71	-28,46	-27,66	-11,65
58	-30,98	-24,11	-30,22	-24,03	-48,17	-41,12	-39,40	-37,87
59	24,07	18,93	15,34	15,07	13,46	24,17	22,74	15,00
60	-6,97	-6,99	-12,69	-9,30	-27,71	-10,88	-11,23	-21,36
61	-2,79	-1,50	-6,02	-3,87	-24,67	-16,08	-15,93	-17,80
62	4,52	2,84	4,05	4,03	8,05	4,81	8,09	7,62
63	0,10	-0,47	6,72	3,28	22,35	14,36	10,49	16,31
64	-7,63	-6,76	-14,04	-11,87	-24,65	-15,82	-14,07	-21,17
65	5,10	5,03	4,51	4,89	7,56	6,33	4,94	7,28
66	2,54	1,42	-0,30	-0,82	-11,04	-3,89	-5,23	-9,26
67	14,62	13,20	18,25	20,30	28,73	6,39	22,63	28,58
68	-16,73	-14,15	-22,40	-22,73	-23,89	-6,30	-22,51	-22,95
69	-1,41	-1,41	-1,93	-2,04	-3,75	-2,63	-2,77	-3,76
70	0,79	0,25	-0,75	-0,61	-1,00	-0,92	-0,12	-0,89
71	13,91	19,26	15,35	23,35	-6,42	-5,05	-5,07	-5,67
72	0,09	-7,21	-6,33	-8,54	0,01	0,03	0,05	0,11
73	-17,63	-14,67	-13,96	-18,92	7,55	6,14	5,61	10,40
Durme	-7,13	-21,57	-34,18	-16,33	-30,36	-33,60	-33,72	-15,57
Gentbrugge	0,0614	0,0153	0,0096	-0,0028	0,0203	0,0071	0,0113	0,0011

## Appendix B: Net sand transport figures for scenarios

This appendix shows for every scenario the net sand transport over different cross sections along the Scheldt estuary and over a spring/neap tidal cycle, a spring and a neap tide. For every scenario the full length of the estuary is shown in one figure and a second figure shows only the Upper Sea Scheldt, the focus area of this study.

## 2050 REF QN A0CN

Figure 51 – Net sand transport over different cross sections along the Scheldt estuary calculated and plotted for a neap and spring tide and a full spring/neap tidal cycle. Scenario 2050 QN REF A0CN. A positive value means transport in downstream direction.

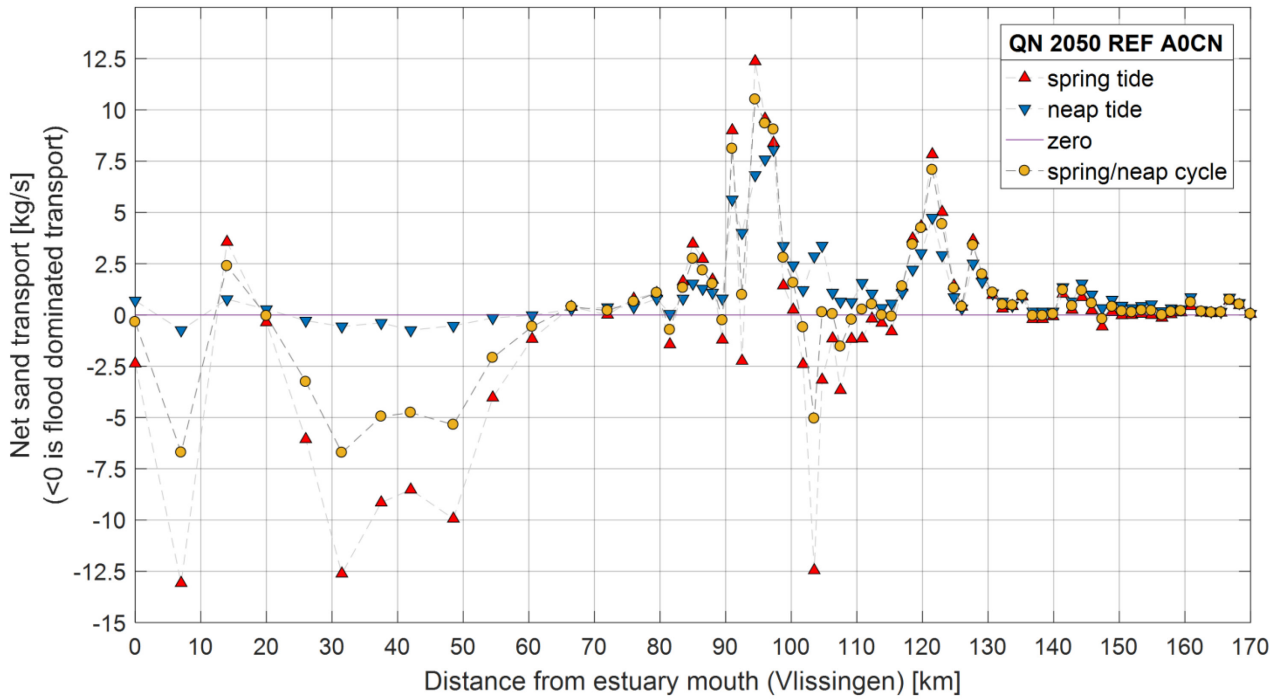
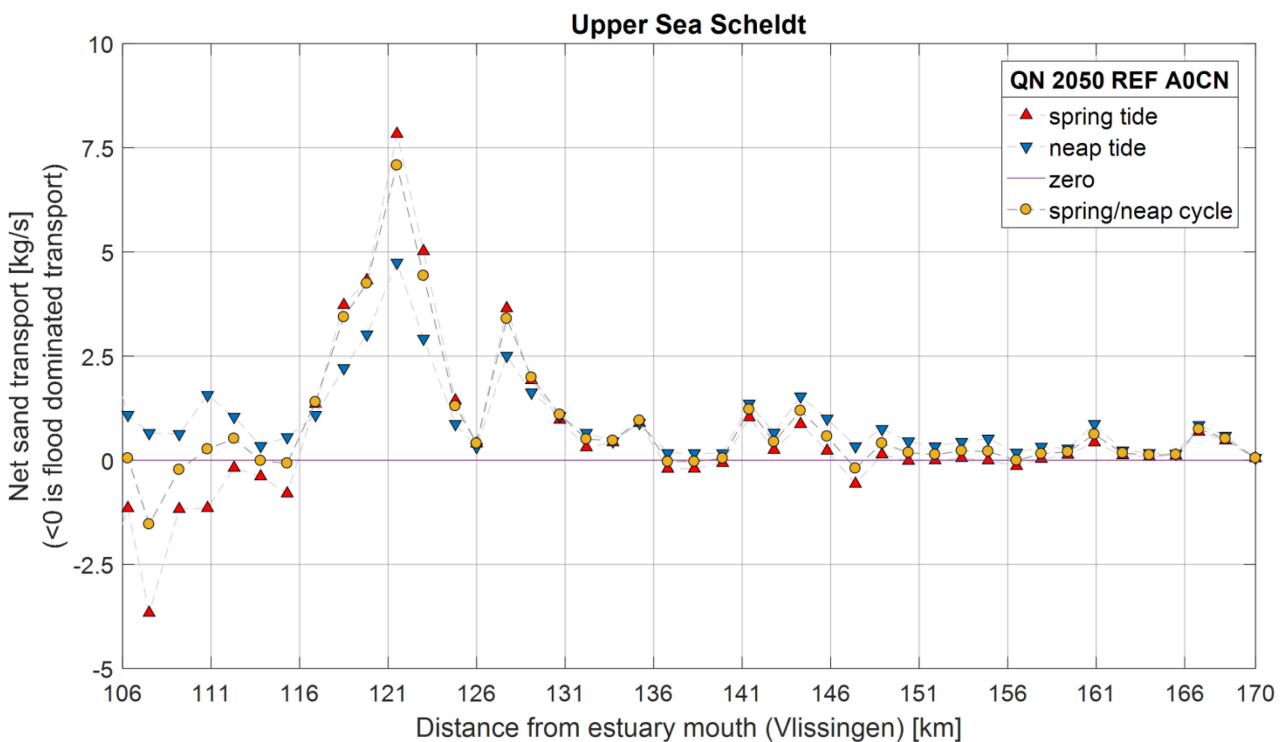


Figure 52 – Net sand transport over different cross sections of the Upper Sea Scheldt calculated and plotted for a neap and spring tide and a full spring/neap tidal cycle. Scenario 2050 QN REF A0CN. A positive value means transport in downstream direction.



## 2050 REF QN AminCL

Figure 53 – Net sand transport over different cross sections along the Scheldt estuary calculated and plotted for a neap and spring tide and a full spring/neap tidal cycle. Scenario 2050 QN REF AminCL. A positive value means transport in downstream direction.

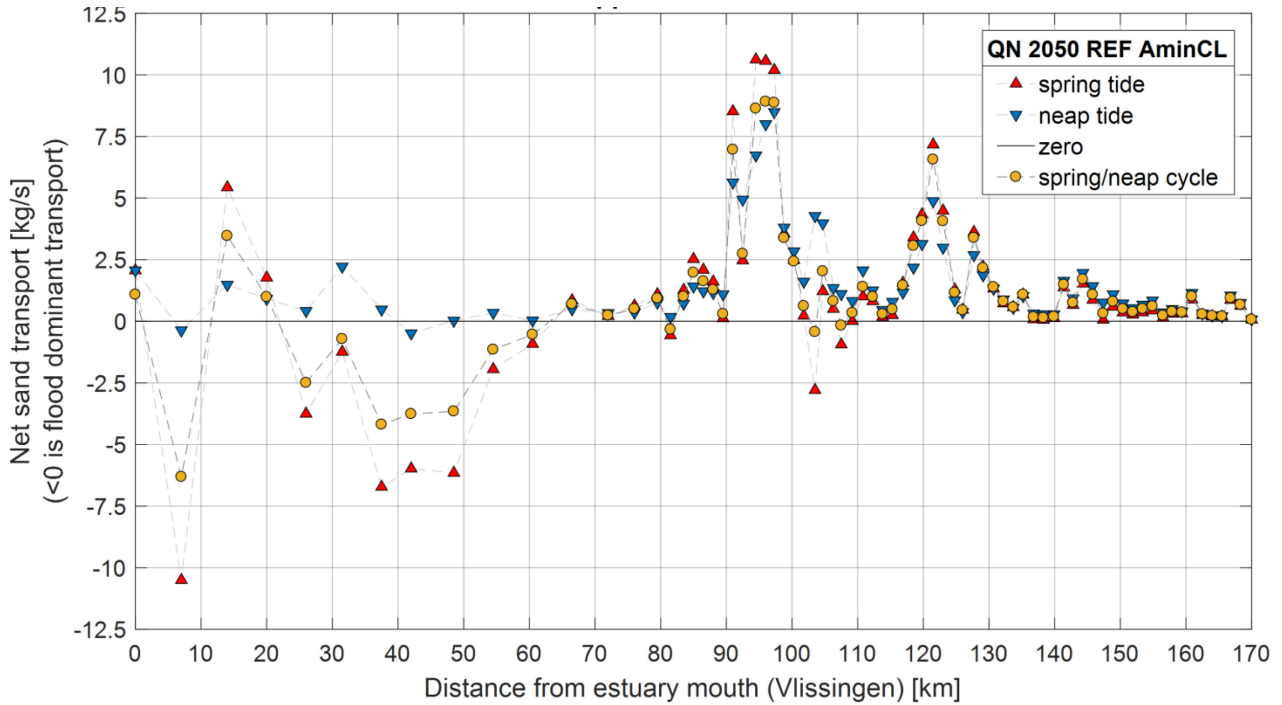
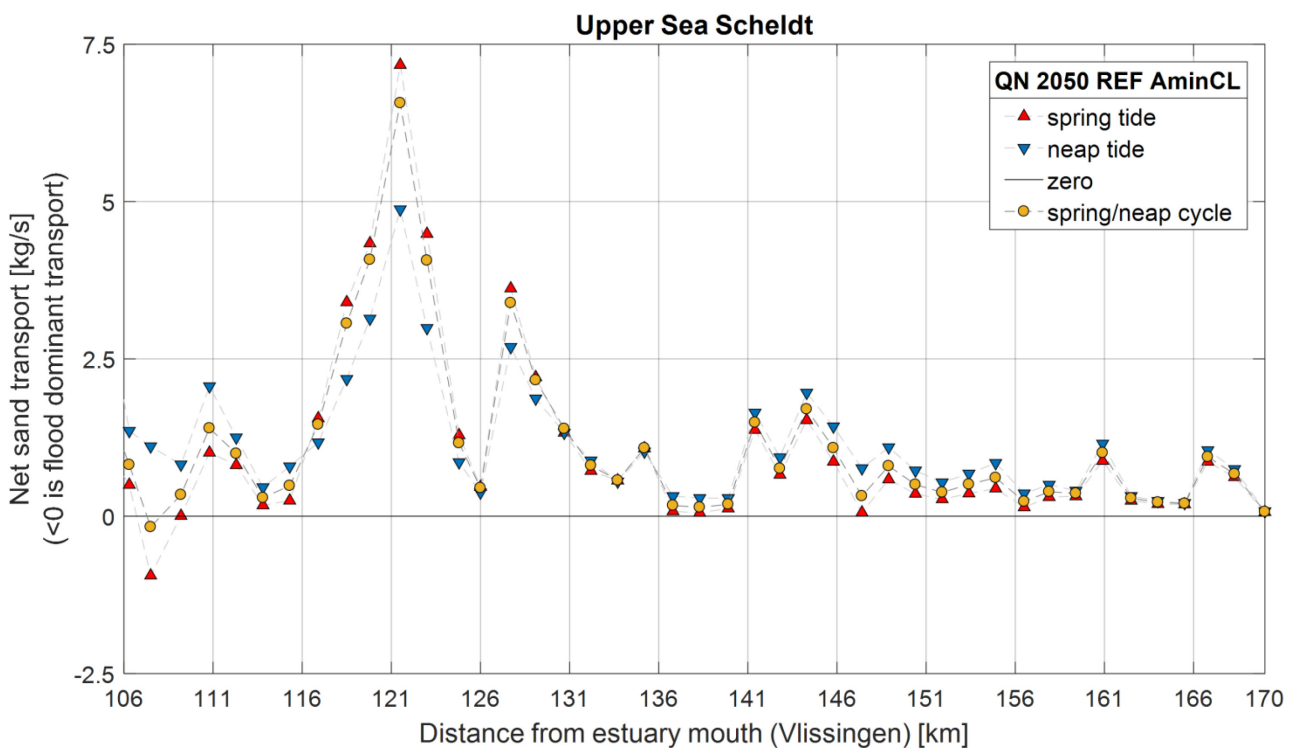


Figure 54 – Net sand transport over different cross sections of the Upper Sea Scheldt calculated and plotted for a neap and spring tide and a full spring/neap tidal cycle. Scenario 2050 QN REF AminCL. A positive value means transport in downstream direction.



## 2050 REF QN AplusCH

Figure 55 – Net sand transport over different cross sections along the Scheldt estuary calculated and plotted for a neap and spring tide and a full spring/neap tidal cycle. Scenario 2050 QN REF AplusCH. A positive value means transport in downstream direction.

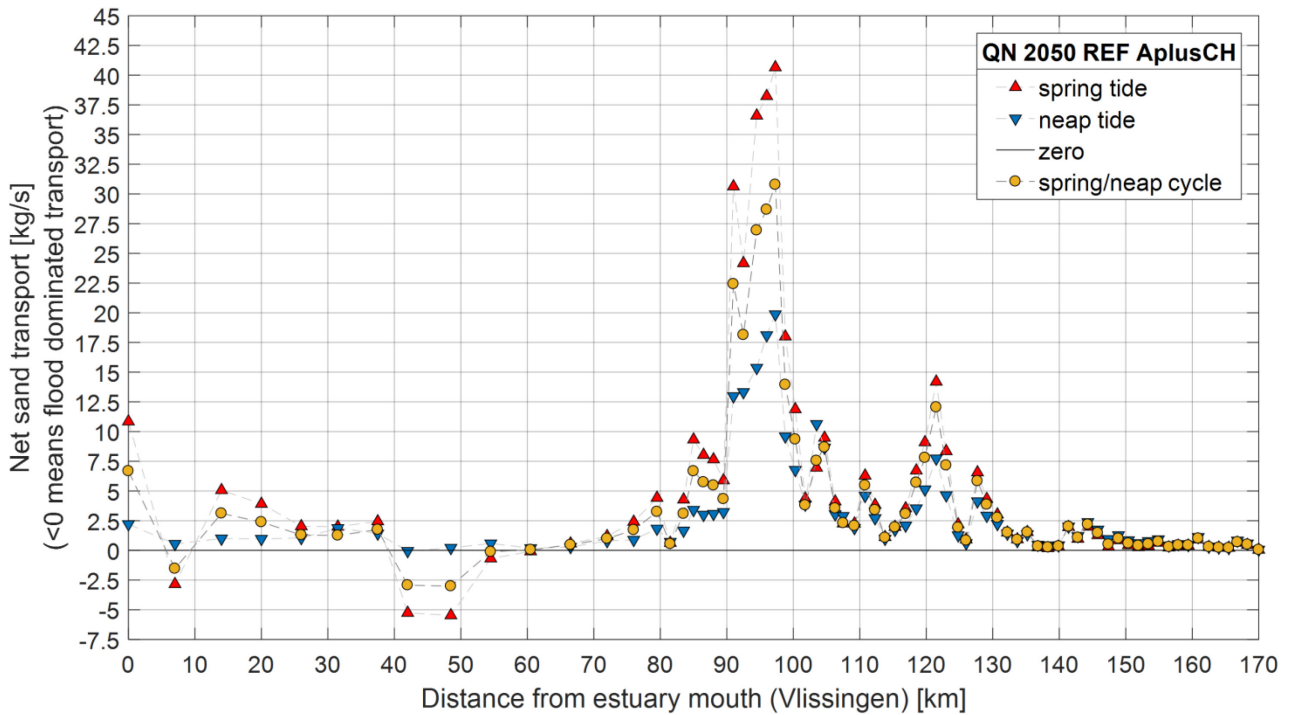
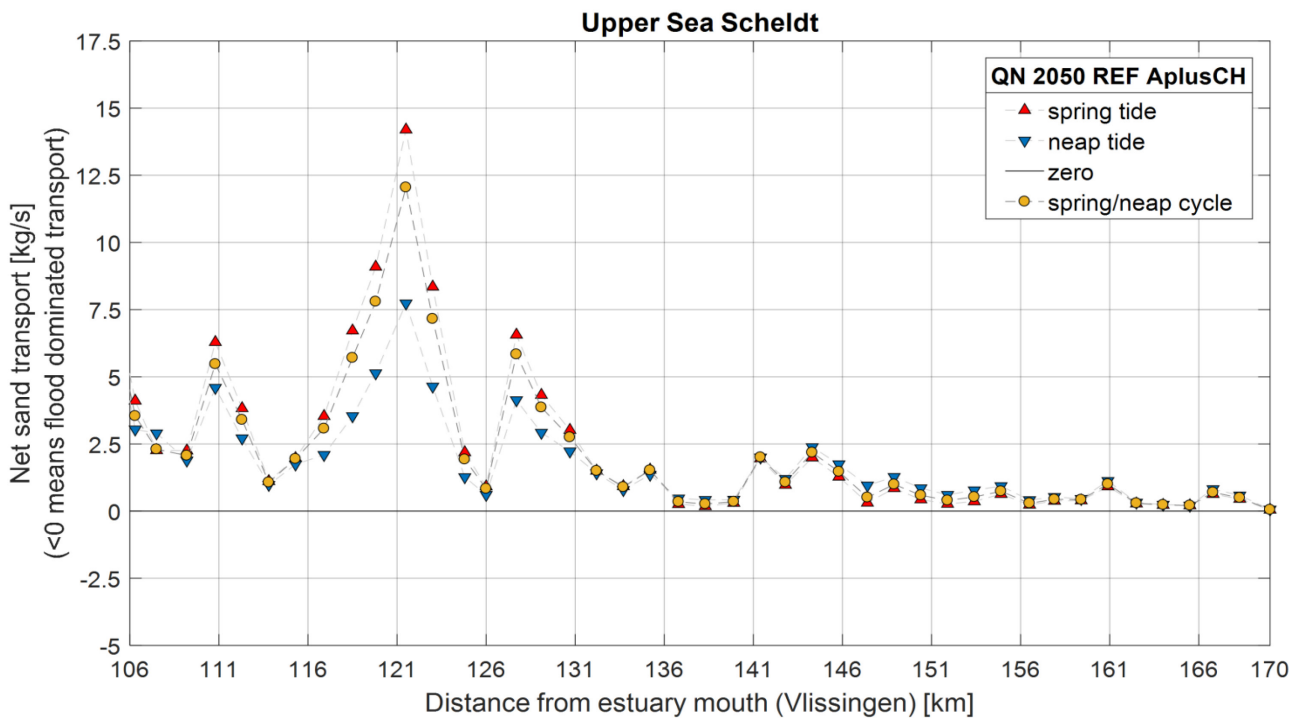


Figure 56 – Net sand transport over different cross sections of the Upper Sea Scheldt calculated and plotted for a neap and spring tide and a full spring/neap tidal cycle. Scenario 2050 QN REF AminCL. A positive value means transport in downstream direction.



## VaG AplusCH

Figure 57 – Net sand transport over different cross sections along the Scheldt estuary calculated and plotted for a neap and spring tide and a full spring/neap tidal cycle. Scenario VaG AplusCH. A positive value means transport in downstream direction.

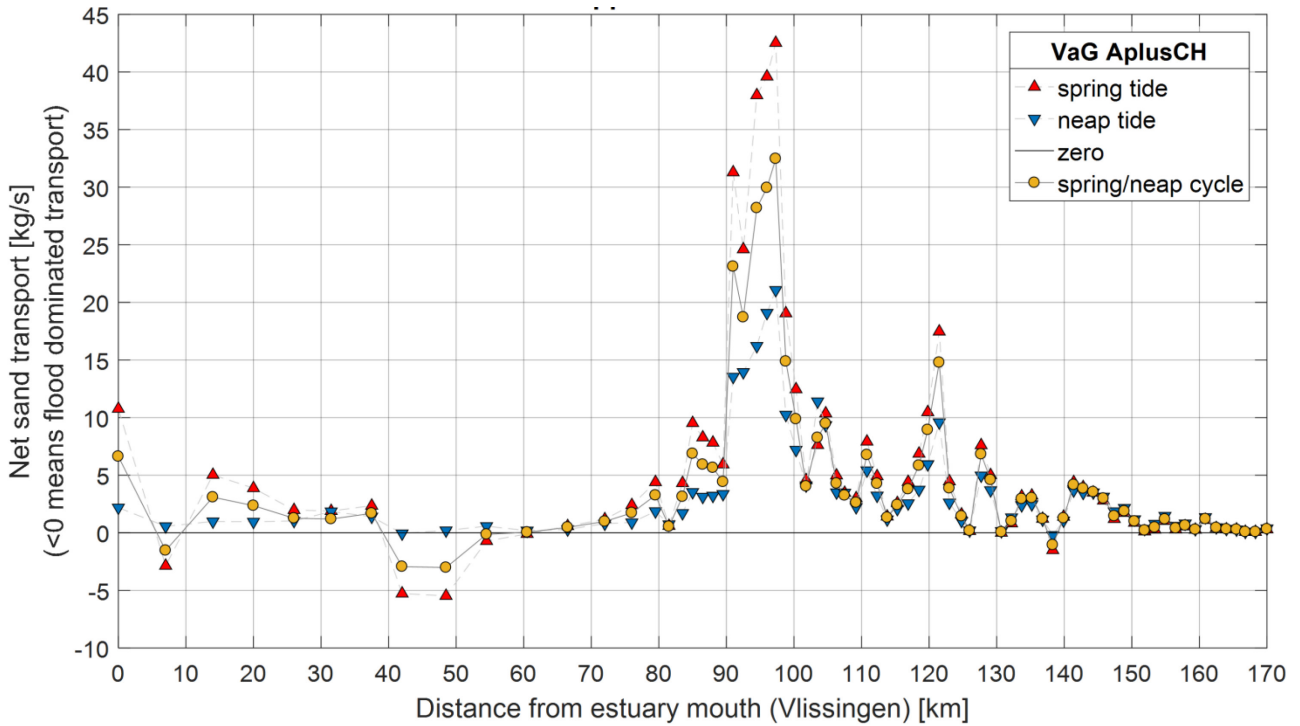
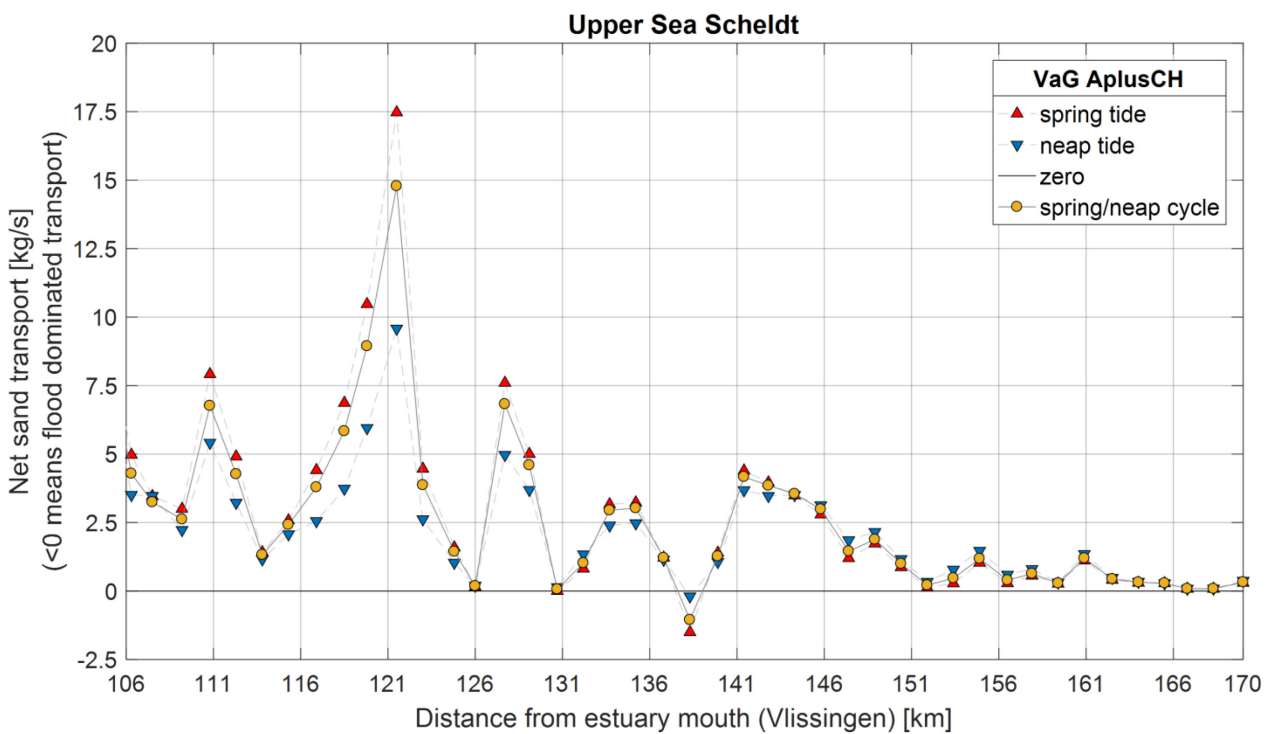


Figure 58 – Net sand transport over different cross sections of the Upper Sea Scheldt calculated and plotted for a neap and spring tide and a full spring/neap tidal cycle. Scenario VaG AplusCH. A positive value means transport in downstream direction.



## VaH AplusCH

Figure 59 – Net sand transport over different cross sections along the Scheldt estuary calculated and plotted for a neap and spring tide and a full spring/neap tidal cycle. Scenario VaH AplusCH. A positive value means transport in downstream direction.

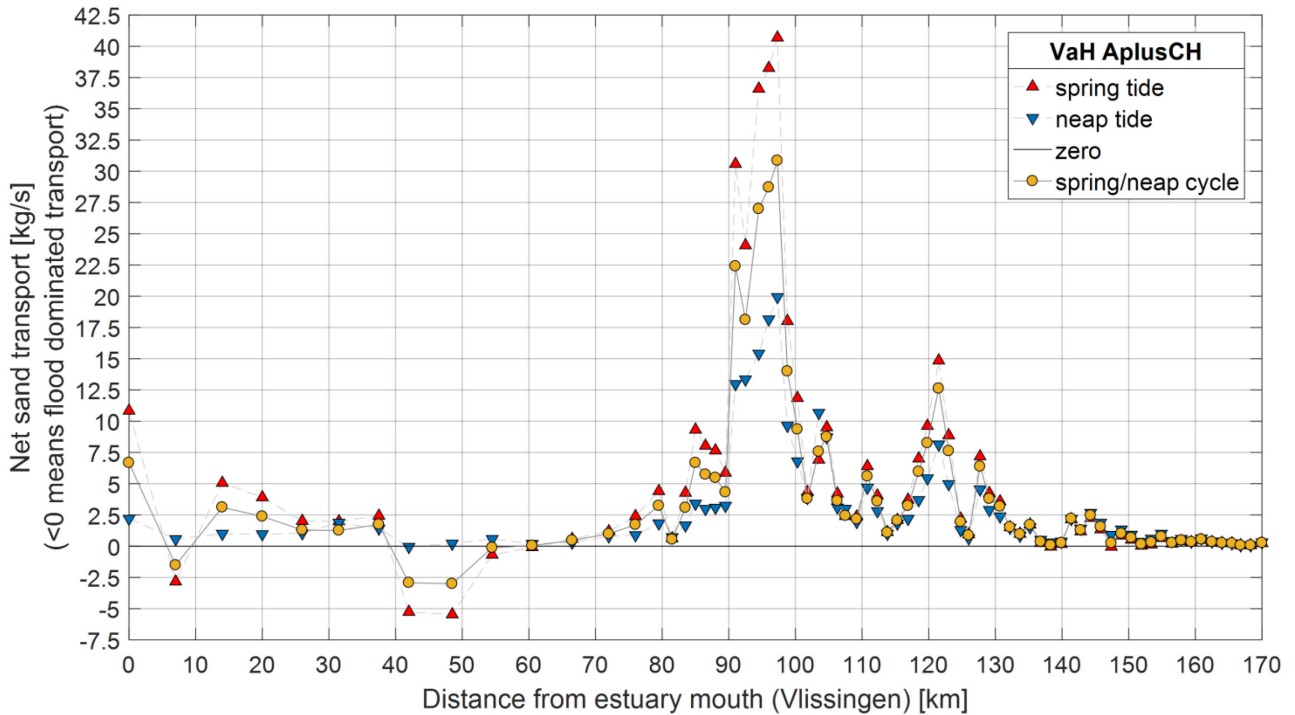
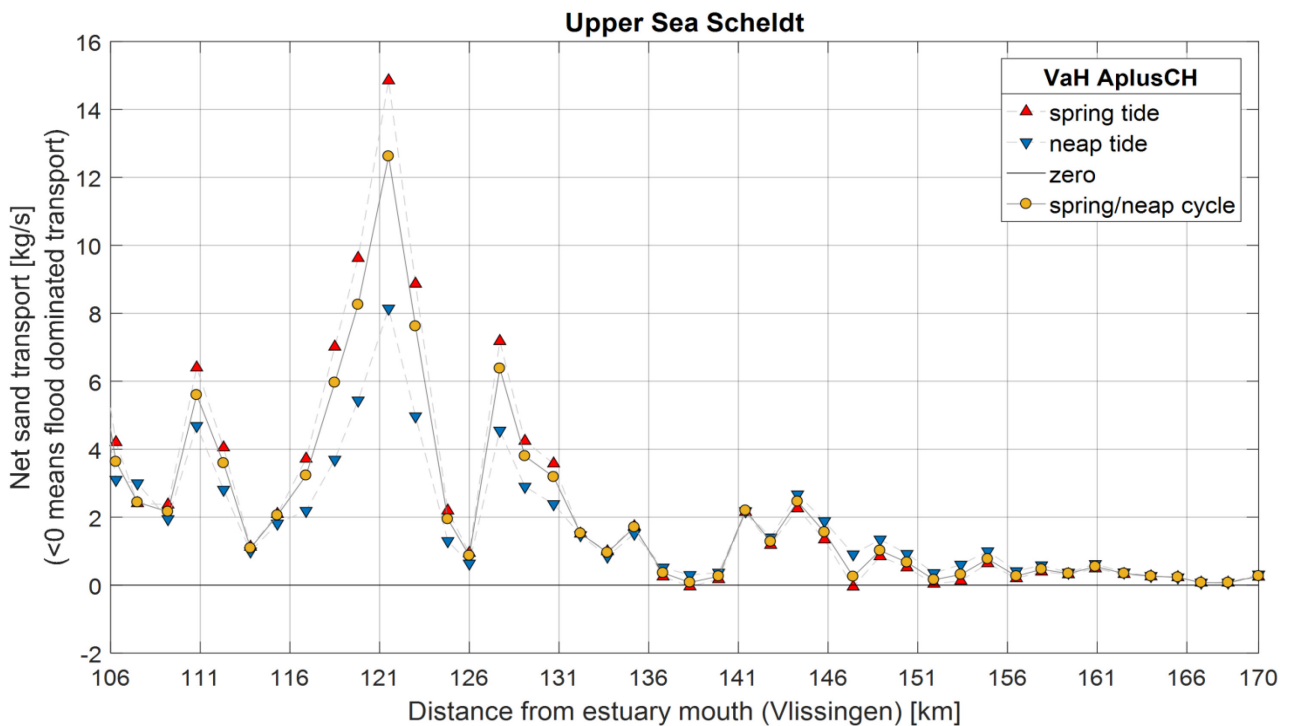


Figure 60 – Net sand transport over different cross sections of the Upper Sea Scheldt calculated and plotted for a neap and spring tide and a full spring/neap tidal cycle. Scenario VaH AplusCH. A positive value means transport in downstream direction.



## Chafing AplusCH

Figure 61 – Net sand transport over different cross sections along the Scheldt estuary calculated and plotted for a neap and spring tide and a full spring/neap tidal cycle. Scenario Chafing AplusCH. A positive value means transport in downstream direction.

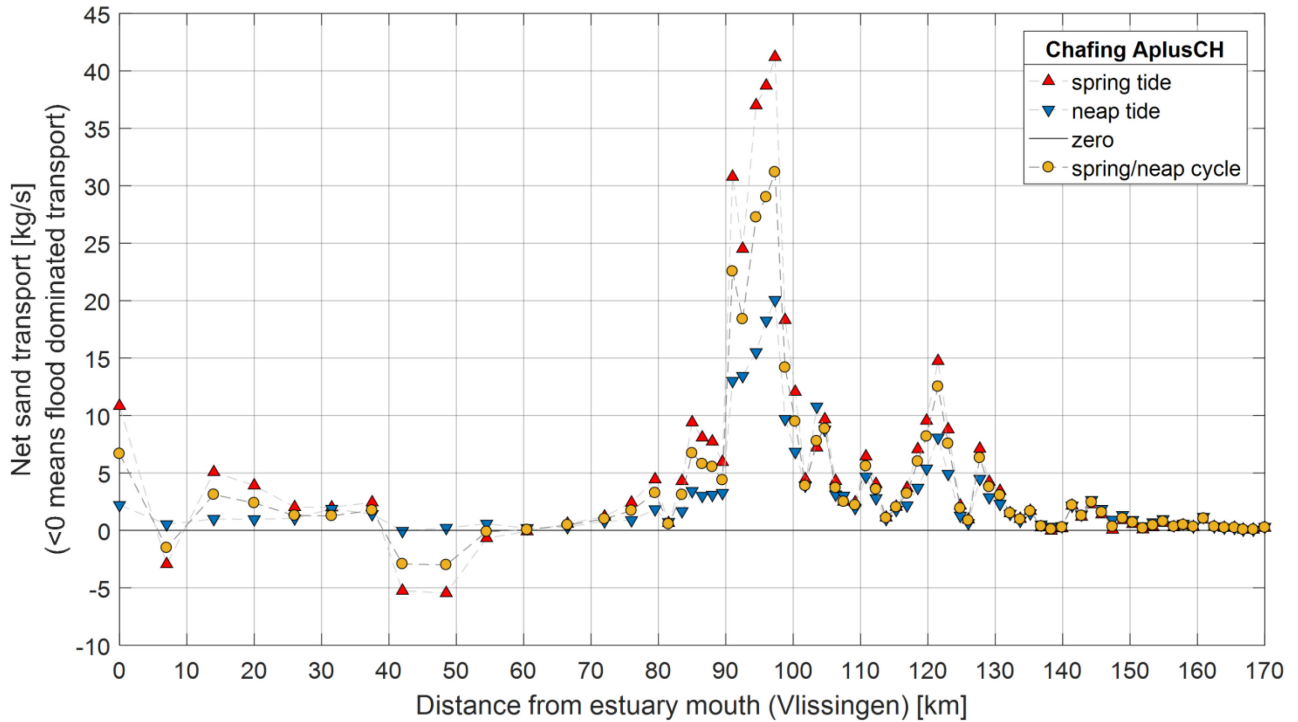
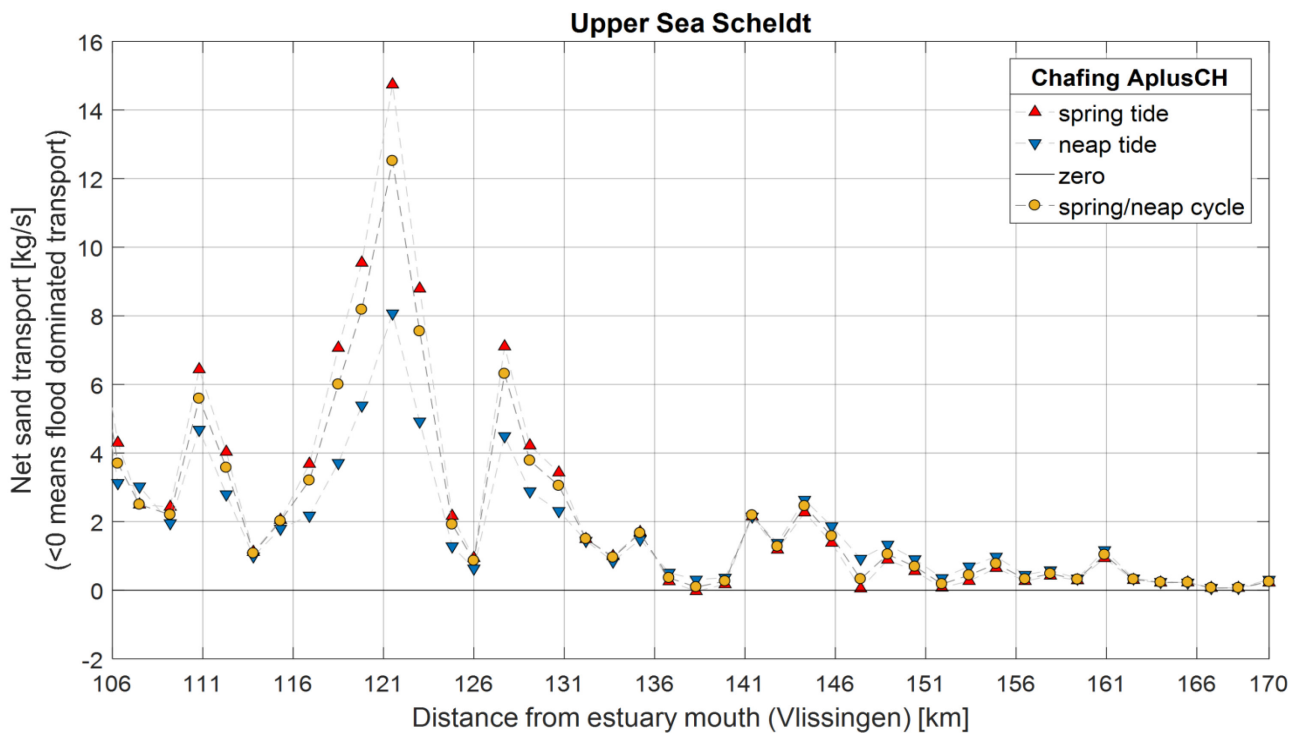


Figure 62 – Net sand transport over different cross sections of the Upper Sea Scheldt calculated and plotted for a neap and spring tide and a full spring/neap tidal cycle. Scenario Chafing AplusCH. A positive value means transport in downstream direction.



DEPARTMENT **MOBILITY & PUBLIC WORKS**  
Flanders hydraulics Research

Berchemlei 115, 2140 Antwerp

**T** +32 (0)3 224 60 35

**F** +32 (0)3 224 60 36

[waterbouwkundiglabo@vlaanderen.be](mailto:waterbouwkundiglabo@vlaanderen.be)

[www.flandershydraulicsresearch.be](http://www.flandershydraulicsresearch.be)